BULK COMPOSITION OF THE TANCO PEGMATITE
AT
BERNIC LAKE, MANITOBA, CANADA

BY

ANDREW STILLING

A Thesis
Submitted to the Faculty of Graduate Studies
In Partial Fulfilment of the Requirements
For the Degree of

MASTER OF SCIENCE

Department of Geological Sciences
University of Manitoba
Winnipeg, Manitoba, Canada

0-612-32962-3

THE UNIVERSITY OF MANITOBA

FACULTY OF GRADUATE STUDIES

*****

COPYRIGHT PERMISSION PAGE

BULK COMPOSITION OF THE TANCO PEGMATITE AT

BERNIC LAKE, MANITOBA, CANADA

BY

ANDREW STILLING

A Thesis/Practicum submitted to the Faculty of Graduate Studies of The University of Manitoba in partial fulfillment of the requirements of the degree

of

MASTER OF SCIENCE

BULK COMPOSITION OF THE TANCO PEGMATITE
AT
BERNIC LAKE, MANITOBA, CANADA

Andrew Stilling

ABSTRACT: The Tanco pegmatite at Bernic Lake, Manitoba, Canada is a highly fractionated rare-element class, LCT family pegmatite with 9 internal zones and is one of the largest complex internally zoned pegmatites in the world. The outer zones of the pegmatite are generally concentric, while the shape of the inner zones, based on underground workings and drill core observations, are very irregular and complex. Tanco presents a unique opportunity to calculate the bulk composition of a pegmatite which, unlike previous works on other pegmatites, does not need to consider structural deformation and/or erosion to reconstruct the original size and shape. Tanco is essentially an undeformed blind pegmatite, with only minimal exposure through erosion at the bottom of Bernic Lake. Almost no reconstructive interpretation is required as the amount of eroded material is negligible and does not affect the over-all bulk composition calculations.

Given the available information from the drill core logs and underground workings on the Tanco pegmatite, it was possible to create the first 3D computer representation of a pegmatite. The model shows a sub-horizontal, bilobate, saddle-shaped body, which dips shallowly to the north and doubly plunges to the east and west. It is about 1990 m in length, 1060 m in width, attaining a maximum thickness of nearly 100 m in the central portions, while thinning out towards the edges. The model also provides the basis for the generation of volumes for the different zones within the pegmatite and bulk composition of the entire pegmatite as a whole. The pegmatite displaces approximately 9.4 million m^3 and has a mass of about 25.0 million metric tons. The proportional volumes of each zone are: zone (10) 0.10%, zone (20) 30.83%, zone (30) 2.69%, zone (40) 28.79%, zone (50) 13.12%, zone (60) 13.56%, zone (70) 7.47%, zone (80) 1.33%, zone (90) 2.11%.

The bulk mineral composition of the pegmatite, by volume, is: quartz 32.54%, albite 25.56%, K-feldspar 22.05%, petalite 9.03%, lithian muscovite 3.00%, muscovite 2.97%, pollucite 1.28%, spodumene 0.92%, amblygonite 0.77%, lepidolite 0.27%.

The bulk chemical composition of the pegmatite is: SiO_2 75.27%, Al_2O_3 13.72%, TiO_2 0.01%, Fe_2O_3 0.00%, FeO 0.12%, MnO 0.19%, MgO 0.01%, CaO 0.21%, SrO 0.0004%, Li_2O 0.76%, Na_2O 3.35%, K_2O 3.50%, Rb_2O 0.58%, Cs_2O 0.48%, P_2O_5 0.94%, B_2O_3 0.05%, BeO 0.0613%, H_2O+ 0.37%, H_2O- 0.03%, F 0.18%, Sc_2O_3 0.0001%, SnO_2 0.0391%, Nb_2O_5 0.0129%, Ta_2O_5 0.0792%, UO_2 0.0063%, PbO 0.0014%, WO_3 0.00004%, ZnO 0.0013%, ZrO_2 0.0051%, HfO_2 0.0017%, Tl_2O 0.0047%, Ga_2O_3 0.0106%, Sb_2O_3 0.0002%, -O=F2 -0.08%, total 99.92% by weight.

The current calculated bulk chemical composition of Tanco is different from the total calculated by Morgan and London, (1990), who included only the central zones and did not include the outer reaches of the pegmatite, thus under-representing zone (20) in particular as well as zones (40), (50), and (70). Improved modelling and modal estimates also contribute to the higher SiO_2 and Na_2O, and at the same time lower Al_2O_3, Li_2O, K_2O, Rb_2O, and P_2O_5 calculated in the present work.

Tanco is slightly poorer in lithium and slightly richer in feldspars when compared to other petalite and spodumene pegmatites. At Tanco the internal evolution of lithium silicate minerals starts inside the petalite stability field and moves into the spodumene stability field, from zones (40), (45), and (50), to zones (60) and (70).

The bulk composition of Tanco and other lithium-rich pegmatites analyzed to date are enriched in feldspars and are impoverished in quartz and lithium aluminosilicates, relative to the minimum in the Li_2O-Al_2O_3-SiO_2-H_2O system. This shift is due to the influence of F, B, and P, as documented in experimental studies.

KEY WORDS: Tanco, Pegmatite, Bernic Lake, Bulk Composition, Volume Calculations, Geology, 3D Computer Modelling.

ACKNOWLEDGEMENTS

Support, advice, and assistance have come from many sources during the span of this research. Such research would have been impossible without the cooperation and support of the Tantalum Mining Corporation of Canada, Ltd. Particular thanks is due to the past and present mine managers Richard Burt and Bill Ferguson, chief geologist Peter Vanstone, mine engineers Heide Townshend and Kevin McMurren, mine geologists Jamie Law and Shane Moran for their assistance and access to all available data.

Additional thanks also goes to the regional geologists at AECL's Whiteshell Research laboratories Dr. Anton Brown, Robert MacGregor, Dan Good, and the late Dr. D.H. Kamineni for their technical assistance and critical discussions.

Access to specialized computer resources was generously provided by Dr. Ian Muirhead at the University of Alberta's Faculty of Engineering, by David Mosscrop at the University of Manitoba's Department of Geography, and by Tanco.

The author is forever grateful to Dr. Petr Černý whose supervision, support, direction, and patience have made this challenging project possible.

TABLE OF CONTENTS

LIST OF TABLES

LIST OF FIGURES

1 INTRODUCTION

1.1 Purpose of the Study

The purpose of this research is to calculate the bulk composition of the Tanco pegmatite by determining the volumes, the mineralogy, and chemistry of the individual zones inside the pegmatite.

The Tanco pegmatite at Bernic Lake, Manitoba, Canada is a highly fractionated rare-element class, LCT family pegmatite with 9 internal zones and is one of the largest complex internally zoned pegmatites in the world. It is a unique pegmatite in that one does not need to consider the missing volumes of material caused by structural deformation and/or erosion, unlike other pegmatites, which require these adjustments when reconstructing their original sizes and shapes. Tanco is essentially an undeformed blind pegmatite, whose only erosional exposure is at the bottom of Bernic Lake. Almost no reconstructive interpretation is required as the amount of eroded material is negligible, and so is its effect on the over-all bulk composition calculations. Another factor that makes Tanco unique among other pegmatites is its densely drilled network of surface and underground holes. Over the past 43 years, 1,355 drill holes totalling over 102 km of core have been driven in and around the pegmatite. Given all the information from core logs and underground workings it was possible to develop and construct the first 3D computer model representation of a pegmatite. The construction of the model along with animated or real time modelling generated the shape and size of the internal zones and of the entire pegmatite. It also provided the basis for the generation of volumes for individual zones for the bulk composition calculations.

This study will describe the mineralogy of the internal zones of the pegmatite before describing the methodology used to create the computerized database, the 3D model representations, and the volume calculations. After that, a brief section on methodology will describe how the mineral modes, compositions, and densities were obtained. Findings from the volume and bulk composition calculations will then be considered and compared to other pegmatites and granites for petrologic considerations.

1.2 Location of the Study Area, and Access

The Tanco mine and pegmatite are located in Manitoba, Canada (**Figure 1.01**). They are situated about 180 kilometres east-northeast of the city Winnipeg on the north western shore of Bernic Lake and is accessible by float plane or via the company's private access roadway off provincial roadways 313 and 315 east-northeast of Lac du Bonnet (**Figure 1.02**).

1.3 History and Previous Work

The pegmatite was initially discovered in the 1920's, when the area was being explored for gold. Tin was found in a narrow vertical pegmatite dyke and in 1929, the Jack Nut Tin Mine acquired the property for assessment. A year later in 1930, the company changed its name to the Consolidated Tin Corporation and began development of the property. They constructed a 10 ton-per-day mill to produce tin concentrates and sank a small shaft down into the pegmatite. They also began diamond drilling to define the pegmatite and discovered in one of the drill cores a deeper spodumene-rich pegmatite. Later that year, work at the mine ceased.

In 1954 the property was re-evaluated for its lithium potential and restaked by Montgary Explorations Limited. The company later changed its name to Chemalloy Minerals Limited and began a systematic diamond drilling program of 7,900 m to define the deeper spodumene pegmatite. With positive results from the drilling program a mining plant was set up, and a shaft was collared late in 1956. In 1957 the shaft was sunk to 93 m and the property was optioned to the American Metal Company Limited (later American Metals Climax) who drilled another 2,000 m. This work along with previous work outlined the extent of the spodumene deposit and found interesting deposits of beryl, lepidolite, amblygonite, pollucite, and tantalum minerals. Between 1959 and 1961, Chemalloy and American Metals extended the shaft to 103 m, completed another 8,800 m of diamond drilling, and 1,800 m of drifting and raising into these deposits, discovering more spodumene, lepidolite, pollucite, and tantalum minerals. By 1962 the lithium market dropped and spodumene production stopped. The mine was then allowed to flood.

In 1967 tantalum markets improved and the mine was de-watered, when a 40/60 joint venture between Chemalloy and Northern Goldfields Investments Limited formed the Tantalum Mining Corporation of Canada, Ltd. (also referred to as Tanco). Within a year, sufficient reserves were established to begin construction of a 500 ton-per-day tantalum

Figure 1.01 Tanco's location within Canada and Manitoba.

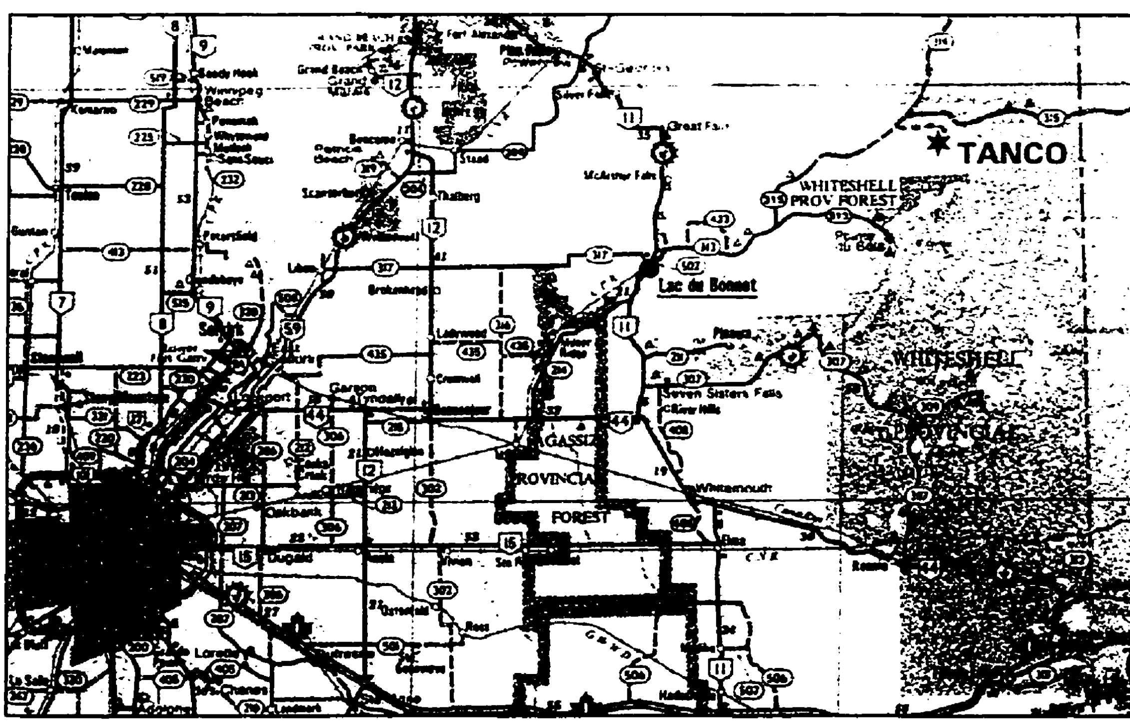

Figure 1.02 Tanco's location relative to Winnipeg.

separation plant and by September of 1969 it was in full operation. Internal problems in July of 1970 put the company under a receiver manager until a settlement and new partners were found in 1972. Chemalloy sold out 24.99% of its share in the Tantalum Corporation to Kawecki Berylco giving them 37.5%, Hudson's Bay Smelting 37.5%, and 25% to the Manitoba Government Development Corporation (Tanco Publication, 1981).

Capacity increases followed, and operations continued until the end of 1982, when tantalum markets and prices tumbled, suspending production temporarily. Operations continued as Tanco turned its attention to recovering high-quality concentrates of refractory spodumene, using parts of the tantalum mill to 'pilot' a spodumene plant, which was operational by the spring of 1984. One year later, construction of a dedicated 300 ton-per-day spodumene plant was finished in association with the tantalum mill. Full-scale production of spodumene and tantalum mineral concentrates commenced in 1986. In 1988 production of tantalum concentrates ceased again because of poor prices. Spodumene production carried Tanco through the lean tantalum years, when the tantalum mill was shut down between 1988 and 1992. Two years later, when tantalum markets recovered, the mill was brought back on line and was in full production by 1996.

In 1993, the Cabot Corporation of Boston, Massachusetts purchased 100% control of Tanco. Retaining the name, they maintained operations under their Speciality Products division, until they consolidated it in 1997 with the Cabot Specialty Fluids division to produce cesium formate from pollucite for heavy drilling fluids (P.J. Vanstone pers. comm. 1997).

1.4 Regional Geology of the Bernic Lake Region

The Tanco pegmatite is located in the southwestern portion of the Superior Province of the Canadian Shield (**Figure 1.03**) in the Bird River Subprovince situated in the southern limb of the Archean Bird River Greenstone Belt (Beakhouse, 1991). The Bird River Greenstone Belt is flanked by the Manigotogan - Ear Falls gneissic belt of the English River Subprovince to the north and by the batholithic belt of the Winnipeg River Subprovince to the south (Beakhouse, 1977). Most of the bedrock formations on the map are dated between 2780 - 2640 Ma, however, several remnant lithologies in the broader vicinity of the greenstone belt have ages in the range of ~ 3 Ga (Černý *et al.*, 1998).

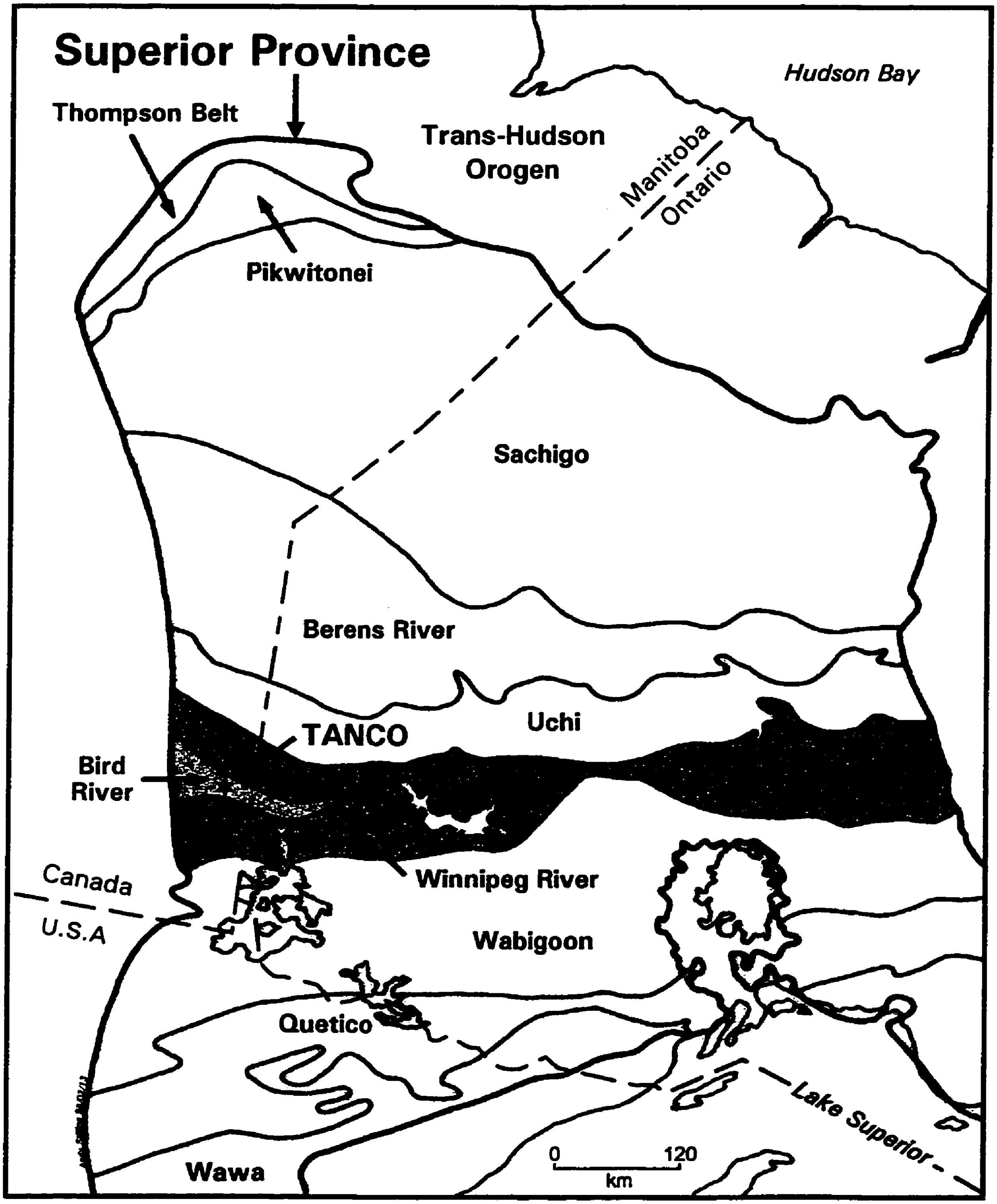

Figure 1.03 Geological map of the Superior Province showing the location of the Winnipeg River, English River (Red), and Bird River (Green) Subprovinces *Modified from Beakhouse, (1991).*

1.4.1 Bird River Greenstone Belt

The Bird River Greenstone Belt is composed of metasedimentary rocks, derived from volcanics, which are shown with synvolcanic to late tectonic intrusive rocks (**Figure 1.04**). The metamorphic rocks of the belt are subdivided into six formations located in and along the principal structural elements in an east to west alignment. These six formations, starting with the oldest, are: 1-Eaglenest Lake, 2-Lamprey Falls, 3-Peterson Creek, 4-Bernic Lake, 5-Flanders Lake, and the 6-Booster Lake formations (Crouse *et al.*, 1979, Černý *et al.* 1981,1998, Trueman, 1980).

1.) The Eaglenest Lake Formation is composed of fine to coarse volcaniclastic metasediments with minor biotite schists, amphibolites, and banded iron formations. The formation exhibits multiple deformations and attendant greenschist-facies metamorphism.

2.) The Lamprey Falls Formation is composed mainly of pillowed, megacrystic, amygdaloidal, and hyaloclastic metabasalt and hypabyssal metagabbro sills, which include the chromite-enriched Bird River Sill. Minor components of the formation also include intercalated tuffs, hyaloclastites, and extensive banded iron formations. These rocks form the underlying keel-like base to the synclinorium, are unmodified by minor deformation, and display dual mineral assemblages of the hornfels and greenschist facies.

3.) The Peterson Creek Formation is a mixture of metarhyolite, volcaniclastic, and epiclastic derivatives, which are intimately infolded and polydeformed along with younger portion of the Bernic Lake formation in the core of the synclinorium. This formation has been metamorphosed to greenschist up to amphibolite facies.

4.) The Bernic Lake Formation is a complex of volcaniclastic metasedimentary rocks and banded iron formation interlayered with pillowed metabasalt, meta-andesite, metadacite, and metarhyolite. The bulk of this formation resides in the core of the synclinorium formed by the greenstone belt and in part by the Peterson Creek formation. This formation attains greenschist and amphibolite-facies metamorphism and was also intruded by stocks and sills of metagabbro, metadorite, quartz-feldspar porphyries, and granodiorite.

5.) The Flanders Lake Formation consists chiefly of lithic and pebbly meta-arenite interbedded with metaconglomerate. Multiple periods of deformation are seen with the infolding of the Peterson Creek and Bernic Lake Formations. The rocks display amphibolite-facies metamorphism.

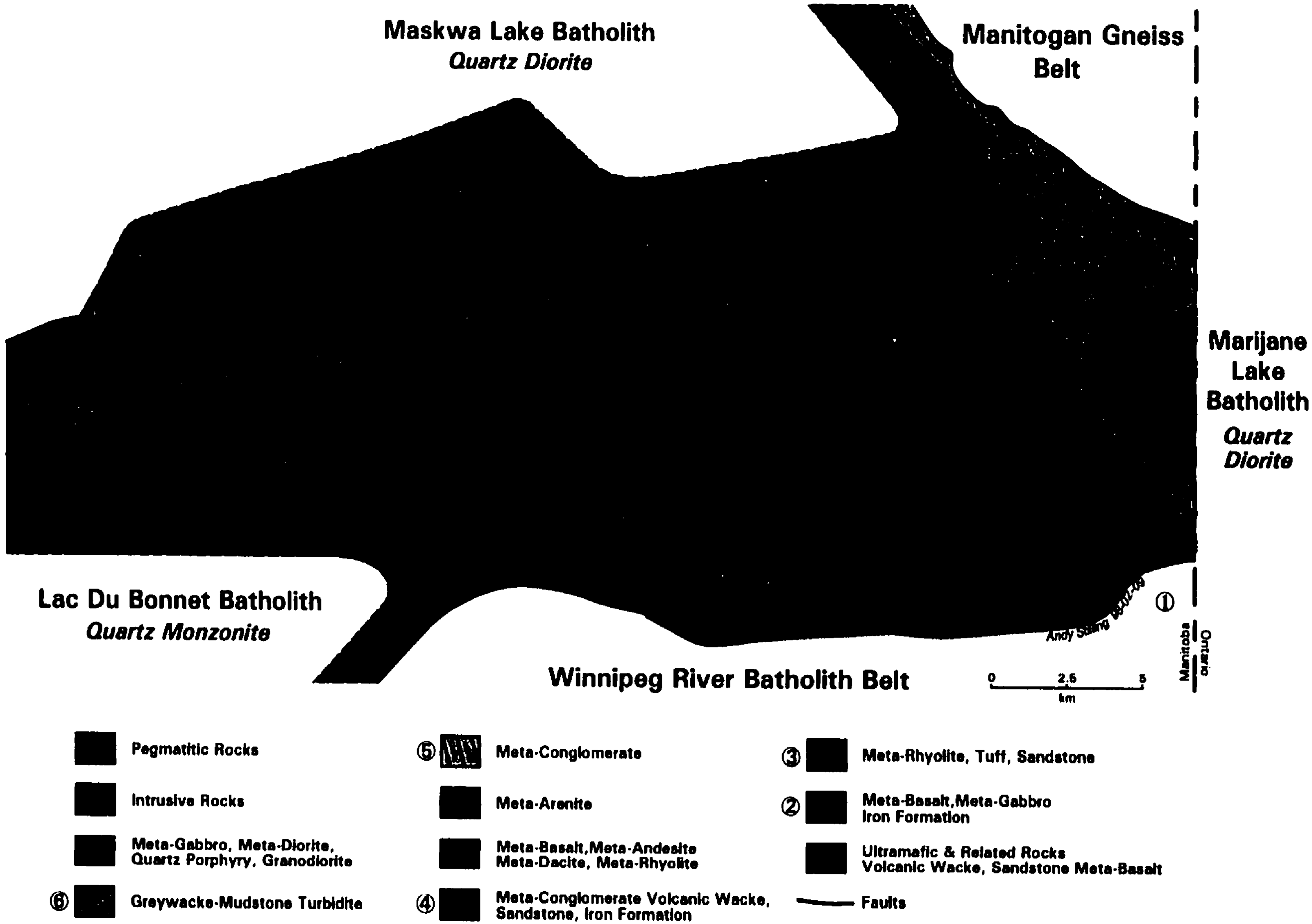

Figure 1.04 Geology of the Bird River Greenstone Belt: 1-Eaglenest Lake, 2-Lamprey Falls, 3-Peterson Creek, 4-Bernic Lake, 5-Flanders Lake, and the 6-Booster Lake formations, *Modified from Crouse et al. (1984) and Morgan & London (1987).*

6.) The Booster Lake Formation is composed of meta-greywacke-mudstone turbidites with interbedded iron formation. They are located along the core of the synclinorium, exhibit a folding event, and are fault-bounded along contacts, forming a monoclinal sequence of lower amphibolite-facies rocks.

1.4.2 Intrusive Rocks

The synvolcanic to late tectonic intrusive rocks, which flank the Bird River greenstone belt to north, east, and southwest have influenced the structural setting and metamorphic regime of the area. The diapiric intrusion of the tonalitic to granodioritic Maskwa and Marijane Lake batholiths in the north and east appears to be emplaced concurrently with the development of tectonic foliation in the layered rocks of the greenstone belt (Crouse *et al.*, 1979). The emplacement of the younger Lac du Bonnet biotite granite batholith to the south, occurred simultaneously with the regional east-west faulting of the greenstone belt. These faults are considered to have acted as the channelways for the subsequent intrusion of pegmatitic granites and pegmatites of the Winnipeg River pegmatite district (Černý *et al.* 1981, 1998).

The Tanco pegmatite is a member of the Bernic Lake pegmatite group in the Winnipeg River district of southeastern Manitoba. This group typically occurs as sheets that penetrate subhorizontal joint systems subnormal to the foliation. These systems had the best chance of opening and dilating, in low pressure shadows developed at major lithological and competency changes along an east-tending fold axis, in response to ductility differences between adjacent units (Černý *et al.* 1981).

This Bernic Lake group harbours the most fractionated and rare-element-enriched (Li, Rb, Cs, Be, Ta, Sn, P, and F) pegmatites of the whole Cat-Lake-Winnipeg River pegmatite field (Černý and Turnock, 1971). The largest of this group is the Tanco pegmatite, which shows the most advanced geochemical fractionation and enrichment. Although the parental source granite of this group does not outcrop at the surface, it is assumed to be situated under the central portion of Bernic Lake (Černý *et al.* 1981, 1998).

2 THE TANCO PEGMATITE

2.1 General Description

The Tanco pegmatite is a sub-horizontal, bilobate, saddle-shaped body which dips shallowly to the north, doubly plunging to the east and west. It is approximately 1,990 m in length, 1,060 m in width, and nearly 100 m in maximum thickness in the central regions, pinching out towards the edges. The known and potential extent of the pegmatite, shown in yellow and orange, are bounded by a heavy black zero-thickness iso-line, which is 5,120 m in circumference, enclosing an area of 855,160 m^2 (**Figure 2.01**).

3D modelling from drill holes in the outskirts of the pegmatite shows the northern contact pinching off abruptly, while the southern tip fingers out gradually in a series of four small parallel dykes. The eastern margin of the pegmatite pinches out in two sub-horizontal fingers. The upper one is abruptly terminated by a large vertical dyke, which is associated with a subvertical fault, while the lower, longer finger turns upwards as it crosscuts the fault. The western extension of the pegmatite is thin and not as well defined. 3D modelling of the hanging-wall and footwall contacts in the western half of the pegmatite show it dipping downwards from the main body at a much greater angle, practically pinching out at the solid line of the western extent, which coincides with pre-existing sub-vertical and sub-horizontal structures. It is a simple pegmatite and may be part of the main pegmatite, however, there is no direct evidence for connecting it to the main body or to determine its extent, based on the only four widely spaced drill holes with minor intersections of pegmatite. It is, therefore, marked with a dashed line in future figures or shown in orange to indicate the possible extent and is not included in the volume calculations.

The drill holes also indicate a set of similar yet simpler and smaller pegmatite dykes sub-parallel to, but below, the main pegmatite. The largest of these is referred to as Lower Tanco. These pegmatite dykes were not included in the bulk composition of the main Tanco pegmatite.

2.2 Structural Setting

The metamorphic host rocks surrounding the pegmatite form a broad anticlinorium-synclinorium pair (**Figure 2.01**). They are sub-vertically to vertically foliated, greenschist- and amphibolite-facies metagabbros and volcaniclastic metasediments, in close proximity to a synvolcanic granodiorite stock to the west (Crouse *et al.*, 1979, A.C. Turnock pers.

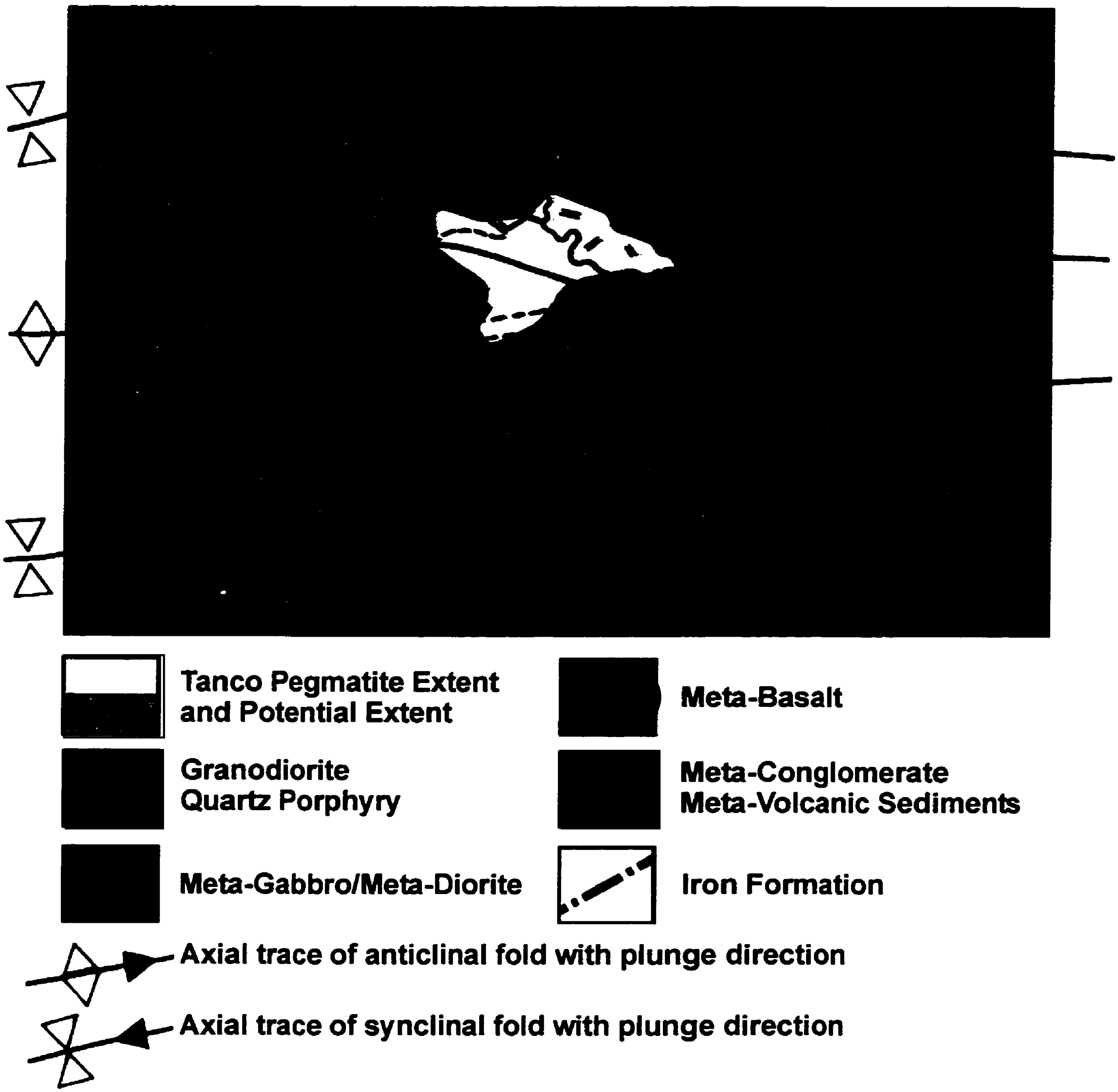

Figure 2.01 Structural and geological setting of the Tanco pegmatite at Bernic Lake, *Modified from Crouse et al. (1979).* Showing the known and potential pegmatite extents in yellow and orange.

comm. 1997). Emplacement of the pegmatite was controlled by pre-existing sub-horizontal east- and west-dipping joints, fractures, and faults that cross-cut the foliation, in a manner similar to the fractures hosting pegmatites at the eastern end of Bernic Lake and at nearby Rush Lake (Brisbin and Trueman 1982).

2.3 Internal Structure: Zoning and Mineral Assemblages

The pegmatite's nine internal zones can be distinguished by the different mineral compositions, textures, and locations within the pegmatite (**Table 2.01**). The principal internal zones are far more complex and often have transition zones between them that do not fit into the standard zoning designation scheme of assigning a zone with a single digit. Transition zones usually have two predominant assemblages and are named in order of their zonal components (*e.g.*. zone (4) and then zone (5) to make a new zone designation (4/5)). This system has been informally in use by the geologists at Tanco and is the basis of a new two digit system. It has been simplified for computer use and coding by removing the slash from the transition zone designation (45). To make the principal zones fit into the new system, zeros were added to their single digit zone numbers (*e.g.* zone (4) equals zone (40)). This zoning designation system is used at the mine and will be used to describe Tanco's zones in this thesis. Volumetrically negligible zones, such as (10) or tiny stringers of zones (30), (80), and (90), are too small to work with and their volumes and compositions were included within the dominant adjacent zones. The dominant portions of zones will be taken into account for the bulk composition calculations.

In addition to the internal zones, a halo of contact exomorphism in the mafic wall rock also exists around the pegmatite. The bulk composition of the pegmatite calculated here does not include the halo of lost volatiles (B, Li, K, Rb, Cs, and F) from the pegmatite into the host rock (Morgan and London, 1987). The calculation is concerned with the composition of the solidified pegmatite rock, not with the composition of the parent magma.

The internal zonal structure can be seen in the cross sections 9100E (**Figure 2.03**), 10200E (**Figure 2.04**), and 9700N (**Figures 2.05 & 2.06**) and in plan in **Figure 2.02**. Zones (10) and (20) generally form concentric shells within each other about the pegmatite. Zones (40) and (50), whose mutual boundaries are transitional, can also be considered shell-like when taken as a single unit. In contrast, the other zones (30, (60), (70), (80), and (90) occur

Table 2.01 Zoning of the Tanco Pegmatite.

Zones		Main Constituents	Characteristic Subordinate (Accessory) & ((Rare)) Minerals	Textural & Structural Characteristics	Geochemically Important Major & (Minor) Elements
	Exomorphic Zone	biotite, tourmaline, holmquistite	(arsenopyrite)	fine-grained reaction rims and diffuse veins	K, Li, B (P, F)
(10)	Border Zone	albite, quartz	tourmaline, apatite, (biotite), (beryl, triphylite)	fine-grained layers	Na (B, P, Be, Li)
(20)	Wall Zone	albite, quartz, muscovite, lithian muscovite, microcline-perthite	beryl, (tourmaline)	medium-grained with giant K-feldspar crystals	K, Na (Li, Be, F)
(30)	Aplitic Albite Zone	albite, quartz, (muscovite)	muscovite, Ta-oxide minerals, beryl, apatite, tourmaline, cassiterite), ((ilmenite, zircon, suphides))	fine-grained undulating layers, fracture fillings, rounded blebs, diffuse viens	Na (Be, Ta, Sn, Zr, Hf, Tl)
(40)	Lower Intermediate Zone	microcline-perthite, albite, quartz, spodumene, amblygonite	lithian-muscovite, lithiophilite, ((lepidolite, petalite, Ta-oxide minerals))	medium- to coarse-grained hetrogeneous	K, Na, Li, P, F ((Ta))
(50)	Upper Intermediate Zone	spodumene, quartz, amblygonite	microcline-perthite, pollucite, lithiophilite, (albite, lithian-muscovite), ((petalite, eucryptite, Ta-oxide minerals))	giant crystals of most major and subordinate minerals	Li, P, F (K, Na, Cs, Ta)
(60)	Central Intermediate Zone	microcline-perthite, quartz, albite, muscovite	beryl, (Ta-oxide minerals), ((zircon, ilmenite, spodumene, suphides, lithiophilite, apatite, cassiterite))	medium- to coarse-grained	K (Na, Be, Ta, Sn, Zr, Hf, Tl)
(70)	Quartz Zone	quartz	((spodumene, amblygonite))	massive, monomineralic	Si (Li)
(80)	Pollucite Zone	pollucite	quartz, spodumene, ((petalite, muscovite, lepidolite, albite, microcline, apatite))	essentially monomineralic	Cs (Li)
(90)	Lepidolite Zone	lithian muscovite, lepidolite, microcline-perthite	albite, quartz, beryl, (Ta-oxide minerals), ((zircon))	fine-grained	Li, K, Rb, F (Na, Be, Ta, Sn, Zr, Hf, Ga)

* Underlined minerals occur in economic quantities in the indicated zones.

(Source: after Černý, 1996, p.8).

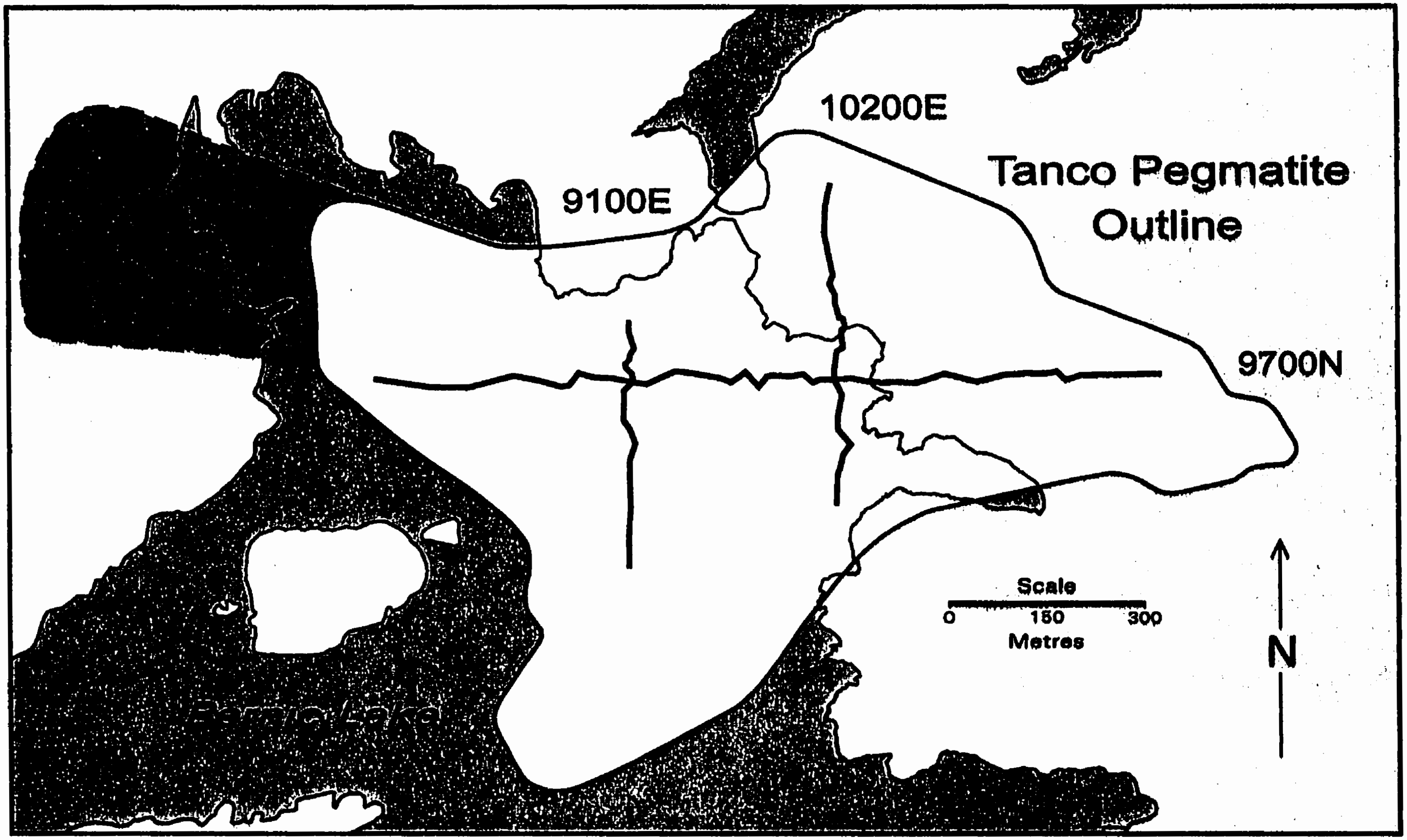

Figure 2.02 Plan view of the Tanco pegmatite - extent outline marked by a heavier solid and dashed zero iso-line. The heaviest black lines in the centre of the isopach map represent three profiles on sections 9100E in Figure 2.03, 10200E in Figure 2.04, and 9700N in Figure 2.05 and 2.06.

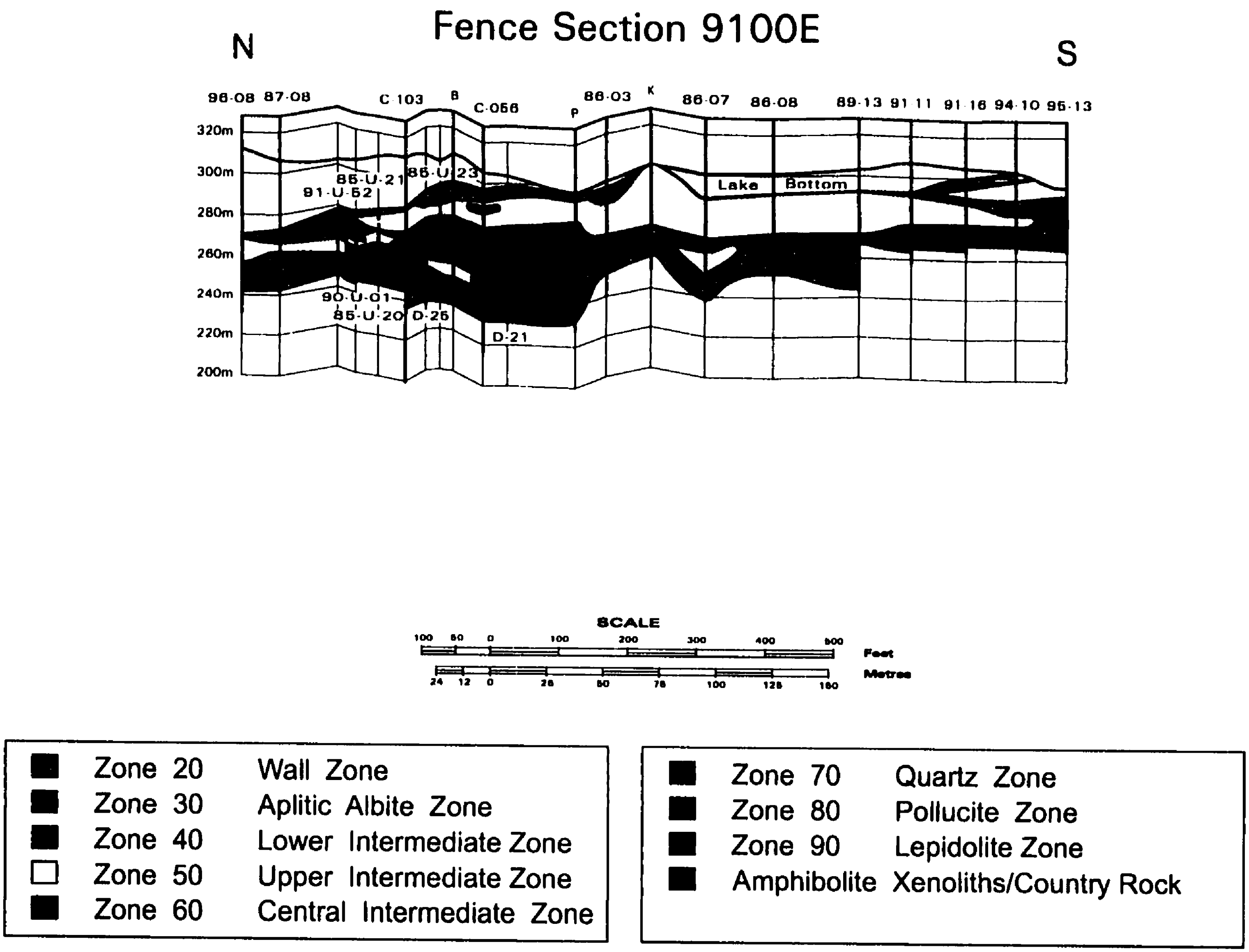

Figure 2.03 N-S fence section 9100E through the Tanco pegmatite looking east; see Figure 2.02 for location in plan view.

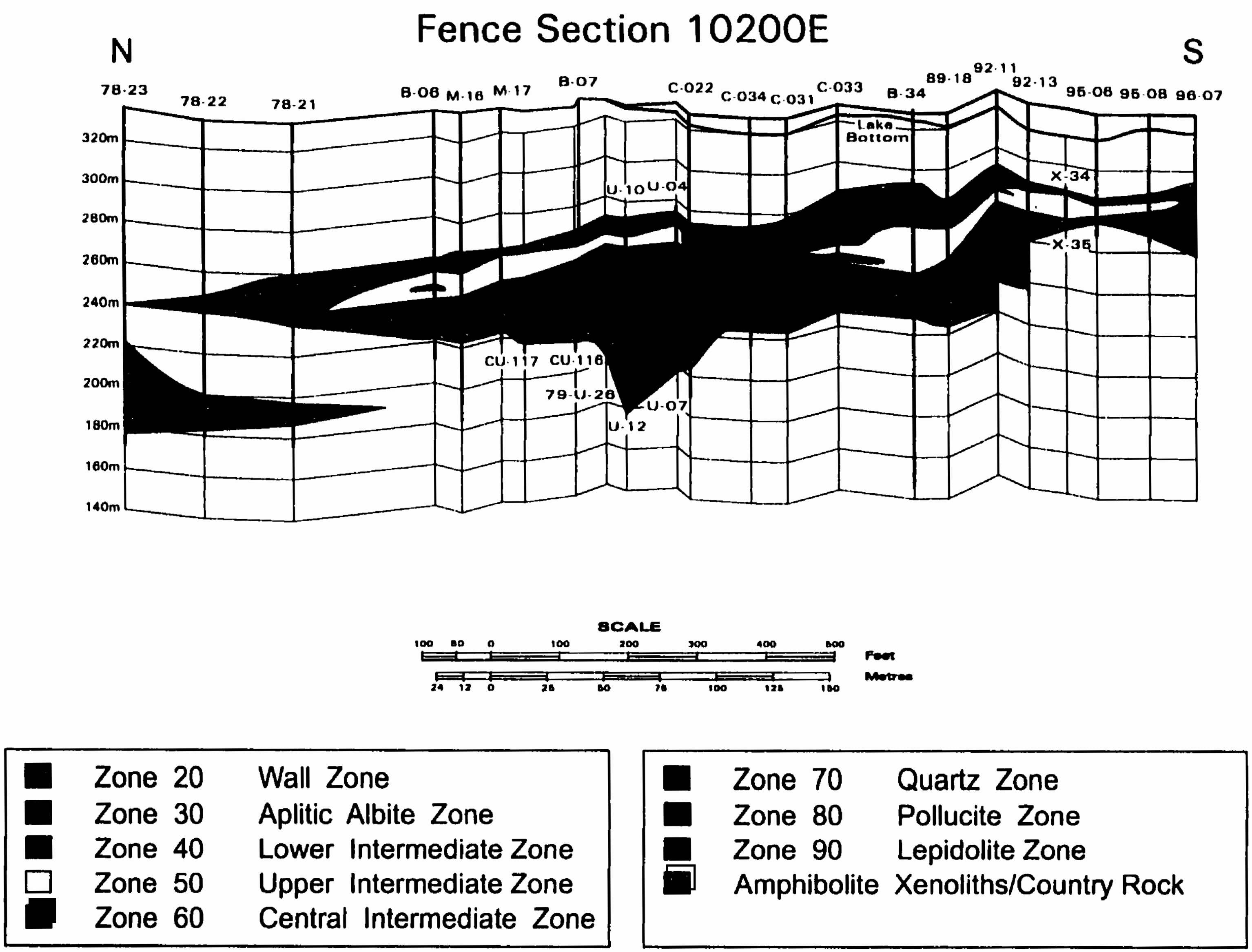

Figure 2.04 N-S fence section 10200E through the Tanco pegmatite looking east; see Figure 2.02 for location in plan view.

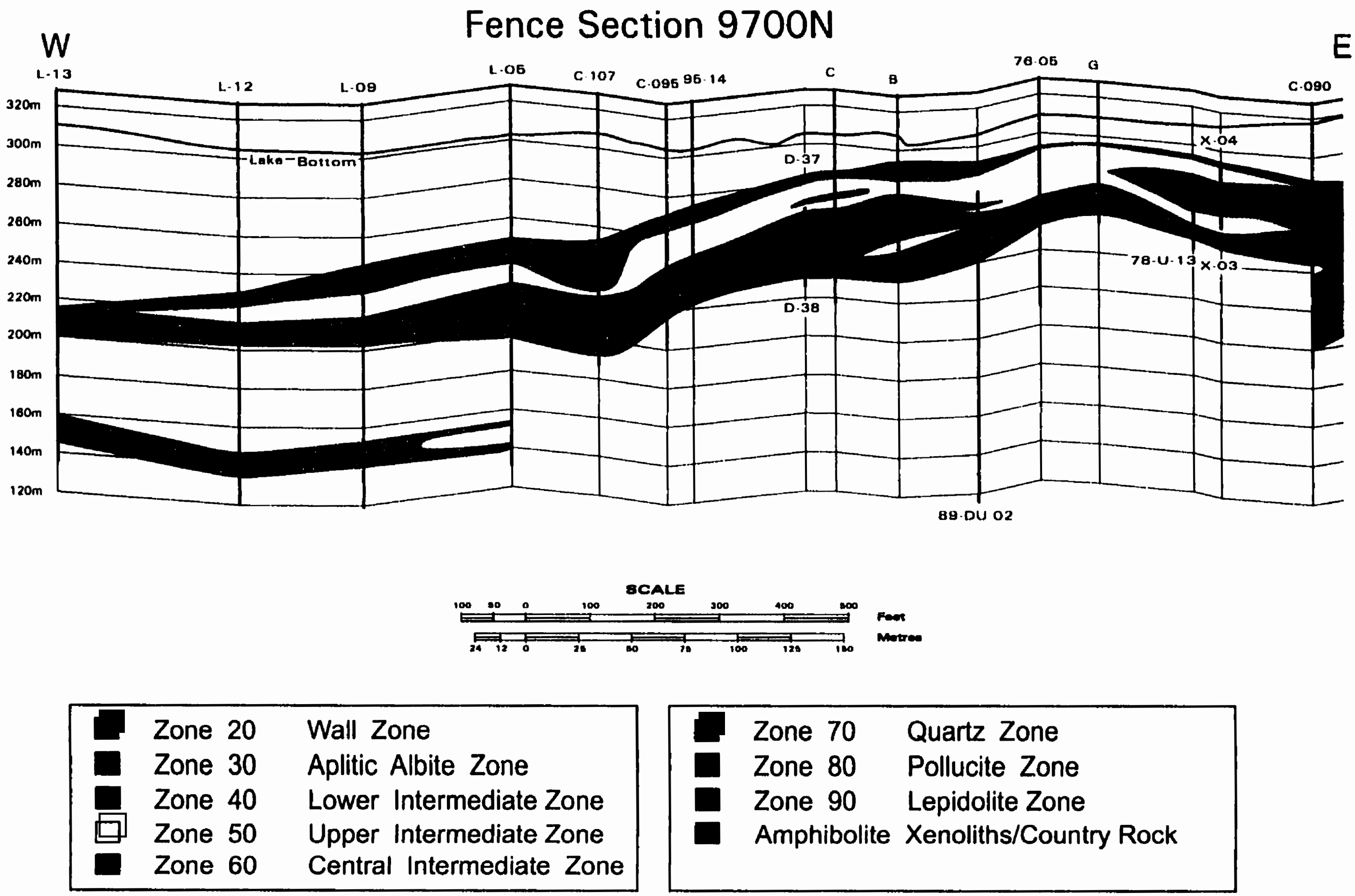

Figure 2.05 Western half of E-W fence section 9700N through the Tanco pegmatite looking north; see Figure 2.02 for location of the sections in plan view. Continued in Figure 2.06.

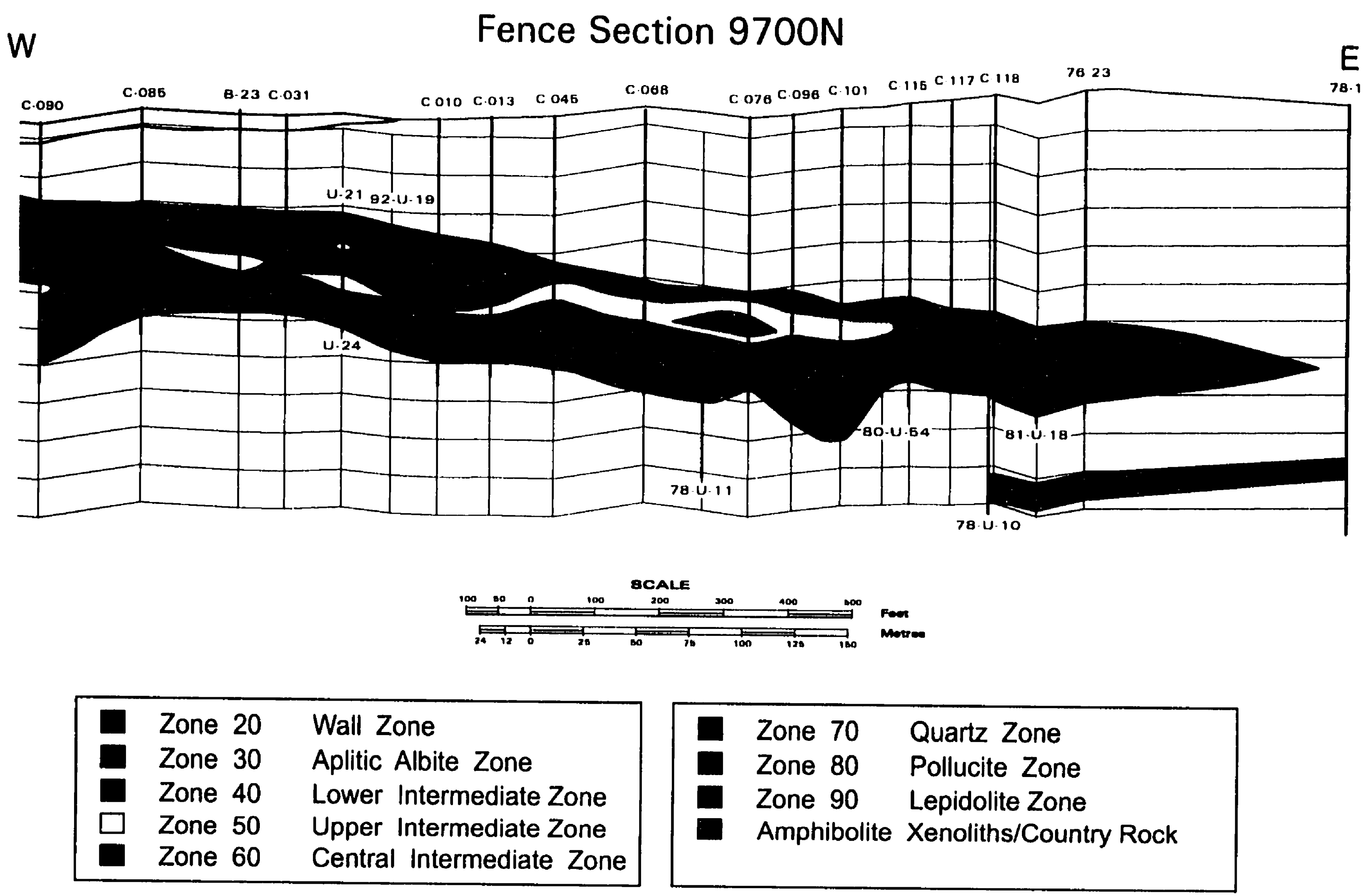

Figure 2.06 Eastern half of E-W fence section 9700N through the Tanco pegmatite looking north; see Figure 2.02 for location of the sections in plan view.

as discontinuous layers or pods within the pegmatite's central upper portion and in the eastern and western lobes (Crouse and Černý, 1972; Crouse *et al.*, 1979, 1984; Černý *et al.*, 1998).

Along the strike and dip of the pegmatite, there is a distinct display of symmetry. At the central crest of the pegmatite, most of its thickness is occupied by the Li-rich zones (40) and (50). These two are separated in both flanks by the intervening zone (60), overlain by quartz (70) and pollucite (80) bodies. Most of the segments of the lepidolite zone (90) occur within and just above the two segments of zone (60), in part transitional into this zone. The aplitic albite zone (30) follows the contacts of quartz core (70) with adjacent zones, and it penetrates particularly the zones (20) and (60). However, late stringers of albite which crosscut and replace most of the primary zones on small local scale, are not necessarily connected with the aplitic albite (30), and are not shown on the diagrams (Černý *et al.*, 1998).

Textural and paragenetic features strongly suggest that the majority of all nine zones were produced by primary crystallization from a liquid/fluid phase. However, zones (10), (30), and in part (90), also show metasomatic relationships with adjacent zones, and small-scale plus very low-volume replacements can be seen within each of the zones (40) to (90) (Černý *et al.*, 1998).

2.3.1 Zone (10): Border Zone

The border zone is the boundary between the host wall rock and the pegmatite. It is usually sharp and ranges from millimetres to 30 centimetres. This zone forms an intermittent concentric shell of very fine grained albite and quartz with biotite, muscovite, apatite, beryl and tourmaline as the common accessory minerals around the entire pegmatite. Tourmaline and beryl crystals up to 20 cm can be found oriented approximately perpendicular to the contact and appear to have grown inwards from the contact. This zone can also be found as a reaction rim around the amphibolite xenoliths in the pegmatite. It is not shown in any of the diagrams, as it is too thin to show up at the scale utilized, and for bulk compositions purposes it has been included in zone (20) as most of the drill logs have not recorded this zone.

2.3.2 Zone (20): Wall Zone

The wall zone, the next inner-most concentric zone is the first majour mineral assemblage of the pegmatite. It consists of albite, quartz, microcline-perthite, muscovite, and lithian muscovite with apatite, beryl and tourmaline as common accessory minerals. Grain size generally increases inwards where large columnar microcline-perthite (up to 3 m) occurs in a matrix of quartz, medium-grained albite (30 cm), and tabular greenish muscovite books (10 cm). Other traits of the zone include columnar curvilarmellar lithian muscovite, columnar tourmaline (20 cm), local metasomatic alteration features, and a generalized colour change from reddish/pinkish to beige/white microcline-perthite in zone (40). The thickness of the zone varies throughout, but is generally thicker on the footwall of pegmatite, reaching a maximum thickness of 38 m in the footwall depression pits.

2.3.3 <u>Zone (30): Aplitic Albite Zone</u>

The aplitic albite zone (30) forms rolling sheet-like layers up to 16 m in thickness, as well as smaller ragged discontinuous lenses in the eastern flank of the pegmatite, where they reside along the contacts of the wall zone (20) with the overlying zones (60) and (70), or grading into zone (60). In the western part of the pegmatite, zone (30) is dispersed as a network within zone (60) and its contacts with zone (20) and (40); continuous and texturally well-defined layered sequences typical of the eastern part of the pegmatite are much less in evidence (Černý *et al.*, 1998). Zone (30) primarily consists of bluish, greenish, and purplish banded saccharoidal albite and is only rarely medium-grained in texture, whereas cleavelandite is uncommon and only exceptionally in contact with the saccharoidal aggregates. It also contains minor quantities of smoky quartz with traces of tourmaline, apatite, lithian muscovite, and spodumene. This zone is also one of the primary producers of Ta and Nb oxide mineralization, along with minor amounts of Be, Sn, Zr, and Hf.

2.3.4 <u>Zone (40): Lower Intermediate Zone</u>

The lower intermediate zone, located mainly in the lower and central portions of the pegmatite is the next innermost adjacent to zone (20). The main constituents are microcline-perthite, albite, quartz, spodumene, and amblygonite-montebrasite with lithian muscovite and lithiophilite as the minor accessory minerals. Lepidolite, petalite, and tantalum oxides are the trace minerals. The zone is a heterogeneous assembly of minerals and assemblages that lack compositional uniformity, exhibiting two texturally characteristic assemblages: (a) Large crystals of pinkish-grey microcline-perthite and spodumene/quartz pseudomorphs after petalite (up to 2 m) embedded in a medium grained quartz, albite, mica matrix and (b) quartz pods (0.5 to 2 m) with amblygonite-montebrasite and spodumene/quartz aggregates; radial rims of cleavelandite and micas usually separate the feldspar-rich assemblages from the quartz accumulations (Crouse and Černý, 1972). This zone is readily distinguished by the absence of tourmaline and beige/white microcline-perthite.

2.3.5 Zone (50): Upper Intermediate Zone

The upper intermediate zone, located mainly in the upper portion of the pegmatite is commonly adjacent to the hanging wall zone (20). It gradually evolves from the lower zone (40) upwards through a gradational transition designated (45), compositionally a mixture of the two zones. If zone (40) and zone (50) were considered as one unit, they would make the next innermost shell-like zone in the pegmatite. Zone (50) consists of chiefly of spodumene/quartz pseudomorphs after petalite, petalite, amblygonite, and quartz with minor amounts of lithian muscovite, microcline-perthite, apatite, lithiophilite, and pollucite. This zone is characterized by gigantic crystals of amblygonite (at least 2 m), microcline-perthite (at least 7 m), and petalite (at least 13 m). There are also rare miarolitic cavities, locally abundant leaching vugs filled with low temperature mineral assemblages, and an almost total disappearance of albite and mica as one moves up through the zone. This zone is the primary producer of anhydrous lithium silicate minerals in the Tanco pegmatite.

2.3.6 Zone (60): Central Intermediate Zone

The central intermediate zone, also known as the MQM (microcline, quartz, and mica assemblage), occupies a large portion of the central eastern and western flanks of the pegmatite, inside a concentric shell of zones (40) and (50), which more or less approximates the shape of the pegmatite. Contacts between zone (60) and adjacent zones are often sharp, or transitional over a couple of metres, which contrasts with the gradational boundaries of many other zones (*e.g.* zones (40) and (50)). The majour components are microcline-perthite, quartz, and albite with minor amounts of lithian muscovite, and trace amounts of beryl, spodumene, wodginite, cassiterite, microlite, tantalite, apatite, lithiophilite, and tapiolite. Within the zone there appear three texturally characteristic assemblages: (a) medium- to coarse-grained microcline-perthite, with minor quartz, beryl, spodumene, and albite, penetrated by fine grained greenish muscovite with tantalum oxides and cassiterite, (b) rounded patches and "waves" of bluish aplitic albite with disseminated tantalum oxides and cassiterite, and (c) grey to smoky quartz, with white and pinkish beryl accumulated along its contacts with feldspar-rich assemblages. The first assemblage is pervasive and forms a matrix in which the other two are regularly distributed with abundant, beryl-enriched quartz pods in the upper part of the zone (Crouse and Černý, 1972). This zone is one of the primary producers of tantalum and niobium oxide minerals in the pegmatite.

2.3.7 Zone (70): Quartz Zone

The quartz zone does not form a true central core, unlike its usual form in other pegmatites. It forms several lens-shaped bodies asymmetrically and predominantly upwardly placed throughout the pegmatite. The zone is predominantly monomineralic, massive, white to faintly rose-coloured quartz with minor amounts of amblygonite-montebrasite, microcline-perthite, apatite, lithiophilite, spodumene, and pollucite, dependent on the neighbouring zones.

2.3.8 Zone (80): Pollucite Zone

The pollucite zone, although petrologically related to the spodumene zone (50), which contains numerous small inclusions of pollucite, is descriptively treated as separate zone because the dimensions of some pollucite bodies are large. In the western half of the pegmatite, several small pollucite blebs (up to 61 x 50 x 5 m) are elongated and parallel to the strike of the pegmatite, whereas in the eastern half there is only one large ore body called the Main Pollucite Zone (180 x 75 x 12 m). Pollucite (80) is mainly located along the upper contacts of zone 50 between the hanging wall portion of zone (20) and (10). This zone is almost entirely composed of monomineralic pollucite, with coarse veining of fine-grained lepidolite, quartz, and feldspar in most of its volume.

2.3.9 Zone (90): Lepidolite Zone

The lepidolite zone is a generic name given to this zone, which contains lithian muscovite as the main constituent. True lepidolite is less common in the pegmatite in general, and in this zone in particular. The two main bodies of this zone form flat-lying, elongated, E - W sheets up to 18 m thick, with several smaller bodies within the central intermediate zone (60) or along its contacts with spodumene-rich zones (40) and (50). Both micas are fine-grained and commonly intergrown with microcline-perthite and quartz along these contacts.

3 METHODOLOGY OF VOLUMETRIC CALCULATIONS

3.1 Data Collection and Storage

The collection of data for this project has been a involved and time-consuming process. Most of the maps and drill core logs generated at Tanco during the past 43 years have been recorded on paper. Only recently, in the last couple of years, have they been stored digitally. Upon starting this project, none of this information was available to the author in digital format. In order to build a computer model of the pegmatite, all the required maps were digitized from the original paper copies on a Calcomp digitizer and then stored in AutoCAD 12 drawing files. In total 1,355 surface and underground drill holes (**Figures 3.01 & 3.02**) with cores logs were coded in a standardized format and manually entered over the course of two years into set of Lotus spreadsheets and DBase databases.

This task was complicated, as over the course of 43 years, the drilling was done for different minerals and by different personel. With the guidance and expertise of the Tanco personel, the extremely time consuming task of re-interpreting drill logs was made easier. Comparisons of independent assessments show that the author's zonal interpretations were in close agreement to those of the mine geologists'. The focus on lumping, for mining purposes, versus that on splitting, for detailed modelling, accounted for interpretational differences.

Given the scale and difficulty in interpreting, authenticating, and revising large geological databases, such as the one constructed from Tanco's maps and core logs, the development of a well designed data storage and retrieval system was necessary. To increase the rate of data entry and to eliminate the possibility of incorrectly typed data, spreadsheets were designed with built-in data prompting, code checking, and automatic error-flagging routines. Once the spreadsheets were setup, databases were constructed to organize and compile all the co-ordinate and core-log spreadsheets into related database files. Over time the they were re-compiled to correct errors and to add new data. Whenever this was done, the compilation program cross-checked the databases looking for inconsistency, as it merged the data for the model-building programs.

3.2 Model Construction

The bulk of the 3D pegmatite model was produced and designed in AutoCAD 12 with custom-written basic programs. They accessed user-defined lists of drill holes from a databases or a spreadsheets to extract their information from the main compiled databases, when building

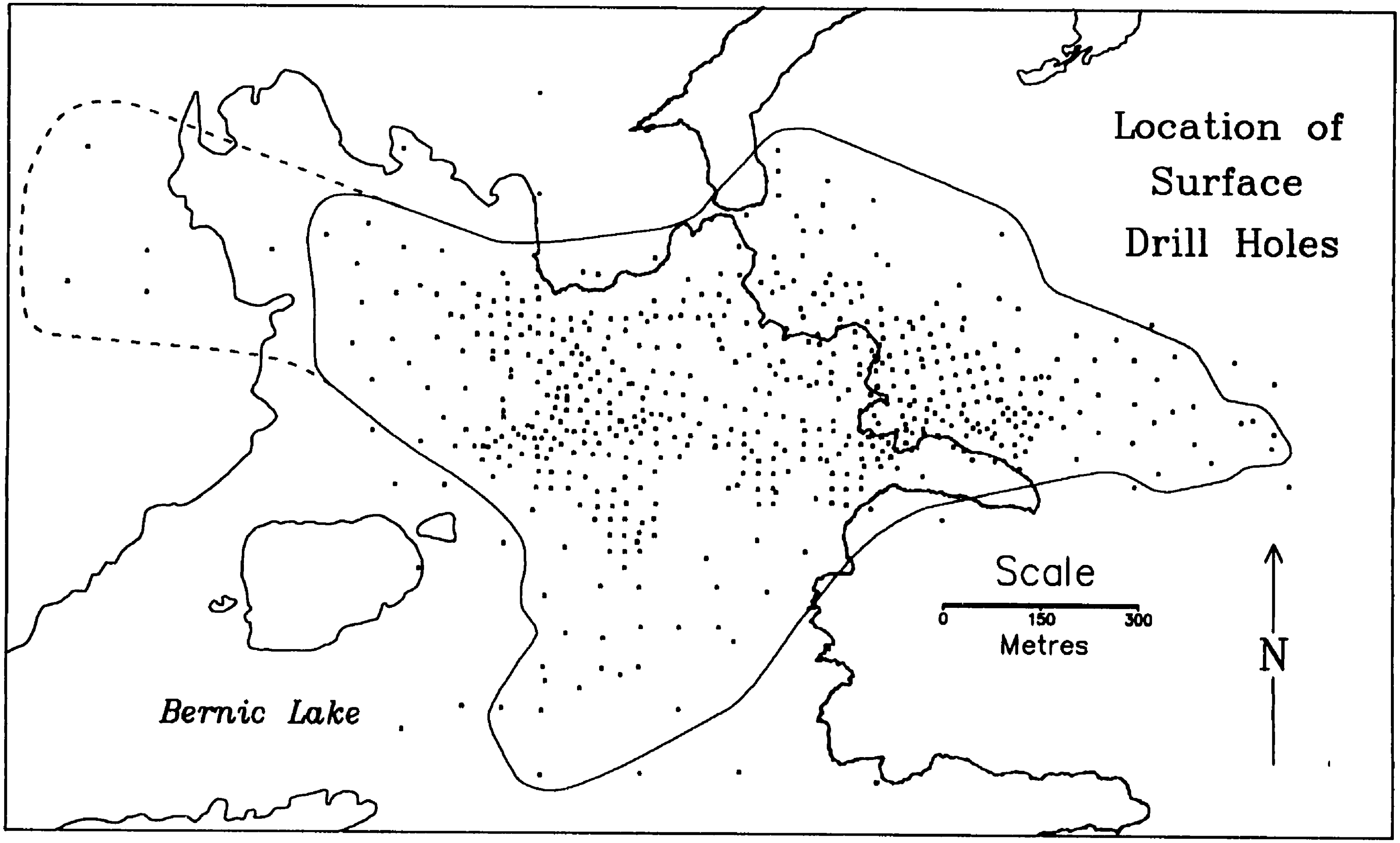

Figure 3.01 Plan view of the Tanco pegmatite showing the location of 583 surface drill holes.

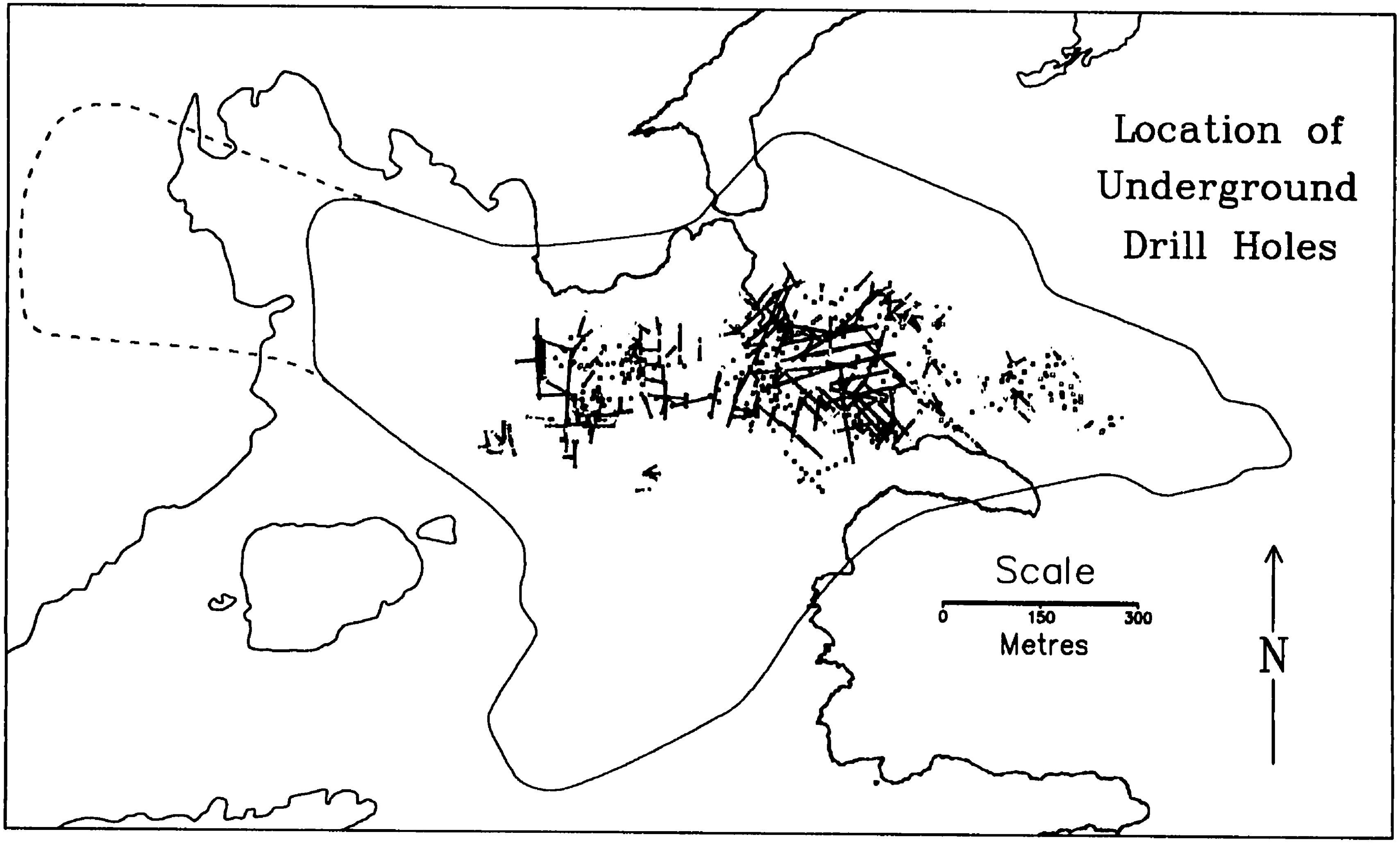

Figure 3.02 Plan view of the Tanco pegmatite showing the location of 736 underground drill holes.

sections, surfaces, or block models. When a segment of the drill hole model was built, it was examined using animated or real time viewing, sectioning, and fly-throughs to visualize the internal structures and relationships within the pegmatite. This allowed one to get inside the pegmatite model to visually spot potential problems and to debug complex geological situations in 3D.

3.3 Volumetric Calculations for Individual Zones

Once the basic structure of the model was built, calculating the volumes for individual zones and for the pegmatite was done by constructing hundreds to thousands of individual **TIN**'s (Triangulated Irregular Network) and **TGRN**'s (Triangularly Gridded Regular Network) trapezoid surfaces between drill holes at drill-core intersections of the hanging-wall and footwall contacts of each zone or body. As an example, **Figure 3.03** shows the western end of the pegmatite's hanging-wall and footwall TIN surface contacts. In the centre of the figure is a green hi-lighted region. This region is shown in **Figure 3.04**, as an example of the drill-core intersections with TIN surfaces for each zone. These surfaces were drawn in three-dimensional CAD space using Auto Miner (a mining software package) and Schreiber's Quick Surf (a surface construction and volume software package), using the Matrox Graphics real-time tools. The resulting block volume trapezoid (**Figure 3.05**) shows the individual zones, which are calculated using Simpson's Trapezoid rule (Press *et al.*, 1992). The individual zone volume components for every TIN in this case are then added up to get the total zone volumes for the entire pegmatite (**Table 3.01**). As each zone in the block uses and shares the same TIN surfaces, the resulting total of all zone volumes is the same as the overall pegmatite volume, unless a zone trapezoid has been missed. Once the zone volumes were totalled, the results were checked against the pegmatite volume calculated from the pegmatite/wallrock contacts minus the amphibolite xenoliths volumes, and the two numbers were found to be identical.

Initially, surfaces were created with TIN's, which are good for flat surfaces with few points or for densely populated surfaces; however, if the surface was complex and distorted, TGRN's were used as they approximate such surfaces closer. Essentially, the denser the grid, the better the approximation to the surface, however, this is offset by exponentially increasing file sizes. Grid sizes from 5 feet (1.52 m) to 50 feet (15.24 m) were tried to optimize file size and reported volumes. File size manageability and volume accuracy converged around the 20 foot (6.09 m) grid size, which was subsequently used for the grid volume calculations.

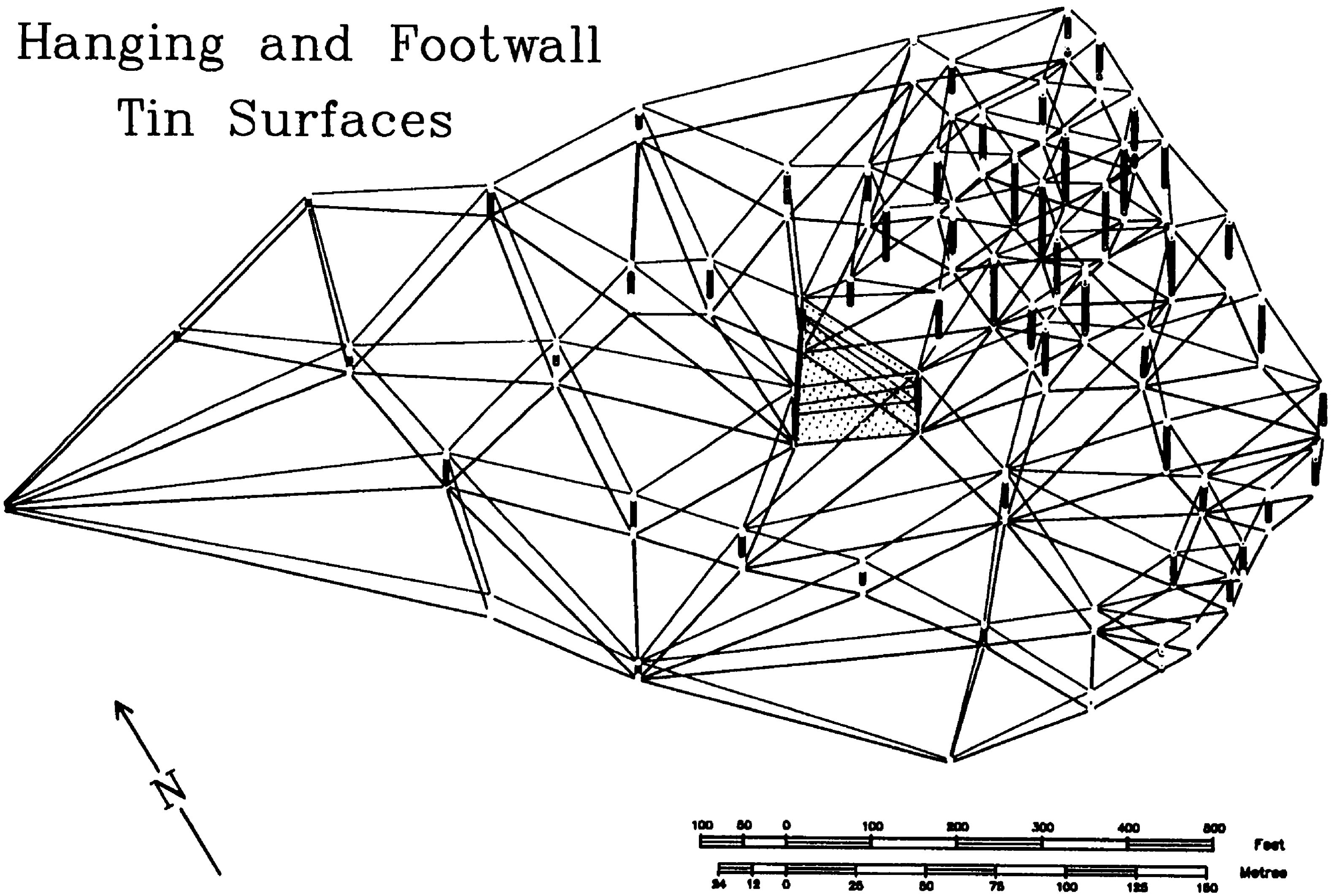

Figure 3.03 TIN surfaces for calculating the volume of the western end of the Tanco pegmatite. Red lines represent the hanging-wall and blue lines the footwall TIN surfaces. Vertical thick lines are the drill-hole intersections of the pegmatite. The green hi-lighted area in the centre is the volume block trapezoid of figures 3.04 & 3.05.

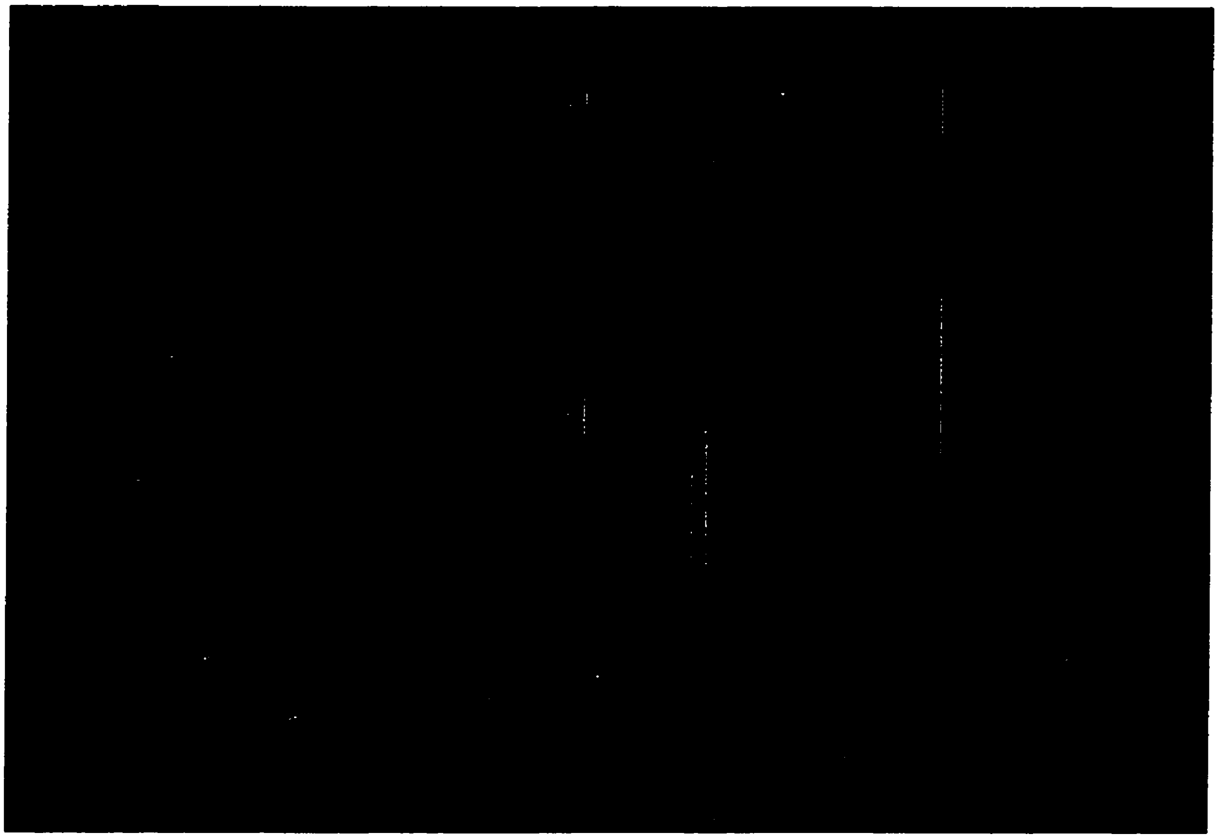

Figure 3.04 Construction of TIN zone surfaces for volume calculation. Vertical lines are the drill holes. Triangles are the zone surfaces attached to the drill holes at the zone and wall rock contacts. Yellow represents zone 20, orange zone 40, and red zone 70. View perspective is looking from above to the north.

Table 3.01 Individual Zone and Total Zone Volumes

Pegmatite Zones	Volumes (ft^3)	Volumes (m^3)	Volumes (km^3)	Volume Percentage
Zone(10)	332,093	9,404	9.40e-06	0.10%
Zone (20)	102,497,721	2,902,413	0.0029	30.83%
Zone (30)	8,935,717	253,031	0.0003	2.69%
Zone (40)	95,690,376	2,709,650	0.0027	28.79%
Zone (50)	43,627,916	1,235,405	0.0012	13.12%
Zone (60)	45,073,066	1,276,327	0.0013	13.56%
Zone (70)	24,820,161	702,829	0.0007	7.47%
Zone (80)	4,423,243	125,252	0.0001	1.33%
Zone (90)	7,024,799	198,920	0.0002	2.11%
Totals	332,425,093	9,413,231	0.0094	100.00%

Given the size of the pegmatite and the viewing perspectives on thin zones, the density of the surface grid lines makes it impossible to display individual zones at a reasonable scale as they show up as indistinguishable solid objects. Instead, data points and isopachs of the individual zones have been used to show the shape and size of the individual zones. The following isopachs were calculated using the vertical distance between the hanging and footwall surfaces created from drill-core zone boundary intersection; they do not represent true thickness even though the pegmatite is almost horizontal. The scales used in the legend of each zone are not identical and were chosen to be proportional to their respective zones. They were done this way to maximize the resolution of the smallest zones.

The border zone (10) was not calculated for reasons explained in the treatment of internal structures in the first paragraph of **Section 2.3** on page 11.

3.3.1 Zone (20): Wall Zone

The wall zone is easily distinguished from other zones in the pegmatite and is recorded in the core logs fairly well. It usually occurs at the contact of the pegmatite and forms the first, outermost, shell which surrounds everything inside the pegmatite. Zone (20) was intersected by 805 drill holes over the known area of the pegmatite 713,106 m^2 (**Figure 3.06**), averaging 1 drill hole per 885 m^2. The zone comprises 30.83% of the pegmatite by volume.

3.3.2 Zone (30): Aplitic Albite Zone

The aplitic albite zone is limited in volume and in extent throughout the pegmatite. Its interpretation has not been consistent throughout the years, and it is was locally combined

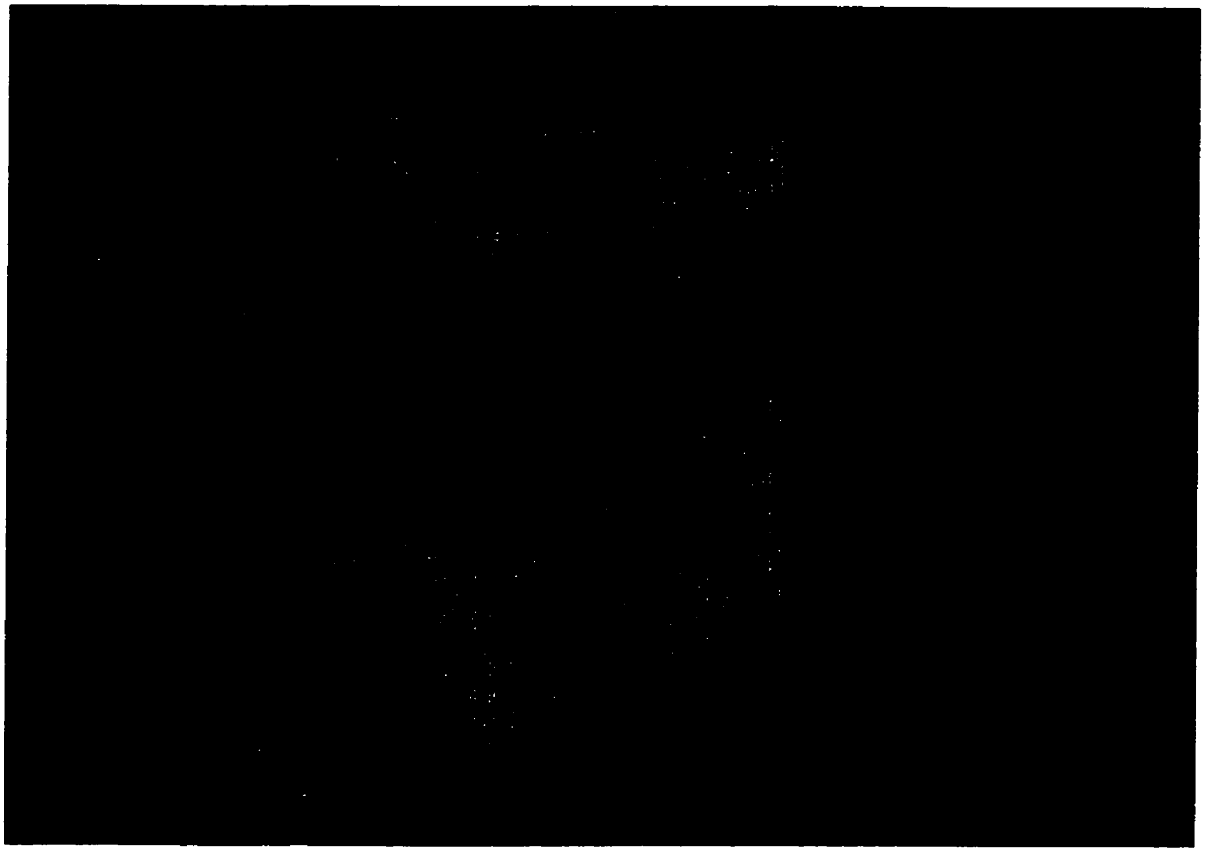

Figure 3.05 Volume block trapezoid shows individual zones, which are calculated using Simpson's trapezoid rule. Yellow represents zone 20, orange zone 40, and red zone 70. View perspective is looking from above to the north.

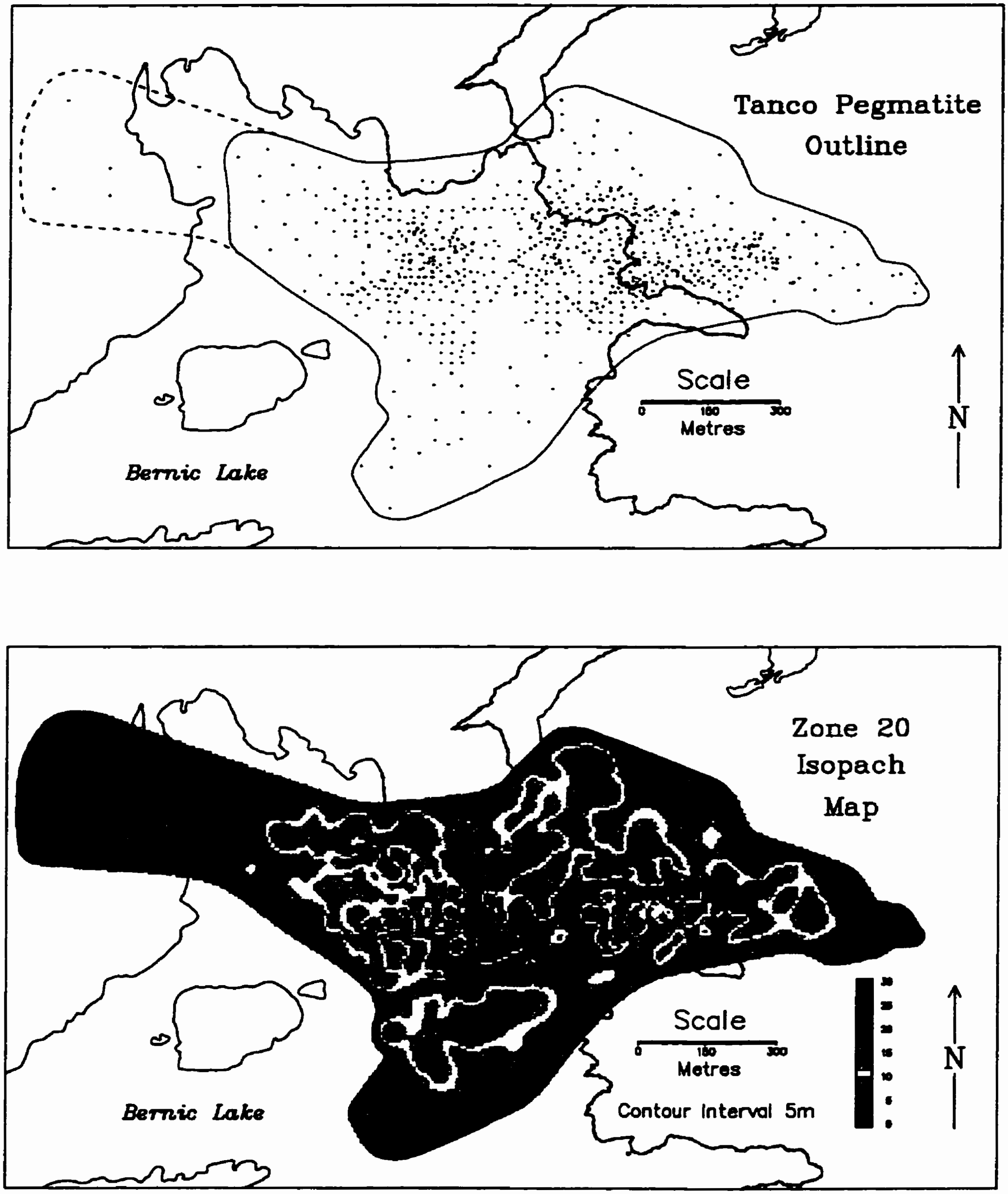

Figure 3.06 Plan view (top) showing drill hole intersections of the zone used to construct the zone 20 isopach map (bottom).

with zone (60). In the present study it was split out of the logs on the basis of high Ta and Sn values and matching mineralogy. Zone (30) was intersected by 121 drill holes over an area of 233,500 m^2 (**Figure 3.07**), averaging 1 drill hole per 1929 m^2. The zone comprises 2.69% of the pegmatite by volume.

3.3.3 Zone (40): Lower Intermediate Zone

The lower intermediate zone, an aggregation of four mineral assemblages, was generally well logged. In a few cases, entire holes were logged as zone (40), even though they may have contained other zones. These holes were sorted out in the present study and split based on their mineralogy, their assays, and their fit into the 3D modeled surfaces. Zone (40) was intersected by 683 drill holes over an area of 528,700 m^2 (**Figure 3.08**), averaging 1 drill hole per 774 m^2. The zone comprises 28.79% of the pegmatite by volume.

3.3.4 Zone (50): Upper Intermediate Zone

The upper intermediate zone has been recorded consistently over the years and is easily identified underground, in drill cores, and from the assays. The zone compliments zone (40) in the upper part of the pegmatite and in part surrounds zone (80). Zone (50) was intersected by 409 drill holes over an area of 395,800 m^2 (**Figure 3.09**), averaging 1 drill hole per 967 m^2. The zone comprises 13.12% of the pegmatite by volume.

3.3.5 Zone (60): Central Intermediate Zone

The central intermediate zone in combination with its rock-forming mineral asseblages has generally been logged well, but was locally combined with zone (40) and confused with zone (30). However, in the present study it was identified and traced from assays, as it is one of the two mineable tantalum ore zones. Zone (60) was intersected by 344 drill holes over an area of 201,000 m^2 (**Figure 3.10**), averaging 1 drill hole per 584 m^2. The zone comprises 13.56% of the pegmatite by volume.

3.3.6 Zone (70): Quartz Zone

The quartz zone is well understood due to its monomineralic nature. It tends to form long thin bodies in the eastern half of the pegmatite, and in the core. Zone (70) was intersected by 286 drill holes over an area of 211,000 m^2 (**Figure 3.11**), averaging 1 drill hole per 737 m^2. The zone comprises 7.47% of the pegmatite by volume.

3.3.7 Zone (80): Pollucite Zone

The pollucite zone is small in total volume, but tends to form a few individual large bodies and many small blebs. The main bodies are volumentrically well defined, whereas the smaller

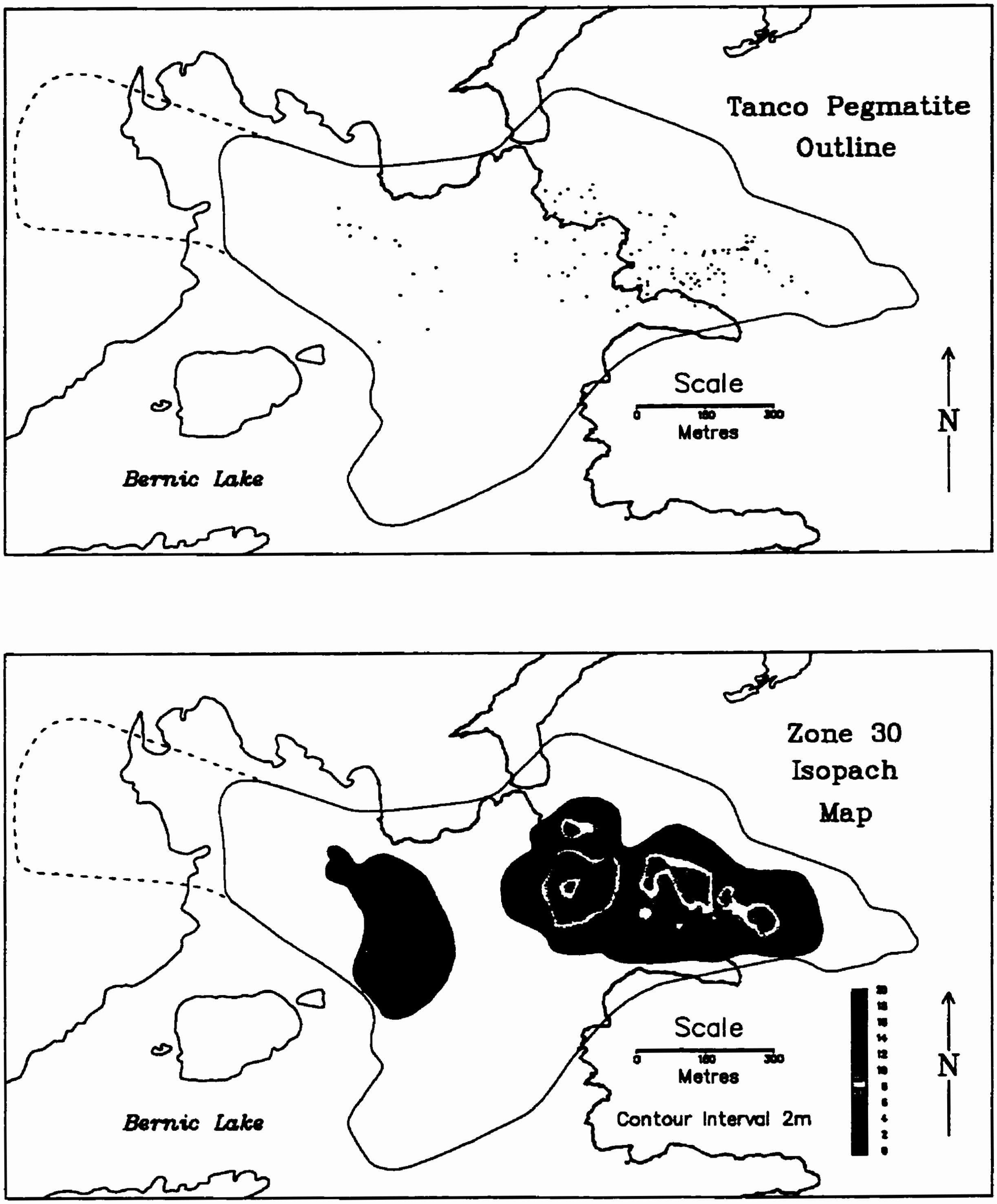

Figure 3.07 Plan view (top) showing drill hole intersections of the zone used to construct the zone 30 isopach map (bottom).

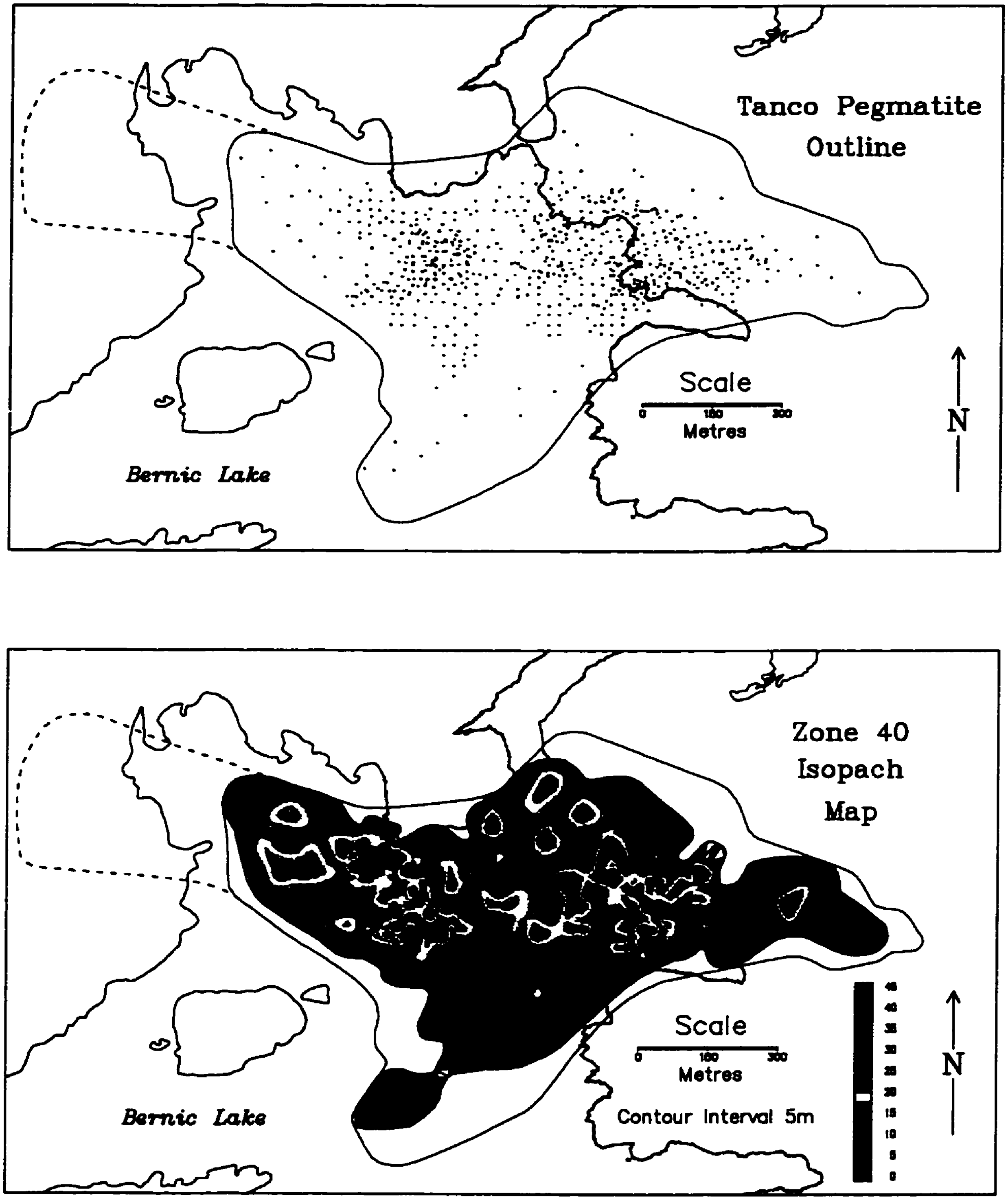

Figure 3.08 Plan view (top) showing drill hole intersections of the zone used to construct the zone 40 isopach map (bottom).

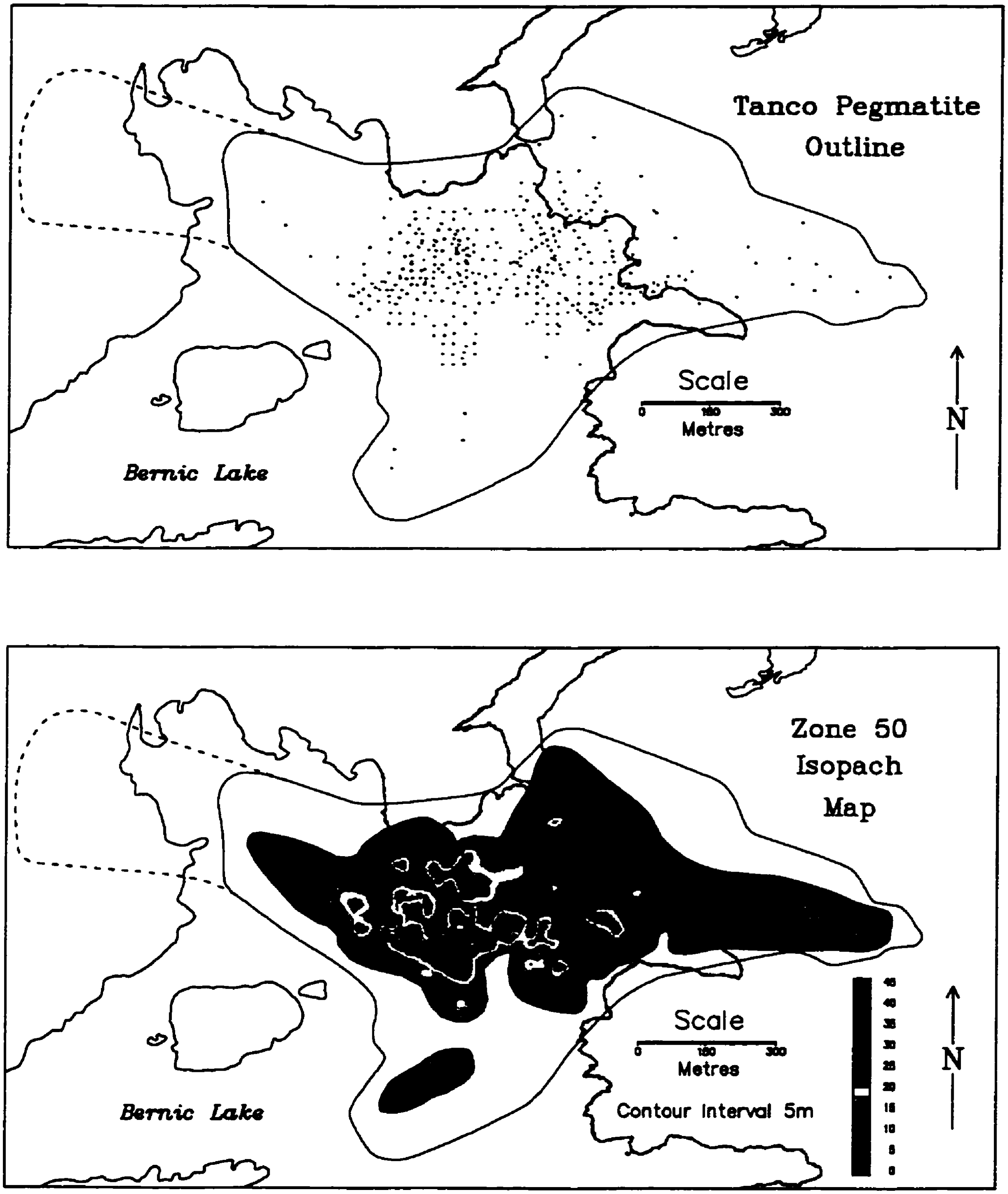

Figure 3.09 Plan view (top) showing drill hole intersections of the zone used to construct the zone 50 isopach map (bottom).

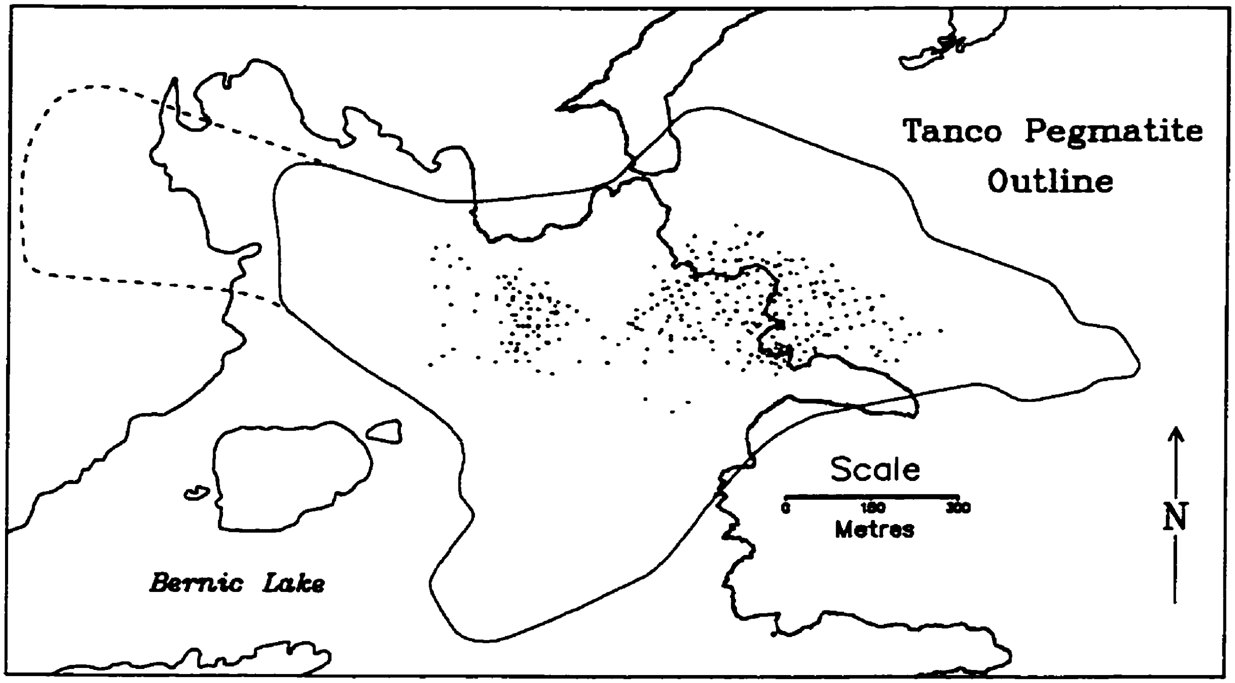

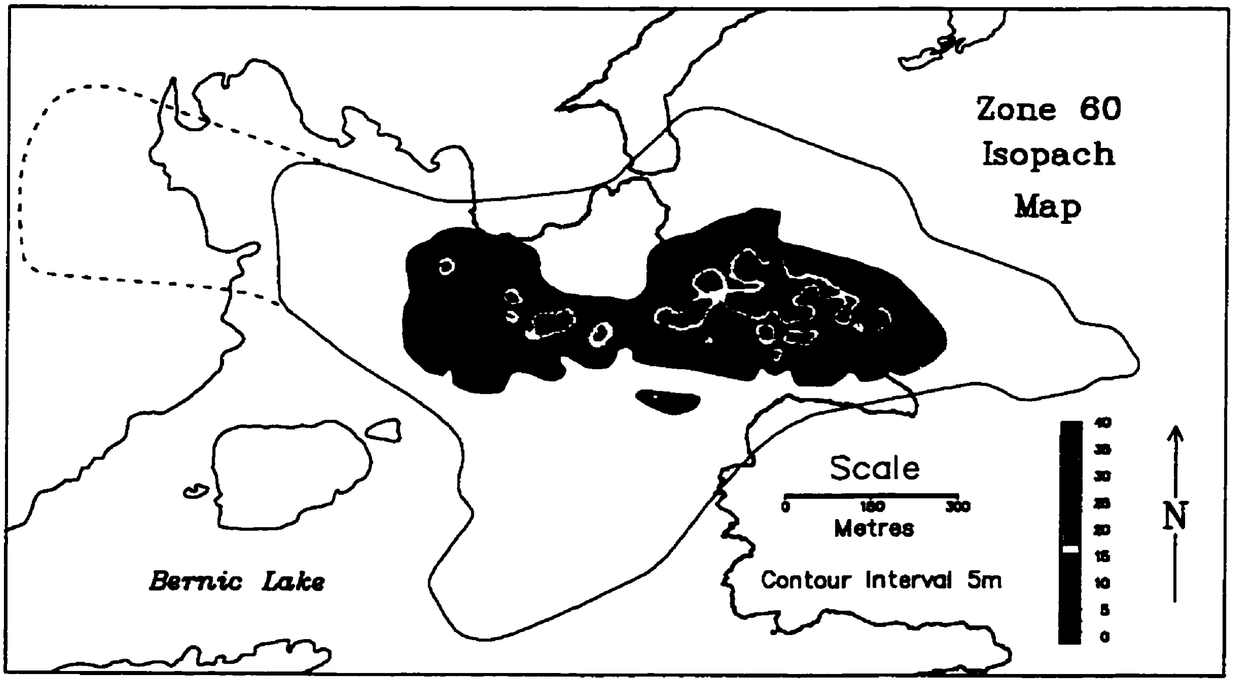

Figure 3.10 Plan view (top) showing drill hole intersections of the zone used to construct the zone 60 isopach map (bottom).

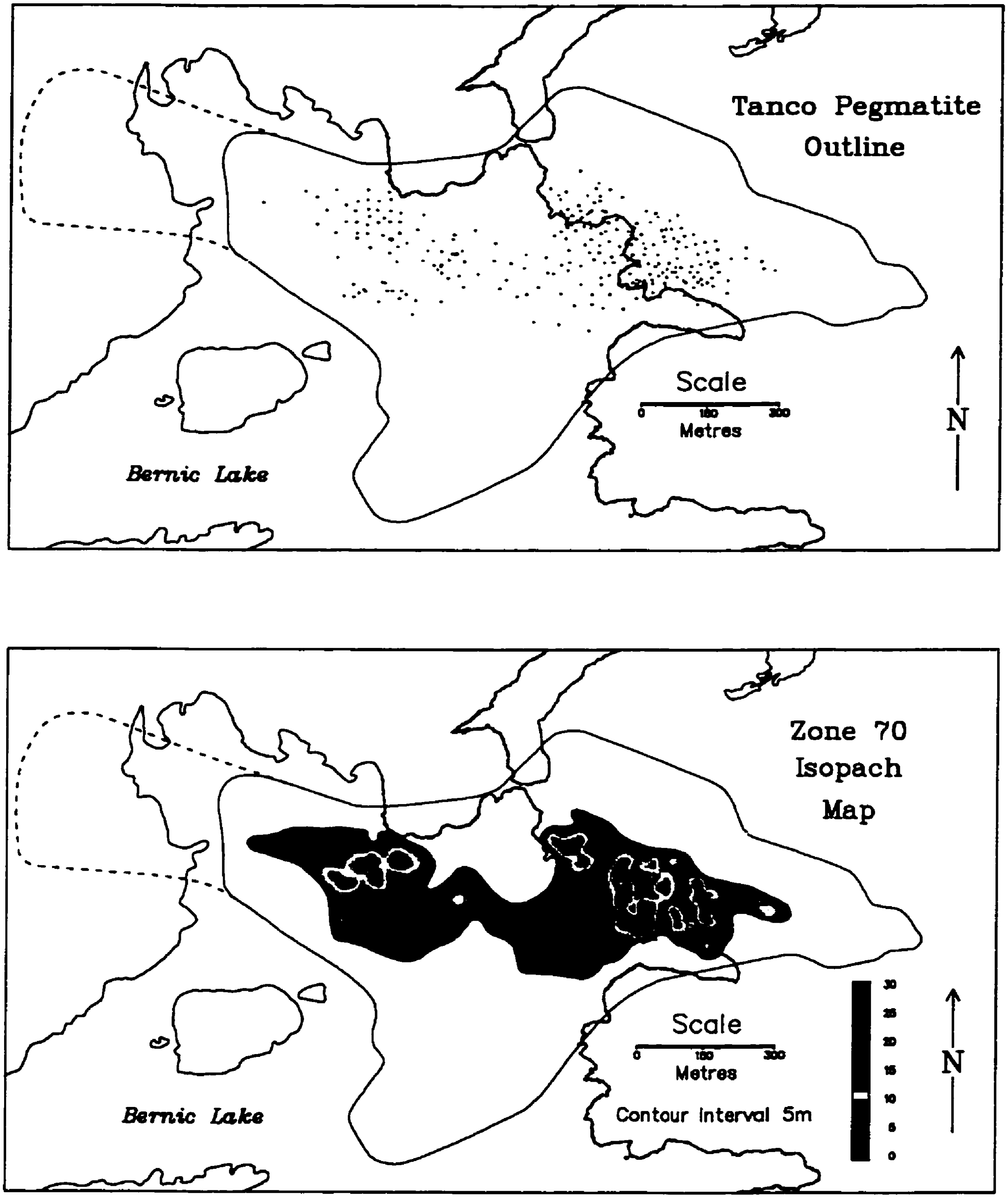

Figure 3.11 Plan view (top) showing drill hole intersections of the zone used to construct the zone 70 isopach map (bottom).

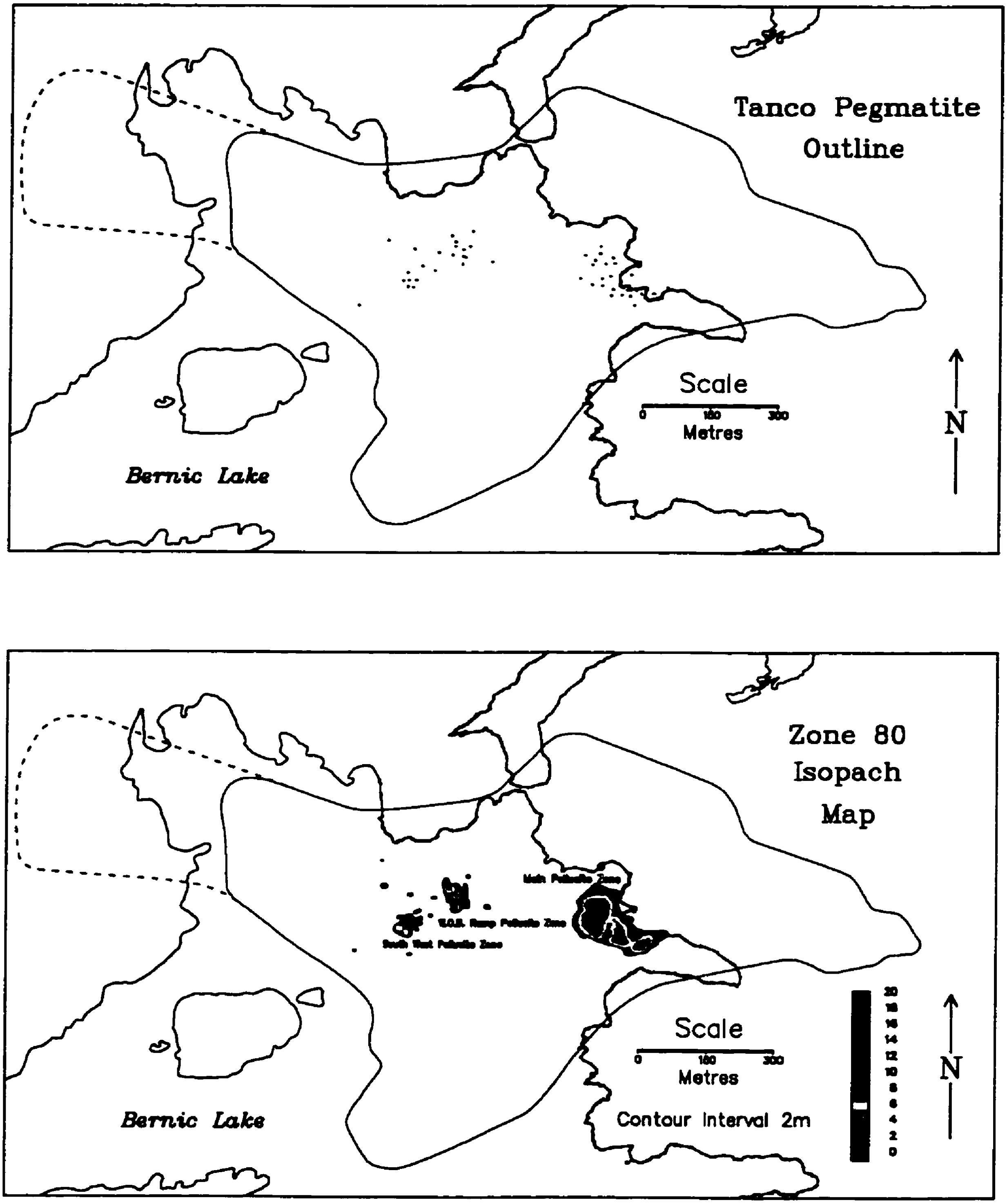

Figure 3.12 Plan view (top) showing drill hole intersections of the zone used to construct the zone 80 isopach map (bottom).

ones are poorly defined and have conservatively interpreted surfaces and volumes. Zone (80) was intersected by 53 drill holes over an area of 21,000 m^2 **(Figure 3.12)**, averaging 1 drill hole per 396 m^2. The zone comprises 1.33% of the pegmatite by volume.

3.3.8 <u>Zone (90): Lepidolite Zone</u>

The lepidolite zone was historically easily distinguished because of its colour and mineralogy in the drill core log. It forms large bodies and thin stringers. Whenever it was encountered in the core logs, but reported as another zone, it was split in out the present study and logged as zone (90). Zone (90) was intersected by 90 drill holes over an area of 50,400 m^2 **(Figure 3.13)**, averaging 1 drill hole per 561 m^2. The zone comprises 2.11% of the pegmatite by volume.

3.4 <u>Volumetric Calculations for the Pegmatite</u>

The surface construction for the entire main body of the pegmatite (*i.e.* hanging-wall and footwall contacts) was generally the easiest task because the black to white contact was consistently identified by all workers all the time. The top surface is sloping, flat, and regular, whereas the bottom surface is pitted and has troughs. These two surfaces pinch out gradually or abruptly depending on the local structural features that controlled the emplacement of the pegmatite.

Sub-vertical and sub-horizontal pegmatite dykes off the main body were observed in the drill-cores. The dykes were constructed into the cross sections and 3D model, however, they are not part of the main pegmatite and were not included in the calculations. Surface exposure of the pegmatite is only known to outcrop in the lake bottom **(Figure 3.14)**. Based on modelling, this spot is minimal in extent and only exposes the outermost contacts of zones (20) and (50). Volume reconstruction of the erosional surface was calculated to be 23,000 m^3, about 0.0024% of the total volume of the pegmatite and its composition does not affect the bulk data. The overall volume calculation for the known pegmatite body is considered to be accurate as the pegmatite intersects 908 drill holes over an area of 713,100 m^2 **(Figures 3.15 and 3.16)**, averaging 1 drill hole per 785 m^2.

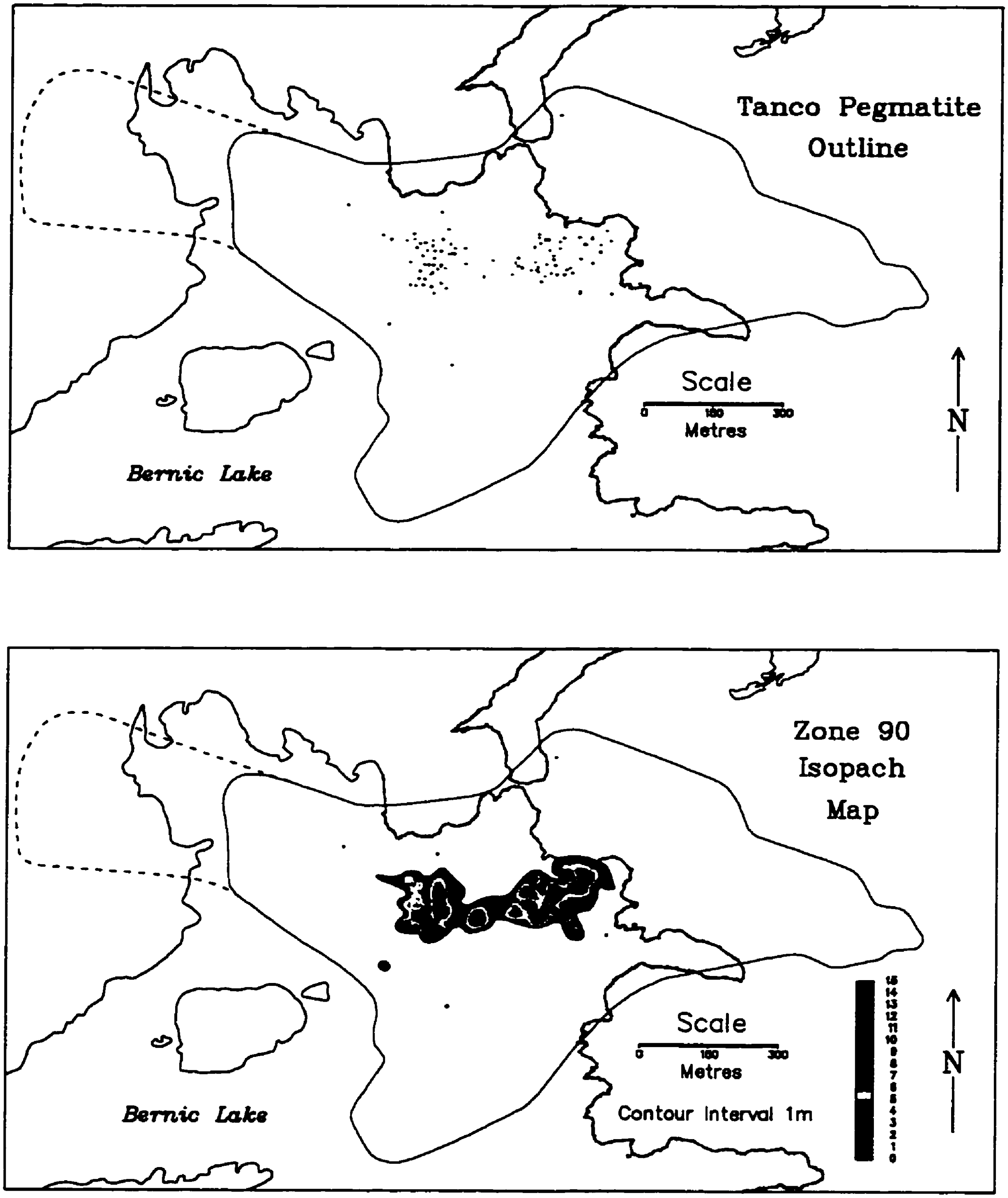

Figure 3.13 Plan view (top) showing drill hole intersections of the zone used to construct the zone 90 isopach map (bottom).

Figure 3.14 Lake bottom exposure of the Tanco pegmatite in red. Lake bottom is brown. Land is green. Tailing pond is blue. White blocks are the head frame for scale and the white line is the outline of the known pegmatite.

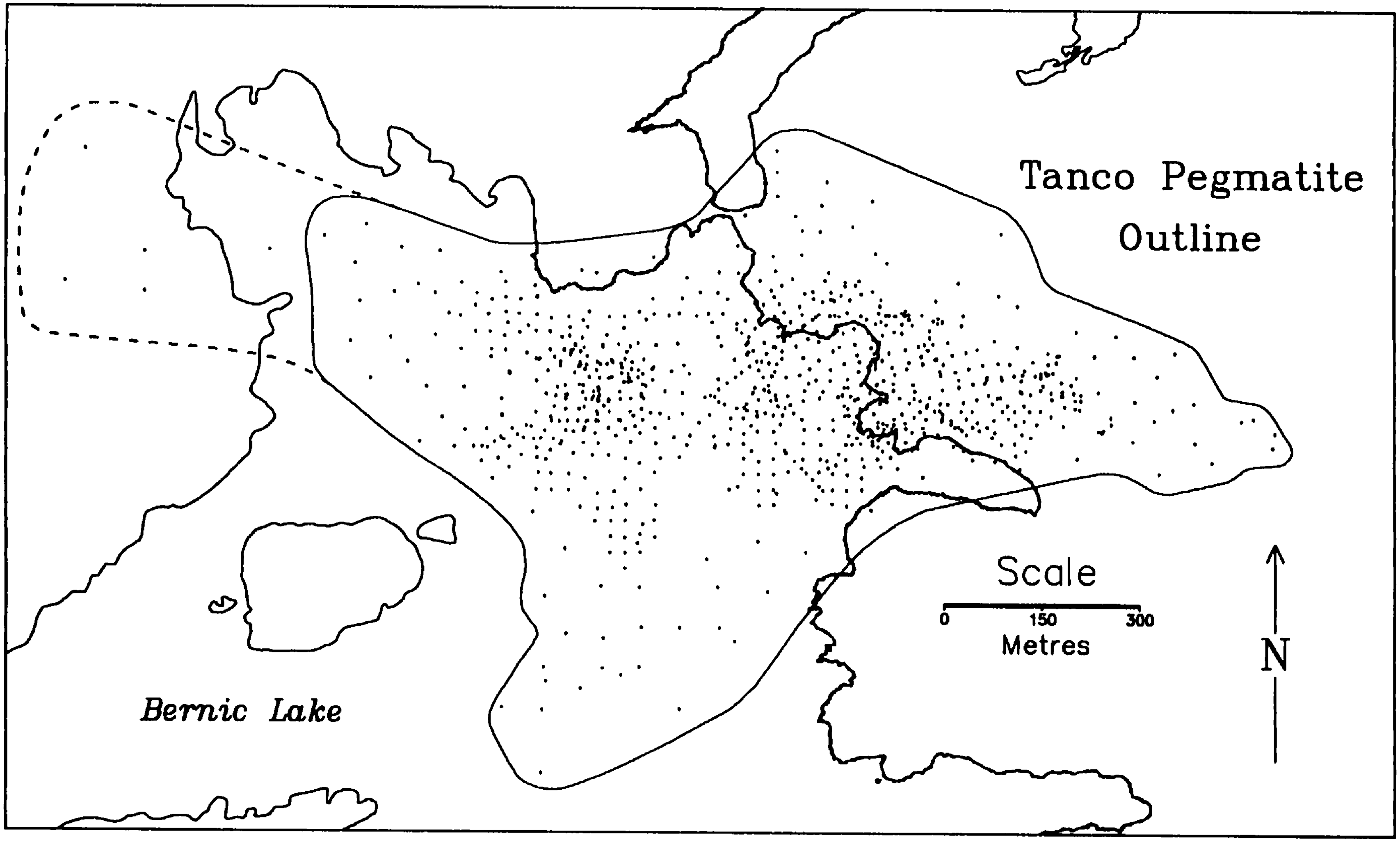

Figure 3.15 Plan view of the Tanco pegmatite and the drill hole intersections used to construct it.

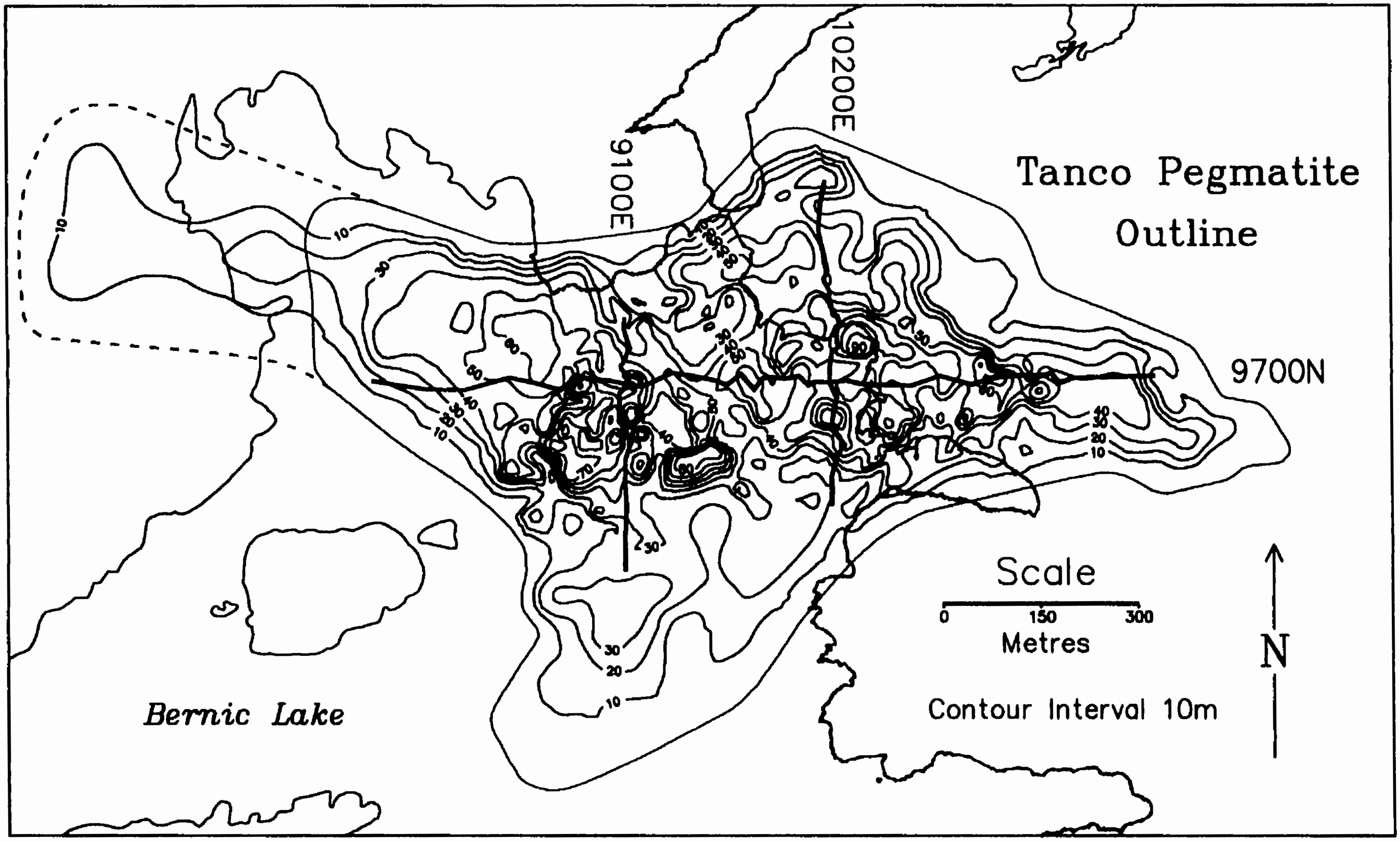

Figure 3.16 Plan view of the Tanco pegmatite – known extent and potential extent outlines marked with a heavier solid and by a dashed zero iso–line. The heaviest black lines in the centre of the isopach map represent three profiles on sections 9100E in Figure 2.03, 10200E in Figure 2.04, and 9700N in Figures 2.05 and 2.06.

4 METHODOLOGY OF MASS COMPOSITION CALCULATIONS

4.1 Modal Mineral Compositions of Individual Zones

Mineral compositions have been estimated for individual zones by examining the drill core, the underground workings, photographic observations, and microscopic studies of fine-grained assemblages. Many years of personal observations and communications by former mine geologists, the current chief mine geologist Peter Vanstone (confidential mine reports and personal communications), by Dr. Dave Teertstra (Teertstra, 1997), Dr. Scott Ercit (Ercit, 1995b), Dr. George Morgan and Dr. Dave London (Morgan & London, D. (1987), the author, and Dr. Petr Černý (Černý *et al.*, 1998) have gone into the compilation and fine-tuning of **Table 4.01**.

The table shows most of the primary minerals, which compose at Tanco in a roughly descending order of abundance by zone. Major components are greater than or equal to 3% by volume and are the most accurate modal estimates, approximately ±5% relative, for the minerals: K-feldspar, albite, quartz, petalite, spodumene, pollucite, most micas, and amblygonite in all zones. Reliability of zones, specifically zone (40) and zone (50), with uneven distributions of very coarse-grained minerals is somewhat lesser. Zone (50) and zone (80) are also correlated with Li_2O and Cs_2O wt% ore grades, based on minerals that make up most of these zones.

Subordinate components are less than 3% and greater than or equal to 1% by volume, and are ±20% relatively accurate for the minerals: beryl, apatite, lithiophilite, tourmaline, eucryptite, and amblygonite.

Minor components, those less than 1% by volume, are about ±40% accurate for: Nb, Ta–oxides, cassiterite, rutile, zircon, and uraninite. Nb, Ta and Sn mineral abundances, however, are in rough agreement with Tanco's published preproduction reserves of tantalum, their recent confidential updates, and their confidential Ta and Sn assay data. Nb, and in part Sn, were then calculated using the mineral chemistries of cassiterite and rutile. Proportions of the Ta-bearing phases were worked out from microscopic observations and from modes of Ta-ore concentrates.

The modal percentage of zircon may be slightly overestimated, but this is compensated for by the recently discovered subordinate Zr and Hf contents of wodginite and ixiolite (Černý, Ercit, Smeds and Groat, ms. in preparation).

Table 4.01 Modal Mineral Composition by Zone

Zones	Zone (10)	Zone (20)	Zone (30)	Zone (40)	Zone (50)	Zone (60)	Zone (70)	Zone (80)	Zone (90)	Tanco
Volumes (%)	0.10%	30.83%	2.69%	28.79%	13.12%	13.56%	7.47%	1.33%	2.11%	100.00%
Quartz	28.7%	36.0%	27.0%	34.0%	11.0%	15.0%	94.5%	5.0%	10.0%	32.54%
Albite	66.0%	40.7%	67.0%	25.0%	7.0%	20.0%	0.1%	5.0%	8.0%	25.56%
K-feldspar		15.0%		24.0%	25.0%	50.0%	2.0%	2.5%	10.0%	22.05%
Muscovite	1.0%	3.0%	3.0%	1.0%	0.1%	12.0%		2.0%		2.97%
Li-muscovite		3.0%		2.0%	0.1%				70.0%	3.00%
Lepidolite			0.1%	0.5%	0.1%	0.1%		7.0%		0.27%
Petalite				10.0%	46.0%		1.0%	1.2%		9.03%
Spodumene				0.3%	5.0%	0.1%	2.0%	1.0%		0.92%
Eucryptite					2.0%					0.26%
Apatite	2.0%	0.1%	0.4%	0.2%	0.1%	0.2%		0.5%	0.1%	0.15%
Lithiophilite	0.1%	0.1%	0.2%	0.5%	1.0%	0.5%			0.2%	0.38%
Amblygonite		0.5%	0.1%	1.5%	1.0%		0.4%	0.5%	0.5%	0.77%
Beryl	0.2%	0.5%	1.0%	0.1%	0.1%	1.0%			0.5%	0.37%
Pollucite				0.5%	1.0%			75.0%		1.28%
Tourmaline	2.0%	1.0%	0.5%	0.1%	0.1%	0.1%				0.38%
Cassiterite		0.01%	0.02%	0.02%	0.01%	0.02%			0.02%	0.01%
Rutile			0.02%		0.02%	0.02%				0.01%
Ferrotapiolite			0.02%			0.01%				0.00%
Columbite Grp		0.02%	0.03%	0.02%	0.02%	0.01%			0.01%	0.02%
Wodginite Grp			0.05%		0.02%	0.05%		0.03%	0.03%	0.01%
Microlite Grp			0.02%	0.02%	0.02%	0.03%		0.01%	0.02%	0.01%
Simpsonite						0.01%				0.00%
Uraninite					0.005%	0.005%			0.005%	0.001%
Zircon			0.02%		0.01%	0.02%			0.02%	0.00%
Biotite	0.1%									0.00%
Totals (%)	100.00%	99.93%	99.48%	99.76%	99.71%	99.18%	100.00%	99.74%	99.41%	100.00%

4.2 Compositions of Individual Minerals

Compositions for individual minerals were taken from many sources. In the cases of albite, K-feldspar, and columbite-tantalite, recalculations were carried out to match the observed mineral compositions in different zones. Ga_2O_3 and Tl_2O values were also added to total mineral compositions from Černý *et al.* (1998) and unpublished data of P. Černý to account for these trace elements in many minerals.

Quartz:
- assumed to be pure $Si0_2$.

Albite:
- calculated for optically estimated Ab-An proportions.

K-feldspar:
- alkali and alkaline earth contents averaged per zone Černý *et al.* (1998), complemented by calculation of other components; P_20_5 for both types of feldspars from London *et al.* (1990), and unpublished data of P. Černý.

Micas:
- from Rinaldi *et al.* (1972), Černý *et al.* (1998) and unpublished data of P. Černý, except for fine-grained veinlet muscovite - D.K. Teertstra (1997).

Petalite, spodumene:
- from Černý & Ferguson (1972), Černý *et al.* (1998).

Eucryptite:
- from Černý, (1972), Černý *et al.* (1998).

Apatite:
- from unpublished data of P. Černý & P. Povondra.

Lithiophilite:
- from unpublished data of A.-M. Fransolet *et al.*

Amblygonite-montebrasite:
- from Černá *et al.* (1972).

Beryl:
- from Černý & Simpson (1977), with modifications for individual zones.

Pollucite:
- from Černý & Simpson (1978).

Tourmaline:
- averages per zone with calculated B_2O_3, LiO_2 and H_2O contents, provided by J.B. Selway (1998, in prep.).

Cassiterite, rutile, ferrotapiolote:

- from Černý *et al.* (1998).

Columbite-tantalite:

- calculated from average Fe/Mn and Nb/Ta ratios per zone Černý *et al.* (1998) and complemented with minor elements from Ercit (1986).

Wodginite, microlite:

- from Ercit (1986) and Černý *et al.* (1998).

Uraninite:

- from Černý *et al.* (1998).

Zircon:

- from Černý & Siivola (1980).

4.3 Densities of Individual Minerals

Densities for individual minerals were taken from many sources. **Table 4.02** summarizes the densities used in the calculations of zone and bulk compositions.

Quartz, albite:

- textbook values from Deer, Howie & Zussman (1962).

K-feldspar:

- interpolated between textbook value for pure potassium microcline (2.55) and Rb- rich microcline from Red Cross Lake from Černý *et al.* (1985).

Muscovite, lepidolite:

- average textbook values from Deer, Howie & Zussman (1962) as the full extent of compositional variability is not yet known.

Lithian muscovite:

- interpolated between muscovite, lepidolite.

Petalite, spodumene:

- as determined on Tanco samples from Černý & Ferguson (1972).

Eucryptite:

- textbook values from Vlasov *et al.* (1962).

Apatite:

- textbook value for fluorapatite end member from Deer, Howie & Zussman (1962) and manganoan apatite determined by Quensel cited in Deer, Howie & Zussman (1962) for a composition close to those analyzed for typical Tanco samples.

Table 4.02 Mineral Density by Zone

Zones	Zone (10)	Zone (20)	Zone (30)	Zone (40)	Zone (50)	Zone (60)	Zone (70)	Zone (80)	Zone (90)
Densities	g/cm3	g/cm3	g/cm3	g/cm3	g/cm3	g/cm3	g/cm3	g/cm3	g/cm3
Quartz	2.66	2.66	2.66	2.66	2.66	2.66	2.66	2.66	2.66
Albite	2.62	2.62	2.62	2.62	2.62	2.62	2.62	2.62	2.62
K-feldspar		2.56		2.57	2.58	2.58	2.58	2.58	2.58
Muscovite	2.83	2.83	2.83	2.83	2.83	2.83		2.83	
Li-muscovite		2.80		2.80	2.80				2.78
Lepidolite			2.75	2.75	2.75	2.75		2.75	
Petalite				2.42	2.42		2.42	2.42	
Spodumene				3.15	3.15	3.15	3.15	3.15	
Eucryptite					2.66				
Apatite	3.20	3.20	3.30	3.30	3.30	3.30		3.30	3.30
Lithiophilite	3.40	3.40	3.40	3.50	3.50	3.50			3.55
Amblygonite		3.03	3.03	3.04	3.04		3.04	3.04	3.04
Beryl	2.75	2.75	2.75	2.78	2.78	2.78			2.78
Pollucite				2.87	2.87			2.87	
Tourmaline	3.16	3.19	3.19	3.10	3.10	3.10			
Cassiterite		6.90	6.90	6.90	6.90	6.90			6.90
Rutile			4.40		4.40	4.40			
Ferrotapiolite			7.90			7.90			
Columbite Grp		6.60	6.60	7.00	7.00	7.30			7.60
Wodginite Grp			7.10		7.10	7.10		7.10	7.10
Microlite Grp			5.50	5.50	5.50	5.50		5.50	5.50
Simpsonite						6.70			
Uraninite					10.00	10.00			10.00
Zircon			5.07		5.07	5.07			5.07
Biotite									

Lithiophilite:

- average values from (Ni et *al.* 1989), for average compositions analyzed for Tanco samples (unpublished data of A.-M. Fransolet *et al.*).

Amblygonite-montebrasite:

- measured in Černá *et al.* (1972) for samples close to zonal averages.

Beryl:

- interpolated from a diagram by Schaller & Stevens from compositions and optical data in Černý & Simpson (1977, Fig.6).

Pollucite:

- measured on a typical sample analyzed by Černý & Simpson (1978).

Tourmaline:

- interpolated for typical average compositions per zone by J.B. Selway in Černý et *al.* (1998) from textbook end-member values Deer, Howie & Zussman (1962).

Cassiterite, rutile:

- textbook values from Deer, Howie & Zussman (1962) adjusted for Fe, Nb substitution.

Ferrotapiolite:

- textbook values from Vlasov *et al.* (1962).

Columbite-tantalite:

- interpolated for average Ta/(Ta+Nb) (at.) ratios per zone Černý *et al.* (1998) from the diagram in Vlasov *et al.* (1964).

Wodginite:

- average value estimated for Tanco compositions from Ercit (1986) and Ercit *et al.* (1995a).

Microlite:

- average textbook value from Vlasov *et al.* (1964); however, the compositional range and consequently the densities are very diversified.

Simpsonite:

- average value from the literature, and calculated for a Tanco sample Ercit *et al.* (1995b).

Uraninite, thorite:

- textbook values from Vlasov *et al.* (1964).

Zircon:

- interpolated for typical Tanco composition Černý & Siivola (1980) from synthetic end-member data of Bideaux *et al.* (1995).

4.4 Bulk Composition Calculations for the Pegmatite

There are two stages involved in calculating the bulk composition of the Tanco pegmatite. The initial stage of this process takes each individual zone of the pegmatite and calculates the corresponding "Zone Composition." This composition is calculated by multiplying the individual minerals in the modal composition of the zone in (from **Table 4.01**) by their densities from that zone (**Table 4.02)** against each elemental oxide for that mineral, calculated from the sources in **Section 4.2**. The resulting product for each elemental oxide of each mineral in the zone is then summed up to create a "Weighted Factor." Individual weighted factors for each oxide are then summed up to create a "Total Factor." The zone composition of the pegmatite represents a normalized composition for all the mineral oxides using the individual weighted factors over the total factor. A weighted zone density is also produced for each zone by summing the products of each mineral mode multiplied by the mineral density. The results of zone compositions can be seen in **Tables 5.01** and **Tables 5.09**.

The final stage of this process takes the individual zone compositions and densities along with the corresponding zone volumes to calculate the "Bulk Composition." It is calculated by multiplying the individual oxides in the zone composition by the zone densities against the zone volumes from **Table 5.10**. The resulting product for each zone oxide in every zone is then summed up to create a weighted factor. Individual weighted factors are then summed up to create a total factor. The bulk composition of the pegmatite represents a composition adjusted to 100% for all the mineral oxides using the individual weighted factors over the total factor. A weighted bulk density is also produced by summing the products of each zone volume multiplied by the zone density. The bulk composition results can be seen in **Table 5.11**.

5 BULK COMPOSITION RESULTS BY VOLUME AND MASS

5.1 Bulk Composition of Individual Zones

The modal mineral compositions and densities of the individual zones shown in the following **Tables 5.01 to 5.09** were taken from **Tables 4.01 and 4.02**. The elemental oxides of each mineral in each zone were taken or calculated from the sources in **Section 4.2**. The normalized density and results of each zone composition appear in the right-most column.

5.2 Individual Zone and Total Zone Volumes

The individual zone and total zone volumes shown in **Table 5.10** are the results of the volumetric calculations for individual zones in **Section 3.4**.

5.3 Bulk Composition of the Pegmatite

Table 5.11 summarizes the Zone Compositions from **Tables 5.01 to 5.09** and Zone Volumes from **Table 5.10** showing the calculated pegmatite bulk composition adjusted to 100% in the right most column.

Table 5.01 Mineral Compositions and Densities in Zone (10)

Mineral	Quartz	Albite	Muscovite	Apatite	Tourmaline	Beryl	Lithiophilite	Zone Comp.
Mode	28.70%	66.00%	1.00%	2.00%	2.00%	0.20%	0.10%	100.00%
Density	2.66	2.62	2.83	3.20	3.16	2.75	3.40	2.66
SiO2	100.00	67.61	43.20		35.85	62.35		74.27%
Al2O3		20.12	34.36	0.02	34.05	17.50		14.32%
TiO2					0.48			0.01%
Fe2O3						0.30		0.00%
FeO			0.32		10.14		18.56	0.27%
MnO			0.07	0.48	0.35		22.73	0.05%
MgO			-0.01	0.01	1.09	0.15	1.52	0.03%
CaO		0.64		55.12	0.29	0.01	1.51	1.76%
SrO				0.06				0.0014%
Li2O			0.37	n.d.		0.29	9.02	0.02%
Na2O		11.44	0.22	0.12	2.12	1.38	0.13	7.51%
K2O			10.12	0.03	0.02	0.05	0.02	0.11%
Rb2O			1.69			0.03		0.02%
Cs2O			0.21			0.45		0.00%
P2O5		0.20		41.56	0.12		44.93	1.19%
B2O3					10.00			0.24%
BeO						12.50		0.0259%
H2O+			6.00	0.12	2.90	1.96		0.14%
H2O-						0.08	1.49	0.00%
F			0.64		0.77			0.03%
Sc2O3								
SnO2								
Nb2O5								
Ta2O5								
UO2								
PbO								
WO3								
ZnO								
ZrO2								
HfO2								
Tl2O								
Ga2O3		0.009	0.085		0.054	0.008	0.002	0.0083%
Sb2O3								
Totals (%)	100.00%	100.02%	97.27%	97.50%	98.23%	97.06%	99.91%	100.00%

Table 5.02 Mineral Compositions and Densities in Zone (20)

Mineral	Quartz	Albite	K-feldspar	Muscovite	Li-muscovite	Apatite	Lithiophilite	Amblygonite	Beryl	Tou
Mode	36.00%	40.70%	15.00%	3.00%	3.00%	0.10%	0.10%	0.50%	0.50%	
Density	2.66	2.62	2.56	2.83	2.80	3.20	3.40	3.03	2.75	
SiO2	100.00	67.60	64.65	43.20	50.00				62.35	
Al2O3		20.06	18.93	34.36	27.50	0.02		34.18	17.50	
TiO2										
Fe2O3								n.d.	0.15	
FeO				0.55	0.30		18.50			
MnO				0.07		0.48	25.71			
MgO				-0.01	0.20	0.01	0.77		0.10	
CaO		0.43	0.20			55.12	0.16	0.02	0.01	
SrO						0.06				
Li2O			0.03	0.52	0.86	n.d.	10.00	9.52	0.80	
Na2O		11.57	1.70	0.90	0.60	0.12	0.20	0.09	1.38	
K2O			13.00	9.20	6.80	0.03		0.01	0.05	
Rb2O			1.20	2.15	2.10				0.03	
Cs2O			0.10	0.18	0.22				0.90	
P2O5		0.35	0.35			41.56	45.85	49.11		
B2O3										
BeO									12.20	
H2O+				6.00		0.12			1.96	
H2O-									0.08	
F				0.64	1.00			6.43		
Sc2O3										
SnO2										
Nb2O5										
Ta2O5										
UO2										
PbO										
WO3										
ZnO										
ZrO2										
HfO2										
Tl2O			0.011	0.010	0.015					
Ga2O3		0.009	0.010	0.085	0.063		0.002	0.007	0.011	
Sb2O3										
Totals (%)	100.00%	100.02%	100.18%	97.86%	89.66%	97.50%	101.18%	99.35%	97.52%	

Densities in Zone (20)

scovite	Li-muscovite	Apatite	Lithiophilite	Amblygonite	Beryl	Tourmaline	Cassiterite	Columbite	Zone Comp.
3.00%	3.00%	0.10%	0.10%	0.50%	0.50%	1.00%	0.01%	0.02%	99.93%
2.83	2.80	3.20	3.40	3.03	2.75	3.19	6.90	6.60	2.65
43.20	50.00				62.35	35.98			76.84%
34.36	27.50	0.02		34.18	17.50	35.27			13.57%
						0.32	0.26	1.80	0.00%
				n.d.	0.15				0.00%
0.55	0.30		18.50			9.73	0.49	3.20	0.17%
0.07		0.48	25.71			0.44	0.33	12.66	0.05%
-0.01	0.20	0.01	0.77		0.10	0.27			0.01%
		55.12	0.16	0.02	0.01	0.08			0.27%
		0.06							0.0001%
0.52	0.86	n.d.	10.00	9.52	0.80	0.10			0.12%
0.90	0.60	0.12	0.20	0.09	1.38	2.20			5.01%
9.20	6.80	0.03		0.01	0.05	0.02			2.41%
2.15	2.10				0.03				0.31%
0.18	0.22				0.90				0.03%
		41.56	45.85	49.11		0.10			0.59%
						10.00			0.12%
					12.20				0.0636%
6.00		0.12			1.96	3.10			0.24%
					0.08				0.00%
0.64	1.00			6.43		0.77			0.10%
							0.07	0.40	0.0002%
							93.36	0.60	0.0247%
							0.25	26.70	0.0134%
							5.67	54.23	0.0286%
								0.20	0.0001%
						0.30			0.0037%
								0.15	0.0001%
0.010	0.015								0.0025%
0.085	0.063		0.002	0.007	0.011	0.054		0.054	0.0108%
97.86%	89.66%	97.50%	101.18%	99.35%	97.52%	98.74%	100.43%	100.00%	100.00%

Table 5.03 Mineral Compositions and Densities in Zone (30)

Mineral	Quartz	Albite	Muscovite	Lepidolite	Apatite	Lithiophilite	Amblygonite	Beryl	Tourmaline	Zircon
Mode	27.00%	67.00%	3.00%	0.10%	0.40%	0.20%	0.10%	1.00%	0.50%	0.02%
Density	2.66	2.62	2.83	2.75	3.30	3.40	3.03	2.75	3.19	5.07
SiO2	100.00	67.55	43.20	47.50				63.35	36.62	28.50
Al2O3		20.08	34.36	28.64	0.02		34.18	16.77	35.97	0.80
TiO2									0.24	
Fe2O3							n.d.	0.07		
FeO			0.30	0.03		16.61			8.12	0.03
MnO			0.07	0.22	0.48	26.66		0.00	0.37	0.02
MgO			-0.01	-0.01	0.01	0.84		0.00	0.44	
CaO		0.43			55.12		0.02	0.12	0.08	
SrO					0.06					
Li2O			0.75	3.50	n.d.	10.00	9.52	1.29	0.10	
Na2O		11.57	0.80	0.19	0.12		0.09	1.68	2.41	
K2O			9.00	9.45	0.03		0.01	0.07	0.02	
Rb2O			2.40	3.59				0.07		
Cs2O			0.25	0.71				2.92		
P2O5		0.38			41.56	45.06	49.11			
B2O3									9.50	
BeO								11.21		
H2O+			6.00	4.38	0.12			2.10	3.00	
H2O-				0.21				0.05		
F			0.64	4.08			6.43		0.97	
Sc2O3										
SnO2										
Nb2O5										
Ta2O5										
UO2										
PbO										
WO3										
ZnO									0.20	
ZrO2										53.00
HfO2										17.60
Tl2O			0.010							
Ga2O3		0.009	0.085	0.063		0.002	0.007	0.011	0.054	
Sb2O3										
Totals (%)	100.00%	100.02%	97.86%	102.55%	97.50%	99.17%	99.35%	99.72%	98.09%	99.95%

e	Amblygonite	Beryl	Tourmaline	Zircon	Cassiterite	Rutile	Ferrotapiolite	Col-Tant	Wodginite	Microlite	Zone Comp.
%	0.10%	1.00%	0.50%	0.02%	0.02%	0.02%	0.02%	0.03%	0.05%	0.02%	99.48%
)	3.03	2.75	3.19	5.07	6.90	4.40	7.90	6.60	7.10	5.50	2.64
		63.35	36.62	28.50							74.54%
	34.18	16.77	35.97	0.80							14.94%
			0.24		0.26	59.40	0.17	1.20	4.59	1.08	0.03%
	n.d.	0.07				1.40			0.87		0.00%
			8.12	0.03	0.49	5.14	12.04	6.62	4.95	0.96	0.12%
)		0.00	0.37	0.02	0.33	0.04	2.06	9.80	6.72	0.36	0.09%
		0.00	0.44								0.00%
	0.02	0.12	0.08							7.88	0.57%
											0.0003%
)	9.52	1.29	0.10						0 08		0.08%
	0.09	1.68	2.41							2.72	7.76%
	0.01	0.07	0.02								0.30%
		0.07									0.08%
		2.92								0.01	0.04%
5	49.11										0.63%
			9.50								0.06%
		11.21									0.1169%
		2.10	3.00								0.24%
		0.05									0.00%
	6.43		0.97							1.82	0.04%
					0.07	0.09	0.06	0.30			0.0003%
					93.36	1.18	0.67	0.30	8.37	0.49	0.0613%
					0.25	4.29	1.50	30.62	9.86	2.59	0.0398%
					5.67	28.90	83.45	50.90	61.78	68.76	0.2127%
										6.01	0.0025%
										1.65	0.0007%
								0.10		0.01	0.0001%
			0.20								0.0012%
				53.00				0.10			0.0205%
				17.60							0.0068%
											0.0003%
2	0.007	0.011	0.054				0.054	0.054	0.054		0.0097%
										0.91	0.0004%
%	99.35%	99.72%	98.09%	99.95%	100.43%	100.44%	100.00%	100.00%	97.26%	95.21%	100.00%

Table 5.04 Mineral Compositions and Densities in Zone (40)

Mineral	Quartz	Albite	K-feldspar	Muscovite	Li-muscovite	Lepidolite	Petalite	Spodumene	Apatite	Lithiophilite	Aml
Mode	34.00%	25.00%	24.00%	1.00%	2.00%	0.50%	10.00%	0.30%	0.20%	0.50%	
Density	2.66	2.62	2.57	2.83	2.80	2.75	2.42	3.15	3.30	3.50	
SiO2	100.00	67.78	64.77	43.20	45.25	51.65	77.85	63.45			
Al2O3		19.91	18.88	34.36	25.90	26.65	16.60	27.40	0.51		
TiO2											
Fe2O3							0.01	0.05			
FeO				0.50	0.07	0.06			0.09	11.81	
MnO				0.07	0.21	0.44			0.77	32.65	
MgO				-0.01	0.37	0.90	0.03	0.01	0.02	0.46	
CaO		0.21	0.02				0.01	0.16	52.30		
SrO									0.38		
Li2O			0.08	0.55	3.97	4.28	4.54	7.87	n.d.	10.00	
Na2O		11.69	1.80	0.80	0.41	0.40	0.05	0.11	0.14		
K2O			13.20	9.00	9.12	8.68	0.05	0.04	0.05		
Rb2O			1.85	2.25	3.46	4.47		0.00			
Cs2O			0.12	0.21	0.79	0.79		0.00			
P2O5		0.40	0.44					0.02	41.81	45.39	
B2O3											
BeO											
H2O+				6.00	6.84	2.13	0.32	0.30	0.08		
H2O-				0.80	0.73		0.14	0.11			
F				0.64	4.18	1.51					
Sc2O3											
SnO2											
Nb2O5											
Ta2O5											
UO2											
PbO											
WO3											
ZnO											
ZrO2											
HfO2											
Tl2O			0.012	0.012	0.023	0.022					
Ga2O3		0.009	0.009	0.085	0.063	0.063	0.007	0.012		0.002	
Sb2O3											
Totals (%)	100.00%	100.00%	101.18%	98.47%	101.39%	102.05%	99.61%	99.54%	96.12%	100.31%	

lite	Spodumene	Apatite	Lithiophilite	Amblygonite	Beryl	Pollucite	Tourmaline	Cassiterite	Columbite	Microlite	Zone Comp.
.00%	0.30%	0.20%	0.50%	1.50%	0.10%	0.50%	0.10%	0.02%	0.02%	0.02%	99.76%
2.42	3.15	3.30	3.50	3.04	2.78	2.87	3.10	6.90	7.00	5.50	2.62
7.85	63.45				63.35	47.07	37.55				76.04%
6.60	27.40	0.51		34.53	16.77	15.95	39.29				12.84%
							0.08	0.26	0.40	1.08	0.00%
.01	0.05			0.11	0.07						0.00%
		0.09	11.81				2.70	0.49	3.28	0.96	0.09%
		0.77	32.65		0.00		1.51	0.33	12.97	0.36	0.24%
.03	0.01	0.02	0.46	0.01	0.00		0.02				0.02%
.01	0.16	52.30		0.17	0.12		0.22			7.88	0.20%
		0.38									0.0009%
.54	7.87	n.d.	10.00	9.86	1.29		1.40				0.82%
.05	0.11	0.14		0.05	1.68	1.59	2.07			2.72	3.38%
.05	0.04	0.05		n.d.	0.07		0.01				3.44%
	0.00				0.07	0.83					0.56%
	0.00				2.92	32.19				0.01	0.23%
	0.02	41.81	45.39	49.32		0.33	0.01				1.47%
							11.00				0.01%
					11.21						0.0119%
.32	0.30	0.08			2.10		3.00				0.26%
.14	0.11				0.05						0.04%
				5.56			1.07			1.82	0.20%
								0.07	0.10		0.0001%
								93.36	0.20	0.49	0.0494%
								0.25	27.34	2.59	0.0158%
								5.67	55.55	68.76	0.0614%
										6.01	0.0025%
										1.65	0.0007%
									0.05	0.01	0.0000%
							0.14				0.0002%
									0.05		0.0000%
						0.010					0.0037%
007	0.012		0.002	0.007	0.013	0.008	0.054		0.054		0.0080%
										0.91	0.0004%
61%	99.54%	96.12%	100.31%	99.62%	99.72%	97.98%	100.12%	100.43%	100.00%	95.21%	100.00%

Table 5.05 Mineral Compositions and Densities in Zone (50)

Mineral	Quartz	Albite	K-feldspar	Muscovite	Li-muscovite	Lepidolite	Petalite	Spodumene	Eucryptite	Apatite	Lithiophilite	Amblygonite
Mode	11.00%	7.00%	25.00%	0.10%	0.10%	0.10%	46.00%	5.00%	2.00%	0.10%	1.00%	1.00%
Density	2.66	2.62	2.58	2.83	2.80	2.75	2.42	3.15	2.66	3.30	3.50	3.04
SiO2	100.00	67.73	63.95	43.20	45.25	51.65	77.85	63.45	45.18			
Al2O3		19.93	18.60	34.36	25.90	26.65	16.60	27.40	43.79	0.51		34.53
TiO2												
Fe2O3							0.01	0.05				0.11
FeO				0.45	0.07	0.06				0.09	10.59	
MnO				0.07	0.21	0.44				0.77	33.50	
MgO				-0.01	0.37	0.90	0.03	0.01		0.02		0.01
CaO		0.21	0.07				0.01	0.16		52.30		0.17
SrO										0.38		
Li2O			0.08	0.32	3.97	4.28	4.54	7.87	11.03	n.d.	10.00	9.86
Na2O		11.69	1.40	0.82	0.41	0.40	0.05	0.11		0.14	0.17	0.05
K2O			13.20	9.42	9.12	8.68	0.05	0.04		0.05		n.d.
Rb2O			2.30	1.81	3.46	4.47		0.00				
Cs2O			0.20	0.12	0.79	0.79		0.00				
P2O5		0.42	0.42					0.02		41.81	45.20	49.32
B2O3												
BeO												
H2O+				6.00	6.84	2.13	0.32	0.30		0.08		
H2O-				0.80	0.73		0.14	0.11				
F				0.64	4.18	1.51						5.56
Sc2O3												
SnO2												
Nb2O5												
Ta2O5												
UO2												
PbO												
WO3												
ZnO												
ZrO2												
HfO2												
Tl2O			0.024	0.011	0.022	0.022						
Ga2O3		0.009	0.009	0.085	0.063	0.063	0.007	0.012	0.017		0.002	0.007
Sb2O3												
Totals (%)	100.00%	99.99%	100.25%	98.10%	101.38%	102.04%	99.61%	99.54%	100.02%	96.12%	99.46%	99.62%

te	Lithiophilite	Amblygonite	Beryl	Pollucite	Tourmaline	Cassiterite	Rutile	Col-Tant	Wodginite	Microlite	Uraninite	Zircon	Zone Comp.
)%	1.00%	1.00%	0.10%	1.00%	0.10%	0.01%	0.02%	0.02%	0.02%	0.02%	0.01%	0.01%	99.71%
30	3.50	3.04	2.78	2.87	3.10	6.90	4.40	7.00	7.10	5.50	10.00	5.07	2.56
			63.35	47.07	37.55							32.20	72.10%
51		34.53	16.77	15.95	39.29								16.69%
					0.08	0.26	59.40	0.30	0.19	1.08			0.02%
		0.11	0.07				1.40		0.98				0.01%
09	10.59				2.70	0.49	5.14	0.79		0.96		0.04	0.15%
77	33.50		0.00		1.51	0.33	0.04	14.70	9.49	0.36		0.20	0.48%
02		0.01	0.00		0.02								0.01%
30		0.17	0.12		0.22				0.06	7.88	1.60	0.02	0.12%
38									0.24				0.0006%
n.d.	10.00	9.86	1.29		1.40								2.99%
14	0.17	0.05	1.68	1.59	2.07					2.72			1.25%
05		n.d.	0.07		0.01								3.38%
			0.07	0.83									0.59%
			2.92	32.19						0.01			0.09%
.81	45.20	49.32		0.33	0.01								1.40%
					11.00								0.01%
			11.21										0.1379%
.08			2.10		3.00								0.20%
			0.05										0.07%
		5.56			1.07					1.82			0.08%
						0.07	0.09	0.05					0.0001%
						93.36	1.18	0.20	14.01	0.49			0.0337%
						0.25	4.29	18.85	2.95	2.59			0.0146%
						5.67	28.90	65.06	71.74	68.76	2.10		0.1168%
										6.01	79.80		0.0182%
										1.65	15.40		0.0037%
										0.01			0.0000%
					0.14								0.0002%
												50.40	0.0100%
												17.40	0.0034%
				0.010									0.0062%
	0.002	0.007	0.013	0.008				0.054	0.054				0.0079%
										0.91			0.0004%
12%	99.46%	99.62%	99.72%	97.98%	100.07%	100.43%	100.44%	100.00%	99.73%	95.21%	98.90%	100.26%	100.00%

Table 5.06 Mineral Compositions and Densities in Zone (60)

Mineral	Quartz	Albite	K-feldspar	Muscovite	Lepidolite	Spodumene	Apatite	Lithiophilite	Beryl	Tourmaline	Cassiter
Mode	15.00%	20.00%	50.00%	12.00%	0.10%	0.10%	0.20%	0.50%	1.00%	0.10%	0.0
Density	2.66	2.62	2.58	2.83	2.75	3.15	3.30	3.50	2.78	3.10	6.
SiO2	100.00	67.64	63.74	43.20	46.72	63.45			63.35	35.30	
Al2O3		19.97	18.70	34.36	27.97	27.40	0.06		16.77	34.70	
TiO2										0.38	0.
Fe2O3						0.05			0.07		
FeO				0.32	0.05		0.10	8.66		12.17	0.
MnO				0.07	0.27		0.89	35.64	0.00	0.38	0.
MgO				-0.01	0.01	0.01	0.01	0.30	0.00	0.05	
CaO		0.21	0.10			0.16	53.50		0.12	0.07	
SrO							0.04				
Li2O			0.06	0.29	3.33	7.87	n.d.	10.00	1.29	0.10	
Na2O		11.69	1.10	0.23	0.19	0.11	0.15	0.20	1.68	1.77	
K2O			13.80	10.80	9.62	0.04	0.04		0.07	0.02	
Rb2O			2.20	1.63	3.23	0.00			0.07		
Cs2O			0.24	0.21	0.59	0.00			2.92		
P2O5		0.48	0.52			0.02	41.35	45.40		0.01	
B2O3										10.20	
BeO									11.21		
H2O+				6.00	4.94	0.30	0.02		2.10	3.20	
H2O-					0.76	0.11					
F				0.64	3.85					0.39	
Sc2O3											0.0
SnO2											93.3
Nb2O5											0.2
Ta2O5											5.6
UO2											
PbO											
WO3											
ZnO										0.42	
ZrO2											
HfO2											
Tl2O			0.020	0.012	0.023						
Ga2O3		0.009	0.011	0.085	0.063	0.012			0.015	0.054	
Sb2O3											
Totals (%)	100.00%	100.00%	100.49%	97.82%	101.62%	99.54%	96.14%	100.19%	99.67%	99.21%	100.43

eryl	Tourmaline	Cassiterite	Rutile	Ferrotapiolite	Col-Tant	Wodginite	Microlite	Simpsonite	Uraninite	Zircon	Zone Comp.
1.00%	0.10%	0.02%	0.02%	0.01%	0.01%	0.05%	0.03%	0.010%	0.01%	0.02%	99.18%
2.78	3.10	6.90	4.40	7.90	7.30	7.10	5.50	6.70	10.00	5.07	2.62
53.35	35.30							22.95		28.50	66.52%
16.77	34.70									0.80	17.92%
	0.38	0.26	59.40	0.17		0.24	1.03				0.02%
0.07			1.40			1.16					0.00%
	12.17	0.49	5.14	12.04	1.45		1.27			0.03	0.12%
0.00	0.38	0.33	0.04	2.06	12.88	10.64	0.42			0.02	0.27%
0.00	0.05										0.00%
0.12	0.07					0.08	7.33		1.60		0.23%
											0.0001%
1.29	0.10										0.16%
1.68	1.77						2.01				2.93%
0.07	0.02										8.20%
0.07											1.30%
2.92							0.00				0.18%
	0.01										0.76%
	10.20										0.01%
11.21											0.1188%
2.10	3.20							1.02			0.81%
											0.00%
	0.39						1.45				0.09%
		0.07	0.09	0.06							0.0001%
		93.36	1.18	0.67		16.66	0.49	1.20			0.0729%
		0.25	4.29	1.50	5.37	2.49	2.07	0.85			0.0084%
		5.67	28.90	83.45	80.25	68.42	66.44	72.25	2.10		0.2134%
							8.27		79.80		0.0204%
							2.22		15.40		0.0043%
							0.01				0.0000%
	0.42										0.0005%
										53.00	0.0205%
										17.60	0.0068%
											0.0113%
0.015	0.054			0.054	0.054	0.054		0.054			0.0186%
							0.78				0.0005%
9.67%	99.21%	100.43%	100.44%	100.00%	100.00%	99.74%	93.77%	98.32%	98.90%	99.95%	100.00%

Table 5.07 Mineral Compositions and Densities in Zone (70)

Mineral	Quartz	Albite	K-feldspar	Petalite	Spodumene	Amblygonite	Zone Comp.
Mode	94.50%	0.10%	2.00%	1.00%	2.00%	0.40%	100.00%
Density	2.66	2.62	2.58	2.42	3.15	3.04	2.67
SiO2	100.00	68.47	63.95	77.85	63.45		97.76%
Al2O3		19.62	18.60	16.60	27.40	34.53	1.33%
TiO2							
Fe2O3				0.01	0.05	0.11	0.00%
FeO							
MnO							
MgO				0.03	0.01	0.01	0.00%
CaO		0.21	0.07	0.01	0.16	0.17	0.01%
SrO							
Li2O			0.08	4.54	7.87	9.86	0.27%
Na2O		11.69	1.40	0.05	0.11	0.05	0.04%
K2O			13.20	0.05	0.04	n.d.	0.26%
Rb2O			2.30		0.00		0.04%
Cs2O			0.20		0.00		0.00%
P2O5			0.42		0.02	49.32	0.23%
B2O3							
BeO							
H2O+				0.32	0.30		0.01%
H2O-				0.14	0.11		0.00%
F						5.56	0.03%
Sc2O3							
SnO2							
Nb2O5							
Ta2O5							
UO2							
PbO							
WO3							
ZnO							
ZrO2							
HfO2							
Tl2O			0.024				0.0005%
Ga2O3			0.009	0.007	0.012	0.007	0.0006%
Sb2O3							
Totals (%)	100.00%	99.99%	100.25%	99.61%	99.54%	99.62%	100.00%

Table 5.08 Mineral Compositions and Densities in Zone (80)

Mineral	Quartz	Albite	K-feldspar	Muscovite	Lepidolite	Petalite	Spodumene	Apatite	Amblygonite	Pollucite
Mode	5.00%	5.00%	2.50%	2.00%	7.00%	1.20%	1.00%	0.50%	0.50%	75.00%
Density	2.66	2.62	2.58	2.83	2.75	2.42	3.15	3.30	3.04	2.87
SiO2	100.00	67.64	63.95	45.09	44.85	77.85	63.45			47.07
Al2O3		19.97	18.60	37.72	26.64	16.60	27.40	0.04	34.53	15.95
TiO2										
Fe2O3						0.01	0.05		0.11	
FeO					0.05			0.06		
MnO					0.38			2.60		
MgO					0.02	0.03	0.01	0.01	0.01	
CaO		0.21	0.07			0.01	0.16	52.93	0.17	
SrO								0.06		
Li2O			0.08		3.38	4.54	7.87	n.d.	9.86	
Na2O		11.69	1.40	0.23	0.19	0.05	0.11	0.29	0.05	1.59
K2O			13.20	10.04	9.43	0.05	0.04	0.05	n.d.	
Rb2O			2.30	1.44	3.18		0.00			0.83
Cs2O			0.20	0.18	0.55		0.00			32.19
P2O5		0.48	0.42				0.02	41.60	49.32	0.33
B2O3										
BeO										
H2O+					4.84	0.32	0.30	0.14		
H2O-					1.60	0.14	0.11			
F				0.19	4.75				5.56	
Sc2O3										
SnO2										
Nb2O5										
Ta2O5										
UO2										
PbO										
WO3										
ZnO										
ZrO2										
HfO2										
Tl2O			0.024		0.021					0.010
Ga2O3		0.009	0.009		0.063	0.007	0.012		0.007	0.008
Sb2O3										
Totals (%)	100.00%	100.00%	100.25%	94.89%	99.94%	99.61%	99.54%	97.76%	99.62%	97.98%

ons and Densities in Zone (80)

dspar	Muscovite	Lepidolite	Petalite	Spodumene	Apatite	Amblygonite	Pollucite	Wodginite	Microlite	Zone Comp.
.50%	2.00%	7.00%	1.20%	1.00%	0.50%	0.50%	75.00%	0.03%	0.01%	99.74%
2.58	2.83	2.75	2.42	3.15	3.30	3.04	2.87	7.10	5.50	2.83
3.95	45.09	44.85	77.85	63.45			47.07			51.49%
8.60	37.72	26.64	16.60	27.40	0.04	34.53	15.95			17.02%
								0.24	1.02	0.00%
			0.01	0.05		0.11		1.16		0.00%
		0.05			0.06				1.33	0.00%
		0.38			2.60			10.64	0.43	0.05%
		0.02	0.03	0.01	0.01	0.01				0.00%
0.07			0.01	0.16	52.93	0.17		0.08	7.22	0.33%
					0.06					0.0004%
0.08		3.38	4.54	7.87	n.d.	9.86				0.43%
1.40	0.23	0.19	0.05	0.11	0.29	0.05	1.59		1.87	1.84%
3.20	10.04	9.43	0.05	0.04	0.05	n.d.				1.17%
2.30	1.44	3.18		0.00			0.83			0.95%
0.20	0.18	0.55		0.00			32.19		0.00	24.99%
0.42				0.02	41.60	49.32	0.33			0.81%
		4.84	0.32	0.30	0.14					0.34%
		1.60	0.14	0.11						0.11%
	0.19	4.75				5.56			1.37	0.36%
								16.66	0.37	0.0128%
								2.49	1.96	0.0023%
								68.42	65.97	0.0655%
									8.73	0.0017%
									2.33	0.0005%
									0.00	0.0000%
.024		0.021					0.010			0.0101%
.009		0.063	0.007	0.012		0.007	0.008	0.054		0.0114%
									0.75	0.0001%
.25%	94.89%	99.94%	99.61%	99.54%	97.76%	99.62%	97.98%	99.74%	93.36%	100.00%

Table 5.09 Mineral Compositions and Densities in Zone (90)

Mineral	Quartz	Albite	K-feldspar	Li-musc Lepid	Apatite	Lithiophilite	Amblygonite	Beryl	Cassiterite	Col-Tant	Wo
Mode	10.00%	8.00%	10.00%	70.00%	0.10%	0.20%	0.50%	0.50%	0.02%	0.01%	
Density	2.66	2.62	2.58	2.78	3.30	3.55	3.04	2.78	6.90	7.60	
SiO2	100.00	67.64	63.74	46.72				63.35			
Al2O3		19.97	18.70	27.97	0.04		34.53	16.77			
TiO2									0.26		
Fe2O3							0.11	0.07			
FeO				0.05	0.06	1.23			0.49	0.75	
MnO				0.27	2.60	43.23		0.00	0.33	14.10	
MgO				0.01	0.01	0.61	0.01	0.00			
CaO		0.21	0.10		52.93	0.12	0.17	0.12			
SrO					0.06						
Li2O			0.06	3.33	n.d.	10.00	9.86	1.29			
Na2O		11.69	1.10	0.19	0.29	0.15	0.05	1.68			
K2O			13.80	9.62	0.05		n.d.	0.07			
Rb2O			2.20	3.23				0.07			
Cs2O			0.24	0.59				2.92			
P2O5		0.48	0.52		41.60	45.52	49.32				
B2O3											
BeO								11.21			
H2O+				4.94	0.14			2.10			
H2O-				0.76				0.05			
F.				3.85			5.56				
Sc2O3									0.07		
SnO2									93.36		
Nb2O5									0.25	11.12	
Ta2O5									5.67	73.97	
UO2											
PbO											
WO3											
ZnO											
ZrO2											
HfO2											
Tl2O			0.020	0.022							
Ga2O3		0.009	0.011	0.063	0.002	0.007		0.015		0.054	
Sb2O3											
Totals (%)	100.00%	100.00%	100.49%	101.62%	97.77%	100.87%	99.61%	99.72%	100.43%	100.00%	9

philite	Amblygonite	Beryl	Cassiterite	Col-Tant	Wodginite	Microlite	Uraninite	Zircon	Zone Comp.
.20%	0.50%	0.50%	0.02%	0.01%	0.03%	0.020%	0.005%	0.02%	99.41%
3.55	3.04	2.78	6.90	7.60	7.10	5.50	10.00	5.07	2.72
		63.35						30.00	54.03%
	34.53	16.77						0.35	23.27%
			0.26		0.24	1.03			0.00%
	0.11	0.07			1.16				0.00%
1.23			0.49	0.75		1.27		0.06	0.04%
43.23		0.00	0.33	14.10	10.64	0.42		0.35	0.32%
0.61	0.01	0.00							0.01%
0.12	0.17	0.12			0.08	7.33	1.60	0.15	0.09%
									0.0001%
10.00	9.86	1.29							2.44%
0.15	0.05	1.68				2.01			1.14%
	n.d.	0.07							8.08%
		0.07							2.48%
		2.92				0.00			0.45%
45.52	49.32								0.52%
		11.21							0.0565%
		2.10							3.50%
		0.05							0.54%
	5.56					1.45			2.75%
			0.07						0.0000%
			93.36		16.66	0.39			0.0597%
			0.25	11.12	2.49	2.07			0.0059%
			5.67	73.97	68.42	66.44	2.10		0.1030%
						8.27	79.80		0.0178%
						2.22	15.40		0.0037%
						0.01			0.0000%
								52.70	0.0194%
								17.60	0.0065%
									0.0176%
.007		0.015		0.054	0.054				0.0464%
						0.78			0.0003%
.87%	99.61%	99.72%	100.43%	100.00%	99.74%	93.67%	98.90%	101.21%	100.00%

Table 5.10 Individual Zone and Total Zone Volumes

Pegmatite Zones	Volumes (ft3)	Volumes (m3)	Volumes (km3)	Density (kg/m3)	Mass (Mg)	Volume Percentage
Zone(10)	332,093	9,404	0.0000	2657.02	24,986	0.10%
Zone (20)	102,497,721	2,902,413	0.0029	2646.25	7,680,509	30.83%
Zone (30)	8,935,717	253,031	0.0003	2639.21	667,804	2.69%
Zone (40)	95,690,376	2,709,650	0.0027	2619.51	7,097,955	28.79%
Zone (50)	43,627,916	1,235,405	0.0012	2563.06	3,166,414	13.12%
Zone (60)	45,073,066	1,276,327	0.0013	2624.66	3,349,930	13.56%
Zone (70)	24,820,161	702,829	0.0007	2667.28	1,874,641	7.47%
Zone (80)	4,423,243	125,252	0.0001	2825.02	353,840	1.33%
Zone (90)	7,024,799	198,920	0.0002	2724.98	542,054	2.11%
Totals	332,425,093	9,413,231	0.0094		24,758,135	100.00%

Table 5.11 Composition of Individual Zones and Bulk Pegmatite

Zone	Zone (10)	Zone (20)	Zone (30)	Zone (40)	Zone (50)	Zone (60)	Zone (70)	Zone (80)	Zone (90)	Bulk Comp
Volume	0.10%	30.83%	2.69%	28.79%	13.12%	13.56%	7.47%	1.33%	2.11%	100.00%
Density	2.66	2.65	2.64	2.62	2.56	2.62	2.67	2.83	2.72	2.63
SiO2	74.27%	76.84%	74.54%	76.04%	72.10%	66.52%	97.76%	51.49%	54.03%	75.27%
Al2O3	14.32%	13.57%	14.94%	12.84%	16.69%	17.92%	1.33%	17.02%	23.27%	13.72%
TiO2	0.01%	0.00%	0.03%	0.00%	0.02%	0.02%		0.00%	0.00%	0.01%
Fe2O3	0.00%	0.00%	0.00%	0.00%	0.01%	0.00%	0.00%	0.00%	0.00%	0.00%
FeO	0.27%	0.17%	0.12%	0.09%	0.15%	0.12%		0.00%	0.04%	0.12%
MnO	0.05%	0.05%	0.09%	0.24%	0.48%	0.27%		0.05%	0.32%	0.19%
MgO	0.03%	0.01%	0.00%	0.02%	0.01%	0.00%	0.00%	0.00%	0.01%	0.01%
CaO	1.76%	0.27%	0.57%	0.20%	0.12%	0.23%	0.01%	0.33%	0.09%	0.21%
SrO	0.0014%	0.0001%	0.0003%	0.0009%	0.0006%	0.0001%		0.0004%	0.0001%	0.0004%
Li2O	0.02%	0.12%	0.08%	0.82%	2.99%	0.16%	0.27%	0.43%	2.44%	0.76%
Na2O	7.51%	5.01%	7.76%	3.38%	1.25%	2.93%	0.04%	1.84%	1.14%	3.35%
K2O	0.11%	2.41%	0.30%	3.44%	3.38%	8.20%	0.26%	1.17%	8.08%	3.50%
Rb2O	0.02%	0.31%	0.08%	0.56%	0.59%	1.30%	0.04%	0.95%	2.48%	0.58%
Cs2O	0.00%	0.03%	0.04%	0.23%	0.09%	0.18%	0.00%	24.99%	0.45%	0.48%
P2O5	1.19%	0.59%	0.63%	1.47%	1.40%	0.76%	0.23%	0.81%	0.52%	0.94%
B2O3	0.24%	0.12%	0.06%	0.01%	0.01%	0.01%				0.05%
BeO	0.0259%	0.0636%	0.1169%	0.0119%	0.1379%	0.1188%			0.0565%	0.0613%
H2O+	0.14%	0.24%	0.24%	0.26%	0.20%	0.81%	0.01%	0.34%	3.50%	0.37%
H2O-	0.00%	0.00%	0.00%	0.04%	0.07%	0.00%	0.00%	0.11%	0.54%	0.03%
F	0.03%	0.10%	0.04%	0.20%	0.08%	0.09%	0.03%	0.36%	2.75%	0.18%
Sc2O3		0.0002%	0.0003%	0.0001%	0.0001%	0.0001%			0.0000%	0.0001%
SnO2		0.0247%	0.0613%	0.0494%	0.0337%	0.0729%		0.0128%	0.0597%	0.0391%
Nb2O5		0.0134%	0.0398%	0.0158%	0.0146%	0.0084%		0.0023%	0.0059%	0.0129%
Ta2O5		0.0286%	0.2127%	0.0614%	0.1168%	0.2134%		0.0655%	0.1030%	0.0792%
UO2			0.0025%	0.0025%	0.0182%	0.0204%		0.0017%	0.0178%	0.0063%
PbO			0.0007%	0.0007%	0.0037%	0.0043%		0.0005%	0.0037%	0.0014%
WO3		0.00010%	0.00008%	0.00003%	0.00000%	0.00000%		0.00000%	0.00000%	0.00004%
ZnO		0.0037%	0.0012%	0.0002%	0.0002%	0.0005%				0.0013%
ZrO2		0.0001%	0.0205%	0.0000%	0.0100%	0.0205%			0.0194%	0.0051%
HfO2			0.0068%		0.0034%	0.0068%			0.0065%	0.0017%
Tl2O		0.0025%	0.0003%	0.0037%	0.0062%	0.0113%	0.0005%	0.0101%	0.0176%	0.0047%
Ga2O3	0.0083%	0.0108%	0.0097%	0.0080%	0.0079%	0.0186%	0.0006%	0.0114%	0.0464%	0.0106%
Sb2O3			0.0004%	0.0004%	0.0004%	0.0005%		0.0001%	0.0003%	0.0002%
Subtotals	100.00%	100.00%	100.00%	100.00%	100.00%	100.00%	100.00%	100.00%	100.00%	100.00%
-F=O2	-0.01%	-0.04%	-0.02%	-0.09%	-0.03%	-0.04%	-0.01%	-0.15%	-1.16%	-0.08%
Totals (%)	99.99%	99.96%	99.98%	99.91%	99.97%	99.96%	99.99%	99.85%	98.84%	99.92%

6 DISCUSSION

6.1 Consideration of Errors

Estimates of error for the bulk composition calculations are not easily determined for some stages of the procedure and vary from qualitative to semi-quantitative. No attempt to work out the cumulative error was attempted, although individual errors were estimated for certain stages of the procedure.

During the data entry, every data point and bit of geological information was checked and double checked against the original drill logs, core logs, and maps. 3D modelling of the compiled data also allowed visual checking and confirmation of the data. Any piece of data that did not correlate was investigated and if shown to be recorded in error, corrected. The mineral descriptions and assays from the core logs have been consistent over time, however, the older zonal interpretations have not. To correct this, the mineralogy of the cores and core logs were re-examined and correlated with current zonal descriptions. Errors from incorrect data and/or misidentified zones have been minimized by rigorous examination.

The accuracy of borehole locations varies with age and location at Tanco. The accuracy of underground and newer vertical surface holes (*i.e.*, since draining the mine in 1967) on the land and lake are not in question because they have been properly surveyed within a few centimetres. Older hole collars on the land were found again and resurveyed with newer survey tools and methods to re-establish their exact locations as some of their locations were in question. Older hole collars on the lake bottom could not be resurveyed as they were hidden beneath the lake and sediments, however, they were surveyed underground when they became exposed in the working. Newer drill holes with good control that became exposed underground were good control points for calculating the drilling drift of holes. Upon examining break-through holes, it was found that most of the drill holes can be considered vertical as they have less than a 3% drift. After back-calculating questionable holes, new locations within 1.5 to 2.5 m can be projected back to the lake bottom and checked against existing co-ordinates. 3D modelling of the surface boreholes with computer generated land and lake bottom surfaces helped to confirm locations using collar elevations and pegmatite intersection mineralogy. Modelling of underground drill holes was also used to confirm locations and orientations. Only 2.6% of the drill holes were rejected as they could not be properly located or referenced. Error from hole locations is minor, when compared to the scale of the pegmatite, and does not significantly influence the construction of volume calculated surfaces, and therefore the zone volumes, noticeably.

Volume calculation errors were not measured as they are difficult to qualify or even to quantify because the zone volumes match the pegmatite volume. This is providing that every given zone trapezoid is accounted for in the total volumes and that each use and share the same trapezoidal surfaces. Thus ruling out under and over volume estimates from the constructed and calculated surfaces. Another potential source of error for the volume calculations is the western extent of the pegmatite. Due to the lack of information in that region it was not calculated. At this time it may or may not be part of the main pegmatite and can only be shown to be one way or another with more drilling in the future. If it is shown to be part of the main pegmatite it would only slightly increase the volumes for zone (20), zone (40), and the pegmatite as a whole.

Modal mineral component estimates of the pegmatite are, on average, semi-quantitative. Major components greater than or equal to 3% by volume and are the most accurate modal estimates, approximately ±5% for the minerals: K-feldspar, albite, quartz, petalite, spodumene, pollucite, most micas, and amblygonite in all zones. Reliability of zones, specifically zone (40) and zone (50) with their uneven distributions of very coarse-grained minerals, is somewhat less. Zone (50) and zone (80) are also correlated with Li_2O and Cs_2O wt% ore grades, based on minerals which make up the majority of these zones.

Subordinate components are less than 3% and greater than or equal to 1% by volume, and are ±20% relatively accurate for the minerals: beryl, apatite, lithiophilite, tourmaline, eucryptite, some apatite, amblygonite.

Minor components, those less than 1% by volume are about ±40% accurate for the minerals of Nb, Ta–oxides, cassiterite, rutile, zircon, and uraninite. Nb, Ta and Sn mineral abundances, however, are in rough agreement with Tanco's published preproduction reserves of tantalum, their recent confidential updates, are in good agreement with their confidential Ta and Sn assay data. Nb and in part Sn were then calculated using the mineral chemistries of cassiterite, rutile, zircon, and, uraninite. Proportions of the Ta-bearing phases were worked out from microscopic observations and from modes of Ta-ore concentrates.

Chemical compositions of individual minerals are quite reliable, even for the interpolated data or for estimates from optical properties. However, the analytical data have been accumulated over the period of 30 years from different laboratories using different techniques, therefore, a quantitative assessment of errors is not feasible. The same applies to the data for mineral densities.

The bulk composition results and errors are a product of six sets of data and methods: borehole locations, computer modelling of volumes, local improvements of volume calculations by underground observations, chemical compositions of minerals, mineral densities, and mineral modes used to calculate the final numbers. The mineral modes are probably the major source of error. All the tabulated data represent direct products of computing, which were not adjusted by rounding-off at any stage to eliminate rounding errors. The significance of the decimal digits for major oxide components, and the accuracy of the values of minor components, must be judged accordingly.

6.2 Modal Trends in Zone Compositions

The outermost zones of the Tanco pegmatite, namely (10), (20) and to a degree (40), tend to be granitic, with substantial albitic plagioclase, K-feldspar and quartz. Intermediate and inner zones, however, distinctly to dramatically deviate from granitic mineral modes, for example zone (30), and tend to be simpler in composition, up to virtually monomineralic, as exemplified by zone (70), the quartz zone. The deviation from granitic composition is accentuated by the appearance of high percentages of Li-silicates, such as petalite (SQUI-Spodumene Quartz Inter-growths) in (50) and lepidolite in (90).

6.3 Chemical Trends in Zone Compositions

Silica content is relatively stable in zones (10) to (40) (**Table 5.11**) but drops through the zones (50), (60), (80) and (90). This trend is "violated" by the quartz zone (70), which corresponds to a classic quartz core of granitic pegmatites in all respects except for its segmentation and irregular spatial distribution.

In contrast to silica, alumina increases slightly from the outer to the inner zones, with the exception of zone (70), as above.

Except for the outermost zones of granitic modal composition, the different alkali metals tend to be concentrated in specific zones. Spodumene, petalite and eucryptite mineralization in zone (50) give it the highest Li_2O value, followed by zone (90), which is associated with lithium-rich micas. Rb_2O and Cs_2O tend to be zone-specific and occur in the central zones of the pegmatite. Rb_2O is concentrated in the feldspars of zones (50) and (60) and in the micas of zone (90), whereas Cs_2O is in zone (80) in pollucite. Na_2O and K_2O show reciprocal trends. Na_2O tends to be higher in the outer zones dropping inwards, whereas K_2O

increases inwards. The alkalis show increasing fractionation from the outside to the inside of the pegmatite.

The volatiles H_2O and F generally tend to increase inwards, while B_2O_3 decreases inwards rapidly and is only concentrated in the outermost zones and in the exocontact.

Traces of Tl and Ga tend to increase inwards and are the highest in the central zones. The highest values can be found in the feldspars and micas of zones (60) and (90).

6.4 Comparison with Other Pegmatites

Results from present work on Tanco are, in many respects, different from the results calculated by Morgan and London (1987). These authors did not include the outer reaches of the pegmatite which were much less explored 11 years ago. They under-represented zone (20) in particular, as well as zones (40), (50), and (70), in their results. Improved modelling and modal estimates also contribute to the higher SiO_2 and Na_2O, and lower Al_2O_3, Li_2O, K_2O, Rb_2O, and P_2O_5, evident from the current analysis (**Table 6.01**).

Tanco, one of the world's largest pegmatites, has the highest observed values of SiO_2, Rb_2O, and P_2O_5 among the fully analyzed rare-element pegmatites and the lowest Al_2O_3 and Li_2O values. However, the absolute differences are rather small, and the bulk composition is generally comparable to those of other pegmatites examined by Filippova (1971, "Siberia"), Burnham & Jahns (1962, Harding pegmatite), Jahns (1953, Pidlite pegmatite), Chackowsky (1987, INCO pegmatite), and Černý (unpublished data, Red Cross Lake pegmatites). Tanco is similar to the Harding pegmatite, which has similar SiO_2, Li_2O, CaO, and MnO, however, it has slightly higher K_2O, lower Al_2O_3 and Na_2O. All other pegmatites have greater amounts of Na_2O than K_2O, with the exception of the Pidlite pegmatite, whereas Tanco has nearly equal amounts of both. The combined Na_2O and K_2O values are nearly the same for all these pegmatites, except the Pidlite pegmatite. Tanco may not have the greatest overall concentration of Cs_2O, but it contains the largest and richest known deposit of pollucite in the world. In highly fractionated zoned pegmatites, lithium and cesium minerals tend to be concentrated in individual and mainly inner zones in the pegmatite, however, these zones represent only a small component of the bulk composition (**Table 6.01**).

6.5 Comparison with Experimental Work

The bulk compositions of Tanco and other lithium-rich pegmatites analyzed to date are slightly enriched in feldspars, and impoverished in quartz and lithium aluminosilicates, relative to the minimum in the Li_2O-Al_2O_3-SiO_2-H_2O system (**Table 6.02 & Figure 6.01,**

Table 6.01 Bulk Composition of Rare-Element Pegmatites

Pegmatite Locations	Siberia [1] USSR	Harding [2] NM	Pidlite [3] NM	INCO [4] MB	RCL [5] MB	Tanco [6] MB	Tanco [7] MB
SiO_2	70.62	75.24	74.5	73.70	72.44	69.74	75.27
TiO_2	0.04	0.05		0.01	0.02	0.01	0.01
Al_2O_3	17.69	14.42	14.8	16.53	16.38	16.50	13.72
Fe_2O_3	0.60	*		0.18	0.00	*	0.00
FeO	0.20	0.65	--	0.08	0.13	0.18	0.12
MnO	0.03	0.18	--	0.16	0.11	0.21	0.19
MgO	0.28	0.01	--	0.05	0.12	--	0.01
CaO	0.65	0.2	0.2	0.13	0.30	0.89	0.21
Li_2O	1.05	0.65	0.7	1.41	1.01	1.18	0.76
Na_2O	4.84	4.23	3.3	3.78	4.69	2.69	3.35
K_2O	1.95	2.74	5.4	1.73	2.29	4.42	3.50
Rb_2O	0.21	0.19	--	0.36	1.1	1.1	0.58
Cs_2O	1.31	0.05	--	0.03	0.87	0.42	0.48
P_2O_5	0.9	0.13	--	<0.01	0.36	1.18	0.94
B_2O_3	--	--	--	--	0.32	0.24	0.05
F	0.65	0.64	0.9	--	0.8	0.2	0.18
$H2O^+$	0.75	--	0.6	0.10	--	--	0.37
Subtotals	101.77	99.38	100.4	98.25	100.96	98.96	99.74
$-O=F_2$	-0.28	-0.27	-0.4	--	-0.32	-0.08	-0.08
Totals	101.49	99.11	100	98.25	100.64	98.88	99.67

* Total Fe as FeO, - not determined.

1 Spodumene-subtype of complex pegmatite with pollucite (Filippova, 1971).

2 Spodumene-subtype of complex pegmatite (Burnham & Jahns, 1962).

3 Lepidolite-subtype of complex pegmatite (Jahns, 1953).

4 Albite-spodumene-subtype of pegmatite (Chackowsky, 1987).

5 Lepidolite-subtype of complex pegmatite with pollucite (Černý, unpublished data).

6 Petalite-subtype of complex pegmatite with abundant lepidolite, amblygonite, & pollucite (Morgan & London, 1987)(London, 1990).

7 Petalite-subtype of complex pegmatite with abundant lepidolite, amblygonite, & pollucite.

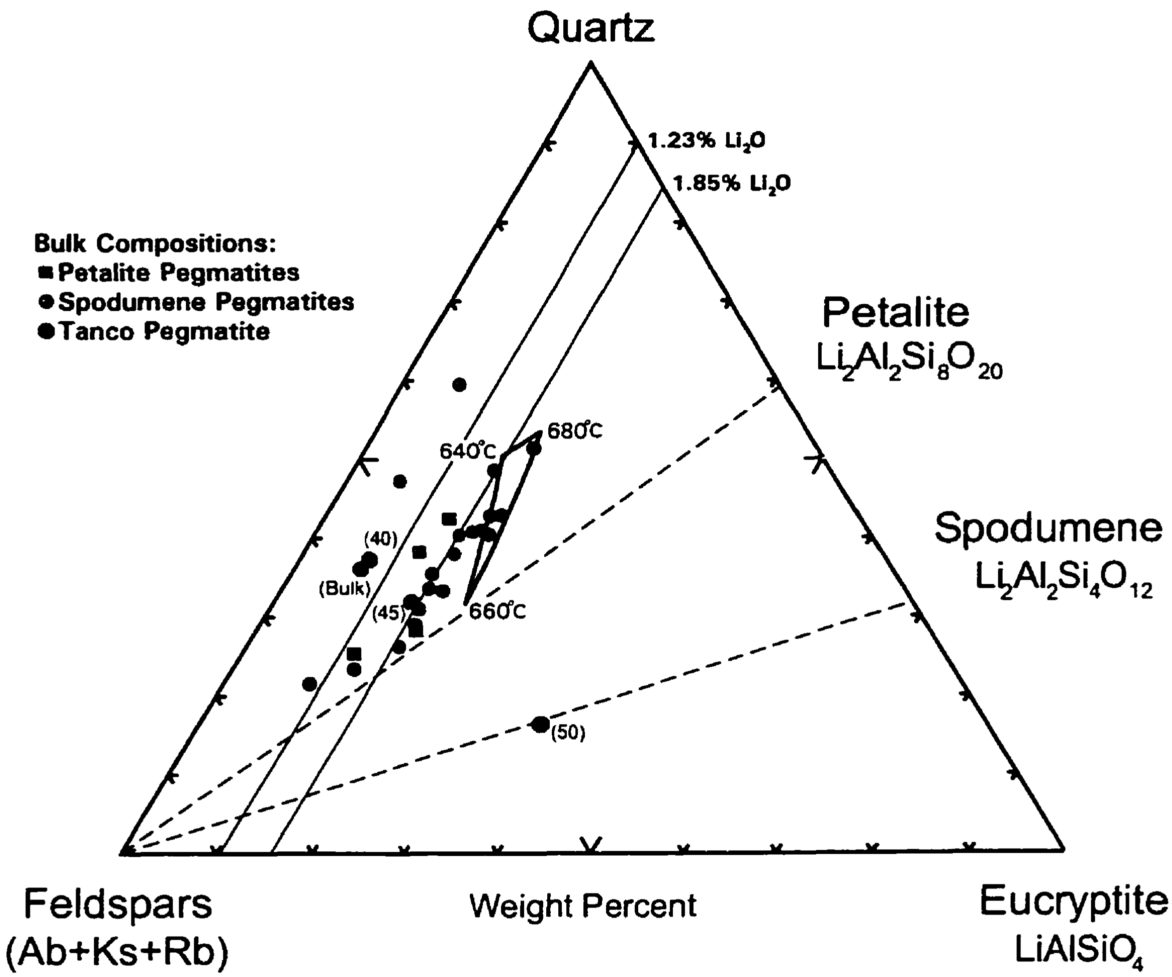

Figure 6.01 Tanco pegmatite bulk composition, composition of zones (40) & (50), and their weighted average (45), versus bulk compositions of petalite and spodumene pegmatites from the literature.
Based on Stewart Fig. 2, (1978).

Zones	Quartz	Alk=>Felds	Li=>Eucr	Totals	Quartz	Feldspar	Eucryptite	Totals
(10)	28.70%	64.27%	0.14%	93.11%	30.82%	69.03%	0.15%	100.00%
(20)	36.00%	57.74%	0.99%	94.73%	38.00%	60.95%	1.04%	100.00%
(30)	27.00%	67.73%	0.66%	95.39%	28.30%	71.00%	0.70%	100.00%
(40)	34.00%	50.88%	6.91%	91.79%	37.04%	55.43%	7.53%	100.00%
(45)	26.80%	45.16%	12.64%	84.60%	31.68%	53.38%	14.94%	100.00%
(50)	11.00%	32.62%	25.21%	68.83%	15.98%	47.39%	36.62%	100.00%
(60)	15.00%	77.72%	1.35%	94.07%	15.94%	82.62%	1.44%	100.00%
(70)	94.50%	2.03%	2.31%	98.83%	95.61%	2.05%	2.33%	100.00%
(80)	5.00%	25.73%	3.60%	34.32%	14.57%	74.95%	10.48%	100.00%
(90)	10.00%	65.97%	20.60%	96.57%	10.36%	68.31%	21.33%	100.00%
(Bulk)	32.54%	51.04%	6.39%	89.97%	36.17%	56.73%	7.10%	100.00%

Table 6.02 Quartz, normative total alkali feldspars, and eucryptite for the Tanco pegmatite zone and bulk compositions

after Stewart, 1978). This shift is due to the influence of F, B, and P, as documented in other experimental studies (London, 1990). These components reduce the silica content of the residual melt, but enhance the albite component.

Even among the spodumene and petalite bearing pegmatites, the bulk Tanco composition is poor in lithium aluminosilicates. However, the weighted bulk composition of the continuous inner zones (40), and, (point (45) in **Figure 6.01**), which solidified simultaneously, falls very close to the bulk composition of the lithium-richest pegmatites (and of inner lithium-rich zones of zoned pegmatites as illustrated in Stewart, 1978).

6.6 Petrochemical Comparison with Fertile Granites

From the petrogenetic viewpoint, it is significant that the large and compositionally granitic zone (20) of the Tanco pegmatite is closely comparable in its bulk mineralogy and chemical composition to the pegmatitic leucogranite phases of nearby fertile granites examined by Goad (1984; *c.f.* also Goad and Černý 1981, Černý *et al.* 1981). The bulk mineralogy, chemical composition in terms of main rock-forming constituents, and the degree of fractionation of rare elements are quite similar (**Table 6.03**). It is only the extreme fractionation attained by the inner zones of the Tanco pegmatite which gives its overall geochemical signature the strong enrichment in Li, Rb, Cs, P, and some other trace elements such as Nb, Ta and Sn.

The comparison is, however, imperfect, as the available compositions of pegmatitic leucogranites come from granite + pegmatite systems other than that which encompasses Tanco; the parent of the Tanco-bearing Bernic Lake pegmatite group is not exposed (Černý *et al.* 1981). Nevertheless, some of the petrochemical features of the Greer Lake pegmatite group (Greer Lake leucogranite), and particularly of the Rush Lake pegmatite group (Osis Lake leucogranite) are closely comparable to those of the Bernic Lake pegmatite group, so the similarities shown in **Table 6.03** can be considered legitimate.

Table 6.03 Representative Chemical Analysis of Pegmatitic Granites

	TNL-1006	OL-1004	OL-1005	GL-1002	GL-1003	ENL-1001	Tanco Zone (20)	Tanco Bulk Comp
SiO2	73.50	72.05	73.40	75.00	75.30	76.00	76.85	75.27
TiO2	0.03	0.03	0.06	0.03	0.04	0.00	0.00	0.01
Al2O3	14.40	15.92	14.80	14.80	14.30	13.98	13.57	13.72
Fe2O3	0.47	0.79	0.44	0.21	0.86	0.59	0.00	0.00
FeO	0.88	0.68	0.68	0.92	0.92	1.10	0.17	0.12
MnO	0.03	0.10	0.02	0.09	0.08	0.09	0.05	0.19
MgO	0.09	0.08	0.03	0.03	0.03	0.04	0.01	0.01
CaO	0.36	0.24	0.33	0.06	0.22	0.32	0.27	0.21
Na2O	3.98	4.08	4.80	2.75	5.20	4.25	5.01	3.35
K2O	5.63	4.98	4.59	5.32	2.19	2.92	2.41	3.50
P2O5	0.05	0.42	0.56	0.03	0.06	0.04	0.59	0.94
CO2	0.09	0.10	0.11	0.09	0.08	0.09	0.00	0.00
H2O+	0.23	0.53	0.39	0.71	0.55	0.56	0.24	0.37
F2	0.01	0.02	0.02	0.06	0.03	0.03	0.10	0.18
Subtotal	99.75	100.02	100.23	100.10	99.86	100.01	99.27	97.88
-F=O2	0.00	-0.01	-0.01	-0.03	-0.01	-0.01	-0.04	-0.08
Total	99.75	100.01	100.22	100.07	99.85	100.00	99.23	97.80
ASI CNKRC	1.08	1.27	1.10	1.42	1.26	1.30	1.18	1.35
ASI CNK	1.08	1.27	1.10	1.42	1.26	1.30	1.20	1.42
Li	28	10	10	119	76	118	544.52	3520.15
Rb	275	318	366	1001	442	391	2846.85	5320.17
Cs	3.2	11	6.2	5.6	2.3	15	302.69	4522.92
Be	0.5	0.7	0.9	1.8	1.7	12	229.44	220.82
Pb	20	11	10	5	11	17		12.67
Ga	62	43	43	65	64	48	80.33	79.21
U	3	5	2	9	8	25		55.44
Zr	5	25	2	N.D.	16	5	0.56	37.43
Hf			0.35		1.25	0.95		14.29
Sn	13	22	18	33	23	13	194.97	308.35
K/Rb	169.95	130.00	104.11	44.12	41.13	61.99	7.02	5.46
K/Cs	14605.10	3758.22	6145.64	7886.24	7904.28	1615.99	66.06	6.42
Mg/Li	19.39	48.25	18.10	1.52	2.38	2.04	0.12	0.02
Zr/Sn	0.38	1.14	0.11		0.70	0.38	0.00	0.12
Zr/Hf			5.71		12.80	5.26		2.62
Al/Ga	1228.95	1959.01	1821.19	1204.79	1182.27	1541.09	893.69	916.58

Sample Locations:

TNL= Tin Lake leucogranite
OL = Osis Lake leucogranite
GL = Greer Lake leucogranite
ENL= Eagle Nest Lake leucogranite

Note:

ASI CNKRC = Aluminium Saturation Index using Ca, Na, K, Rb, and Cs
ASI CNK = Aluminium Saturation Index using CA, Na, and K

7 SUMMARY and CONCLUSIONS

(i) A 3D model of the Tanco pegmatite and its inner zones was constructed from a dense network of underground and surface drill holes in and around the pegmatite, locally improved from underground exposures. The resulting model shows a nearly blind sub-horizontal, bilobate, saddle-shaped pegmatite dipping shallowly to the north and doubly plunging to the east and west. The pegmatite is about 1990 m in length, 1060 m in width, and at its thickest point nearly 100 m, thinning out toward the edges.

(ii) The pegmatite displaces about 9.4 million m^3 and has a mass of 25.0 million metric tons. Proportions of individual zones by volume are as follows: zone (10) 0.10%, zone (20) 30.83%, zone (30) 2.69%, zone (40) 28.79%, zone (50) 13.12%, zone (60) 13.56%, zone (70) 7.47%, zone (80) 1.33%, zone (90) 2.11%.

(iii) Using the mineral compositions, mineral densities, and the volumes of individual zones, the bulk mineral composition of the pegmatite (via compositions of individual zones) was calculated to be: quartz 32.54%, albite 25.56%, K-feldspar 22 05%, petalite 9.03%, lithian muscovite 3.00%, muscovite 2.97%, pollucite 1.28%, spodumene 0.92%, amblygonite 0.77%, lepidolite 0.27% by volume.

(iv) The bulk chemical composition of the pegmatite is: SiO_2 75.27%, Al_2O_3 13.72%, TiO_2 0.01%, Fe_2O_3 0.00%, FeO 0.12%, MnO 0.19%, MgO 0.01%, CaO 0.21%, SrO 0.0004%, Li_2O 0.76%, Na_2O 3.35%, K_2O 3.50%, Rb_2O 0.58%, Cs_2O 0.48%, P_2O_5 0.94%, B_2O_3 0.05%, BeO 0.0613%, Sc_2O_3 0.0001%, SnO_2 0.0391%, Nb_2O_5 0.0129%, Ta_2O_5 0.0792%, UO_2 0.0063%, PbO 0.0014%, WO_3 0.00004%, ZnO 0.0013%, ZrO_2 0.0051%, HfO_2 0.0017%, Tl_2O 0.0047%, Ga_2O_3 0.0106%, Sb_2O_3 0.0002%, H_2O^- 0.03%, F 0.18%, -O=F2 -0.08%, total 99.92% by weight.

(v) The current Tanco bulk composition is different from the previous calculations by Morgan and London (1990). They used a broad E-W belt across the pegmatite as representative of the whole body, thus under-representing zone (20) in particular as well as zones (40), (50), and (70) in their results. Improved modelling and modal estimates contribute to the higher SiO_2 and Na_2O, and lower Al_2O_3, Li_2O, K_2O, Rb_2O, and P_2O_5 in the present work.

(vi) The bulk composition of Tanco and other lithium-rich pegmatites analyzed to date are enriched in feldspars, and impoverished in quartz and lithium aluminosilicates, relative to the minimum in the experimental Li_2O-Al_2O_3-SiO_2-H_2O system as examined by Stewart (1978). This shift is due to the influence of F, B, and P, as documented in experimental studies (London, 1990).

REFERENCES

Beakhouse, G.P. (1977). "A Subdivision of the Western English River Subprovince," Canadian Journal of Earth Science, vol. 14, pp. 1481-1489.

Beakhouse, G.P. (1991). "Winnipeg River Subprovince; *in* Chapter 8," Geology of Ontario, Ontario Geological Survey, Special Volume 4, Part 1, 14, pp. 279-301.

Brisbin, W.C. (1986). "Mechanism of Pegmatite Intrusion," American Mineralogist, vol. 71, pp. 644-651.

Brisbin, W.C. and Trueman, D.L. (1982). "Dilational Mechanics of Fractures During Pegmatite Emplacement, Winnipeg River Area," Manitoba Geological Association of Canada/Mineralogical Association of Canada, Joint Annual Meeting, Winnipeg, Program with Abstracts, No. 7, p.40.

Burnham, C.W. and Jahns, R,H. (1962). "A Method for Determining the Solubility of Water in Silicate Melts," American Journal of Science, vol. 260, pp. 721-745.

Černá, I., Černý, P., and Ferguson, R.B. (1972). "The Tanco pegmatite at Bernic Lake Manitoba. III, Amblygonite-montebrasite:," Canadian Mineralogist, vol. 11, pp. 643-659.

Černý, P. (1972). "The Tanco pegmatite at Bernic Lake Manitoba. VII, Eucryptite," Canadian Mineralogist, vol. 11, pp. 708-713.

Černý, P. (1991). "Rare-Element Granitic Pegmatites. Part I: Anatomy and Internal Evolution of Pegmatite Deposits," Geoscience Canada, vol. 18, pp. 49-67.

Černý, P., Ercit, T.S., and Vanstone, P.J. (1998). Mineralogy and Petrology of the Tanco Rare-Element Pegmatite, Southeastern Manitoba. International Mineralogical Association, 17th General Meeting, Toronto, Ontario, Canada, July 13-17.

Černý, P. and Ferguson, R.B. (1972). "The Tanco pegmatite at Bernic Lake Manitoba. VI, Petalite and spodumene relations," Canadian Mineralogist, vol. 11, pp. 690-707.

Černý, P., Pentinghaus, H., and Macek, J.J. (1985). "Rubidium Microcline from Red Cross Lake, Northeastern Manitoba," Geological Society of America, Bulletin, vol. 69, p. 803-836.

Černý, P. and Siivola, J. (1980). "The Tanco pegmatite at Bernic Lake Manitoba. XII, Hafnium Zircon," Canadian Mineralogist, vol. 15, pp. 489-499.

Černý, P. and Simpson, F.M. (1977). "The Tanco pegmatite at Bernic Lake Manitoba. IX, Beryl," Canadian Mineralogist, vol. 15, pp. 489-499.

Černý, P. and Simpson, F.M. (1978). "The Tanco pegmatite at Bernic Lake Manitoba. X, Pollucite," Canadian Mineralogist, vol. 16, pp. 325-333.

Černý, P., Trueman, D.L., Ziehlke, D.V., Goad, B.E., and Paul, B.J. (1981). The Cat Lake-Winnipeg River and the Wekusko Lake Pegmatite Fields, Manitoba. Manitoba Department of Energy and Mines, Mineral Resources Division, Economic Geology Report ER80-1.

Chackowsky, L.E. (1987). Mineralogy, Geochemistry, and Petrology of Pegmatitic Granites and Pegmatites at Red Sucker Lake and Gods Lake, Northeastern Manitoba: Unpublished M.Sc. Thesis, University of Manitoba, Winnipeg, Canada.

Crouse, R.A. and Černý, P. (1972). "The Tanco Pegmatite at Bernic Lake Manitoba. Part I: Geology and Paragenesis," Canadian Mineralogist, vol. 11, pp. 591-608.

Crouse, R.A., Černý, P., Trueman, D.L., and Burt, R.O. (1979). "The Tanco Pegmatite, Southeastern Manitoba," Canadian Mining and Metallurgical Bulletin, vol. 72, no. 802, pp. 142-151.

Deer, W.A., Howie, R.A., and Zussman, J. (1962). Rock-forming Minerals. Vol 3 of Sheet Silicates. London: Longmans.

Ercit, T.S. (1986). The Simpsonite Paragenesis; the Crystal Chemistry and Geochemistry of Extreme Ta Fractionation: Ph.D. Thesis, University of Manitoba, Winnipeg, Canada.

Ercit, T.S., Černý, P., and Hawthorne, F.C. (1995a). "The Crystal Chemistry of Simpsonite," Canadian Mineralogist, vol. 30, pp. 663-671.

Ercit, T.S., Černý, P., and Hawthorne, F.C. (1995b). "The Wodginite Group II. Crystal Chemistry," Canadian Mineralogist, vol. 30, pp. 613-631.

Ferreira, K.J. (1984). The Mineralogy and Geochemistry of the Lower Tanco Pegmatite, Bernic Lake, Manitoba, Canada: Unpublished M.Sc. Thesis, University of Manitoba, Winnipeg, Canada.

Filippova, Yu.I. (1971). "Geochemistry of Rare Elements in Weakly Differentiated Pollucite Bearing Pegmatites of Siberia," in Pegmatite Rare Element Deposits, vol. 4, pp. 44-58. [in Russian].

Goad, E.B. (1984). Pegmatitic Granites of the Winnipeg River Area, Southeastern Manitoba: MSc. Thesis, University of Manitoba, Winnipeg, Canada.

Hutchinson, R.W. (1959). "Geology of the Montgary Pegmatite," Economic Geology, vol. 54, pp. 1525-1542.

Jahns, R.H. (1953). "The Genesis of Pegmatites. II. Quantitative Analysis of Lithium-Bearing Pegmatite, Mora County, New Mexico," American Mineralogist, vol. 38, pp. 1078-1112.

London, D. (1990). "Internal Differentiation of Rare Element Pegmatites; A Synthesis of Recent Research," Geological Society of America, Special Paper 246, p. 35-50.

London, D. and Burt, D.M. (1982). "Chemical Models for Lithium Aluminosilicate Stabilities in Pegmatites and Granites," American Mineralogist, vol. 67, pp. 494-509.

Morgan VI, G.B. and London, D. (1987). "Alteration of Amphibolitic Wallrocks around the Tanco Rare-Element Pegmatite," American Mineralogist, vol. 72, pp. 1097-1121.

Ni, Y., Yang, Guo, L., Zhou, T. and Ling, Y. (1989). "Triphylite-Lithiophilite series in China," Acta Petrologica et Mineralogica, vol. 8, no. 2, pp. 144-155.

Norton, J.J. (1970). "Composition of a Pegmatite, Keystone, South Dakota," American Mineralogist, vol. 55, pp. 981-1002.

Norton, J.J. (1994). "Structure and Bulk Composition of the Tin Mountain Pegmatite, Black Hills, South Dakota," Economic Geology, vol. 89, pp. 1167-1175.

Press, W.H., Teukolsky, S.A., and Vettering, W. (1992) Numerical Recipes Example Book. Cambridge, England: Cambridge University Press.

Rinaldi, R., Černý, P., and Ferguson, R.B. (1972). "The Tanco pegmatite at Bernic Lake Manitoba. VI, Lithium-rubidium-cesium micas," Canadian Mineralogist, vol. 11, pp. 690-707.

Selway, J.B. (1998). The Compositional Evolution of Tourmaline in Pegmatites: Ph.D. Thesis *in press*, University of Manitoba, Winnipeg, Canada.

Stewart, D.B. (1978). "Petrogenesis of Lithium-Rich Pegmatites," American Mineralogist, vol. 63, pp. 970-980.

Teertstra, D. (1997). Reactions of (K-Rb)-Feldspars - from Rare Element Granitic Pegmatites: Ph.D. Thesis, University of Manitoba, Winnipeg, Canada.

Trueman, D.L. (1980). Stratigraphy, Structure, and Metamorphic Petrology of the Archean Greenstone Belt at Bird River, Manitoba: Ph.D. Thesis, University of Manitoba, Winnipeg, Canada.

Vlasov, K.A. ed. (1964). "Geochemistry and Mineralogy of Rare Elements and Genetic Types of their Deposits," Mineralogy of Rare Elements. English translation Jerusalem, vol. 3, p. 945.

APPENDIX 1
DATA

Due to the confidential nature of the drill core data used in this thesis, these data can not be released publicly. Access to this information depends solely on the discretion of the Tantalum Mining Corporation of Canada Ltd., a division of Cabot Specialty Fluids.

IMAGE EVALUATION TEST TARGET (QA-3)

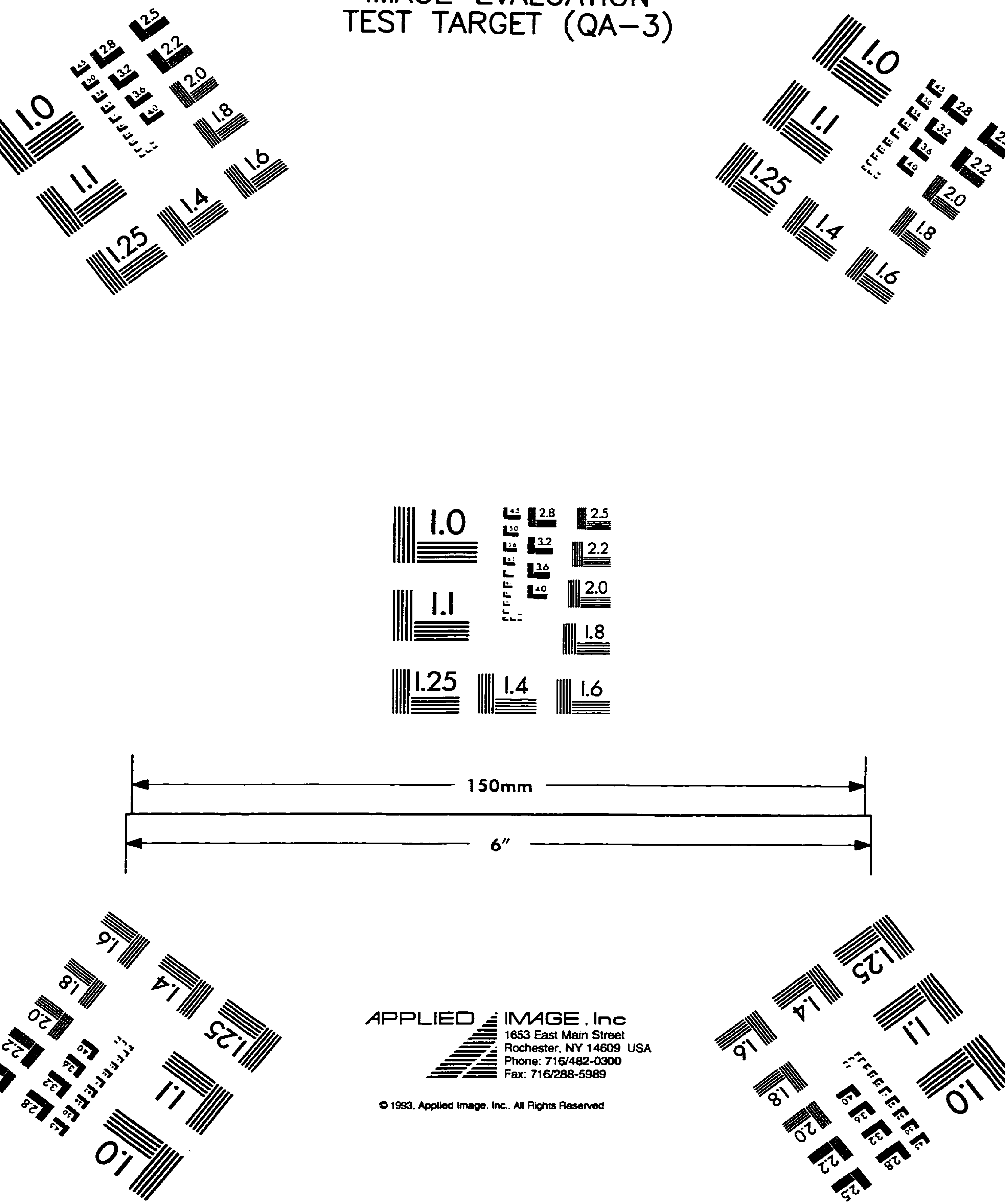

APPLIED IMAGE, Inc
1653 East Main Street
Rochester, NY 14609 USA
Phone: 716/482-0300
Fax: 716/288-5989